Smart Grid Energy Management based on IoT and Computational Intelligence

Submitted in partial fulfillment of the requirements
of the degree of

Doctor of Philosophy

by

Swati Sharda
(Roll No. 2k17/PhD/IT/01)

Supervisors:

Prof. Kapil Sharma
Prof. Mukhtiar Singh

Information Technology
DELHI TECHNOLOGICAL UNIVERSITY DELHI
2022

Dedicated to my beloved parents.

DECLARATION

I hereby declare that the dissertation entitled "Smart Grid Energy Management based on IoT and Computational intelligence" to be submitted for the Degree of Doctor of Philosophy is my original work and the dissertation has not formed the basis for the award of any degree, diploma, or fellowship of similar other titles. It has not been submitted to any other University or Institution for the award of any degree or diploma. I also declare that I have adhered to all principles of academic honesty and integrity and have not misrepresented or fabricated or falsified any idea/data/fact/source in my submission.

Swati Sharda

Roll No. 2K17/PH.D/IT/01

Date: 16 August, 2022

CERTIFICATE

This is to certify that the thesis entitled "Smart Grid Energy Management using IoT and Computational Intelligence" submitted by Ms. Swati Sharda, Roll no. 2k17/Ph.D/IT/01 as a full time research scholar in the Department of Information Technology, Delhi Technological University for the award of the degree of *Doctor of Philosophy*, is a record of bonafide work carried out by her under our supervision. The contents of this report have not been submitted and will not be submitted either in part or in full, for the award of any other degree or diploma in this institute or any other institute or university. The thesis fulfills the requirements and regulations of the University and in our opinion meets the necessary standards for submission.

Place: Delhi

Date: 2 May,2022

Prof. Kapil Sharma
Supervisor
HOD, IT Department
DTU

Prof. Mukhtiar Singh
Co-supervisor
Electrical Department
DTU

ACKNOWLEDGEMENTS

I wish to express my sincere appreciation to those who have contributed to this thesis and supported me in one way or the other during this amazing journey of my research. I wish to record a deep sense of gratitude to **Prof. Mukhtiar Singh**, my supervisor for his valuable guidance and constant support at all stages of my Ph.D study and related research.

He motivated me to take challenges and supported me to work upon the inter-disciplinary problem. His guidance, timely suggestions, enthusiasm, dynamism, and immense knowledge about the subject have been a true inspiration for me. I am highly obliged for his valuable and unlimited support in my Ph.D journey.

I would like to express my sincere gratitude to my supervisor and Head of Department (IT) **Prof. Kapil Sharma**, for helping and supporting through all the phases of my Ph.D research. I am thankful for his unlimited support on my personal front and guiding me on life skills. His encouragement and suggestions helped me to solve challenges occured throughout the research journey.

I thank to my seniors & colleagues, **Dr. Sangeeta, Dr. Ashish tripathi, Dr. Aakash Seth** who were always present there with me during my research discussion and suggestions.

I would also like to give special thanks to my husband **Mr. Ankit Sharda** and my family as a whole for their continuous support and understanding when undertaking my research and writing my project.

Finally, I would like to thank GOD, for letting me through all the difficulties.

Swati Sharda

Roll No. 2K17/PH.D/IT/01

ABSTRACT

Booming demand, depleting natural resources, deregulation, generation capacities, and grids are some of the factors that are a concern for energy efficiency. In Smart grid era, Demand Side Management (DSM) plays an indispensable role in development of sustainable cities and societies. Based on the current practice of utility system, the load shape objectives can be characterized into six categories: peak clipping, valley filling, load shifting, strategic conservation, strategic load growth, and flexible load shape. Out of these six classical approaches: "peak clipping" and "load shifting" are most widely applicable and relevant for energy efficiency using DSM [121]. Home Energy Management System (HEMS) lies under the umbrella of DSM, it allows residential consumers to supervise and manage the power usage of their appliances to reduce their electricity bills. Since, residential consumers are more concerned about their energy bills as well as comfort, energy optimization with multiple objectives grips valuable and resourceful usage of electricity. Therefore, the usage awareness and scheduling optimization alone have the potential to reduce consumption by 15% in private households.

The stochastic problem of scheduling optimization in HEMS involves arbitrary dynamics of renewable energy, consumer demand, consumer behavior, and electricity price. For consumers, energy storage and load scheduling can provide effective means in reducing their electricity costs. Further, the limited battery capacity, the finite optimization time period and interaction with energy storage devices complicates the energy scheduling and control decisions. DSM in HEMS using load shifting technique is a challenging optimization research problem, where the main aim is to have optimal utilization of available energy resources while reducing the electricity bills. Reducing the complexity of scheduling optimization helps in the judicial use of power consumption by the effective control of smart home appliances.

The research work focuses around the development of scheduling algorithm for the consumer which aims to minimize the electricity price without compromising the comfort time period of using various home appliances. First, a comprehensive survey regarding the major factors affecting the optimized management solution and consequent decision making in HEMS

has been performed. Second, a robust deep learning algorithm for solar irradiance forecasting has been developed. It can forecast GHI value using various weather parameters in different seasons as well as at different steps (1-step, 2-step, 12 steps ahead). Third, deep learning ensemble model has been utilized to forecast appliances' power utilization. Using dynamic Item set counting (DIC) algorithm, association between multiple appliances has been determined. Fourth, a real time scheduling algorithm has been proposed which takes into account the forecasted PV power, appliance power, battery constraints, various other constraints and forecast the 24- hour schedule of the appliances which minimizes the electricity price without compromising the comfort. Fifth, smart grid reliability problem has been assessed by modelling it using graph computational model and assessing the reliability through various indices .

Contents

List of Tables

List of Figures

Nomenclature

S	Set of unique entities in dataset.
n	Total number of entities in dataset.
s_α	Specific entity α of data set.
$X_{\alpha,t}$	Total features of α element at time t.
$o_{\alpha,t}$	Observed inputs of α element at time t.
$v_{\alpha,t}$	Time based vectors of α element at time t.
w	Size of look back window.
τ	Future predicted time steps $\in \{1, \tau_{max}\}$.
q	Specific quantile $\in \{50, 90, 95\}$.
$\delta_{ch}, \delta_{dch}$	Battery's charge and discharge efficiency.
$Batt\_E(h)$	Energy in the battery at hour h (kWh).
$Batt\_SOC(h)$	SOC of battery at hour h.
$Batt\_SOC_{\max}(h)$	Maximum SOC of battery at hour h.
$Batt\_SOC_{\min}(h)$	Minimum SOC of battery at hour h.
$Batt^{cap}$	Capacity of battery(kWh).
$Batt^{ch}(h)$,$Batt^{dch}(h)$	Battery's charging and discharging power at hour h.
$Batt^{ch}_{\max}$,$Batt^{dch}_{\max}$	Battery's maximum charging and discharging power.
$D_{ns}(h)$	Power demand of non-shift able loads at hour h(kW).
$D_p(h)$	Power demand at hour h (kWh).
D^n_{sh}	Power demand of nth shift able load at hour h (kW).
D_{total}	Total demand from the customers.

E_{ij}	Energy requirement for energy phase j in appliance i.(technical specification of appliances)
E_{ij}^{k}	Energy assigned to energy phase j of appliance$i$ during the whole period of time slot k.
E_{peak}	Energy consumed in peak hours.
$P_{batt}(h)$	Battery net output power at hour h(kW) (positive means charging, negative means discharging)
$P_{grid}(h)$	Power transferred between main grid and HEMS at hour h(kW).
$P_{grid}^{\max}(h)$	Maximum power received by household from grid at hour h(kW).
$status_n(h)$	The operation state of n^{th} shift able load at hour h 1: on,0: off.
$T_{out}^{\min}, T_{out}^{\max}$	Minimum and maximum outlet temperature in water tank($^{\circ}F$).
T_{out}^{i}	water temperature in the tank at interval i ($^{\circ}F$).
$T_{room}^{\min}, T_{room}^{\max}$	Minimum and maximum room temperature($^{\circ}F$).
T_{room}^{i}	Room temperature at interval i ($^{\circ}F$).
TOC_n	The number of n^{th} shift-able load's operation cycle time.
m	Sequence length.
k	Batch size.
I	Input measurements within a sequence.
d	Dimension of input embedding.
Q	Query vector of attention module.
K	Key vector of attention module.
V	Value vector of attention module.
(a,b)	Node pair within hidden layer of deep learning network.
W^{Q}	Weight matrix of query vector.
W^{K}	Weight matrix of key vector.

W^V	Weight matrix of value vector.
W^o	Weight matrix of learnable weights.
K_{dim}	Dimension of key vector.
h	Number of heads for multi-head self attention.
d_h	Output dimension of h heads.
β	Iterator for different heads in multi-head self attention.
d_model	Dimensionality of input and output of the Transformer encoder.
y_i	Observed value of GHI for sample i.
$\hat{y}_i$	Predicted value of GHI for sample i.
$\omega, \hat{\omega}$	Domain of training and testing data respectively.
W	Weight matrix of RSAM model for quantile forecasts.
$\hat{\phi}(t, \tau)$	Trained RSAM model for τ step ahead prediction starting from time t.
κ	Number of hidden layers in deep neural network.
η	Number of neurons at each hidden layer.
AMI	Advanced Metering Infrastructure.
BESS	Battery Energy Storage System.
CPP	Critical Peak Price.
DIC	Dynamic Itemset Counting.
DR	Demand Response.
DSM	Demand-side management.
ECL	Electrical Controllable Loads.
EV	Electric vehicle.
EWH	Electric Water Heater.
FFNN	Feed Forward Neural Network.

HVAC	Heating, Ventilation, and Air Conditioning.
ICT	Information and communication technologies
IoT	Internet of things.
RNN	Recurrent Neural Network.
RTP	Real-time price.
SOC	State of charge.
TCL	Thermostatically Control Loads.
ToU	Time-of-use.

Chapter 1

Introduction

1.1 Background

In Smart grid era, Demand Side Management (DSM) plays an indispensable role in the development of sustainable cities and societies. Booming demand, crucial natural resources, deregulation, generation capacities, and grids are some of the factors that are a concern for energy efficiency. The various DSM techniques are shown in Figure 1.1.

"Smart grid is a modernized version of the traditional grid that enables bidirectional flow of energy and uses two-way communication and control capabilities that will lead to an array of new functionalities and applications"; definition by National Institute of Standards and Technology (NIST), USA. The smart grid armed with advanced sensors, enhanced computational power and robust communication infrastructure has inherent self-healing capability, is consumer-friendly and is vigilant to physical and cyber attacks. HEMS lies under the umbrella of DSM; it allows residential consumers to supervise and manage the power usage of their appliances to reduce their electricity bills. Today domestic electricity use accounts for 30% of global energy consumption. The stochastic problem of scheduling optimization in HEMS involves

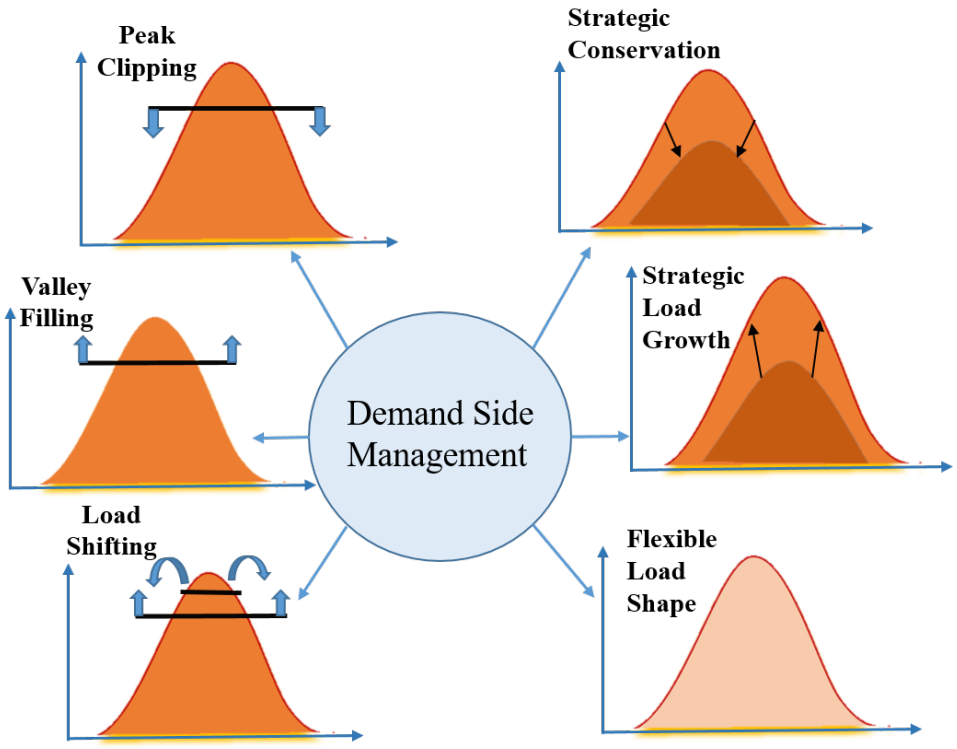

Figure 1.1: Different ways of Demand side management

arbitrary dynamics of renewable energy, consumer demand, consumer behavior, and electricity price. For consumers, energy storage and load scheduling can provide effective means in reducing their electricity costs. Furthermore, the finite battery capacity, the finite optimization time period, and interaction with energy storage devices complicates the energy scheduling and control decisions.

1.2 Motivation

- Demand side management (DSM) in is a very active research area in smart grid in which there is an increased need to explore the challenges imposed by various parameters such as PV integration, different categories of appliances, different power requirements, pricing etc.
- Many works have reported the study of DSM optimization, among which very few studies barely attempted to develop optimization algorithm for real time DSM (including various constraints).

- There are challenges in implementation of load shifting as difference in consumer behavior, pricing, appliance power usage trends, association between appliances, location, weather etc.
- The data obtained from the new generation advanced IoT devices along with advanced cloud integration techniques provide an opportunity to develop improved scheduling algorithms for consumers which minimize electricity cost without compromising consumer comfort.

1.3 Research objectives

In this thesis, for demand side management using load shifting, the real-time scheduling algorithm using different pricing schemes has been developed. In this context, the challenges and opportunities of DSM, solar irradiance forecasting at different time-steps and seasons, consumer behavior learning and detection of attacks on smart grid has been discussed.

- Modeling and characterization of load of smart household appliances including their operating cycles (TCL and ECL).
- Green energy modeling and its optimal utilization for load shifting in time varying price environment.
- Utility Load Reshaping to optimize the energy cost envelope of consumer using computational intelligence techniques.
- Development of Scheduling Algorithm to optimize cost and comfort trade-off of consumer incorporating real time constraints.
- Integration of machine learning techniques to understand the usage pattern of consumer smart appliances and implement self-learning algorithms to enable user comfort and save energy.
- Design of demand response strategy to schedule working cycles of different appliances based on user load and renewable energy forecasting and its optimal utilization to achieve reduced carbon footprint without affecting user comfort.

These objectives are fulfilled by using cutting-edge deep learning techniques for multivariate solar irradiance forecasting and consumer appliances power forecasting. Then, a real-time scheduling algorithm using the forecasting results has been proposed, which schedules the home appliances according to consumer comfort and minimizes the electricity cost and peak-to-average (PAR) ratio of the consumer.

1.4 Thesis outline

The subject matter of the thesis is presented in the following five chapters;

- ✓ Chapter-1 provides an overview of smart grid and demand side management (DSM). Different techniques of DSM and role of IoT in Home Energy Management System (HEMS) has been discussed. It also emphasizes the motivation of the research and objectives.
- ✓ Chapter-2 elucidates the challenges and opportunities of DSM in HEMS. It discusses the different optimization techniques used for DSM. Thorough investigations of different parameters affecting DSM and challenges in distribution network are included in this chapter.
- ✓ Chapter-3 describes the solar irradiance forecasting using self-attention based deep learning model. The training and testing phases of model, multi-step forecasting, seasonal variations and the data sets used for this study are incorporated in this chapter.
- ✓ Chapter-4 discusses the consumer behavior learning model. The power forecasting of various appliances used by consumer using Ensemble deep learning model and association between different appliances using DIC algorithm.
- ✓ Chapter-5 highlights the real time optimization algorithm which uses solar irradiance forecasting and consumer behavior learning resulting the 24-hour schedule for the appliances usage under different pricing schemes.
- ✓ Chapter-6 discusses the smart grid communication reliability issues in ICT networks and solution using computational graph.

✓ Chapter-7 summarizes the proposed methodologies and the discussions of the results, including the important findings of the studies. The future scope of the research works are proposed successively, following the conclusion on the basis of important extracts and understanding of the subject of interest.

Chapter 2

Overview and Challenges of DSM in HEMS

2.1 Introduction

DSM evolved during the 1970s and can be defined as "*to plan, implement and monitor activities designed to influence customer uses of electricity in ways that will produce desired changes in the utility's load shape*" [215, 36, 65]. DSM is beneficial for both consumers and energy providers. It allows the active participation of consumers by reshaping its load profile through informed decisions to have optimal energy consumption which leads to a reduction in peak load demand and hence helps in maintaining the stability of the overall power system network [139]. This chapter discusses the following points in detail:

1. The architecture of smart home with smart devices integrated with photo-voltaic (PV) and electric vehicle (EV).
2. A detailed description of the major factors affecting load management and control decision making in a smart home.

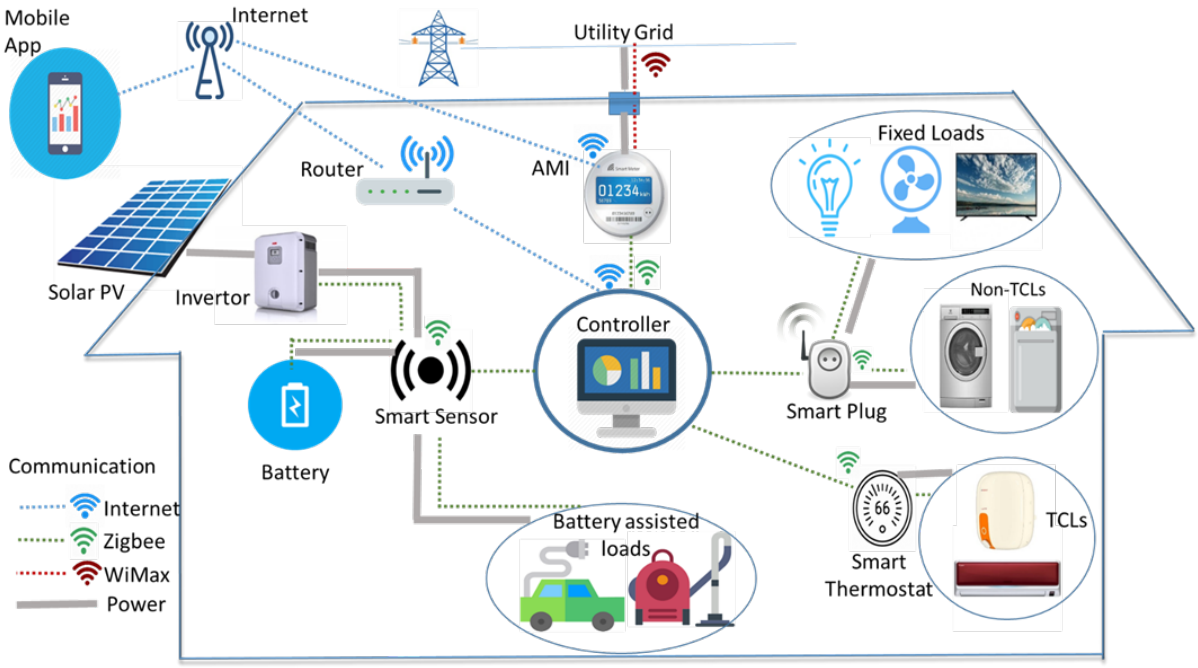

Figure 2.1: IoT based Smart Home

3. A focused taxonomy for the categorization and prioritization of appliances in the smart home.
4. A detailed review of different types of optimization techniques for the solution of load scheduling problem.

2.2 IoT based HEMS

HEMS is the cluster of smart home appliances having in-built communication capability that creates an environment for energy management. IoT is now becoming one of the most commonly used technology for communication and control of various devices confined to the Home Area Network (HAN)/Local Area Network (LAN). The IoT based HEMS architecture is presented in Fig. 2.1. Key elements that make up the environment are described below:

2.2.1 Smart Appliances

Smart Appliances are integrated with IoT enabled technology to interact with smart devices such as smartphones or tablet allowing remote access to the homeowner. These appliances can communicate wirelessly with the smart meter and participates in reducing energy consumption by automatically adapting to changes in availability of power and dynamic tariff [76]. Various factors that influence consumers for the purchase of smart home appliances are mentioned in [151]. These are 1) utility of appliance; 2) consumer satisfaction; 3) cost-saving; 4) ease of control. Privacy, control, and interoperability among smart appliances, majorly affect the consumer purchase decision. IoT based home appliance controlling system as implemented in [233] solves the interoperability issues and enhances user interaction with smart appliances.

2.2.2 Advance Metering Infrastructure (AMI)

AMI is an important tool empowering the customer to play an active role in the electricity consumer market as it enables the bi-directional communication between smart meter installed at consumer premises and utility grid. It is also one of the main component of IoT enabled HEMS which is responsible for data collection, transfer, remote monitoring, privacy and security of consumer information and displaying dynamic tariff information etc. [27]. Since AMI contains detailed information about consumers' data consumption habits, it imposes many security challenges related to revealing consumer lifestyle [158]. Moreover, the vulnerabilities in terms of data theft or manipulation, power theft, cyber and physical attacks are becoming serious issues for utility as well as law enforcement agencies [153]. These security issues and attack scenarios have been extensively investigated in the literature. Various key establishment algorithms have been proposed in the literature to ensure confidentiality and integrity for secure communication between AMI and utility [157, 254, 231, 134]. However, the complexity, computational burden and security related claims of these algorithms are still debatable.

Table 2.1: Communication Technologies for Smart Home

Technology	Spectrum	Data rate	Coverage range	Applications	Limitation
WiFi	2.4 GHz	11 Mbps	100 m	Monitoring and Controlling	Security, Interference
Zigbee	2.4 GHz	250 Kbps	30-50 m	AMI	Low data rate, Short range
WiMAX	3.5GHz	Upto 75 Mbps	10-50 Km	AMI, Demand response	Not widespread
5G	1-6 GHz	Upto 10 Gbps	1000 feet	AMI, Demand response	Cybersecurity

2.2.3 Smart Thermostat

A smart thermostat is a device used in thermostatically controllable loads for learning temperature preferences of consumers. It also facilitates the consumers by providing remote access and communicates with AMI according to price signals [125]. Sensing, machine learning, and network communication feature embedded in programmable thermostat makes them smart. Such thermostats embedded with proximity, motion sensors, and its learning algorithm adapts to set temperature according to the user's historical preferences at different times of the day [58]. Further, the energy consumption profile based on consumer usage pattern guides the user for efficient energy management. Google Nest learning thermostat [219], iDevices thermostat [95], Ecobee [47] are some examples of smart thermostats available in the market.

2.2.4 Smart Plugs

A smart home plug is an electric device that makes existing home appliances to act like smart devices. It can identify the type of attached home appliance based on the energy consumption profile of that appliance. With the inbuilt wireless communication protocols, it can connect to the wireless home network so that a user can measure the energy consumption and control the electronic device plugged into the smart plug over the internet [161]. Security vulnerabilities related to smart plugs have been discussed in [132]. TP-Link Hs110 [220], Centralite ZigBee plug-in [167], iDevices smart plug [16] are some examples of smart plugs available in the market.

2.2.5 Communication Technologies

Communication between different components of a smart home is a key aspect of realizing the smart home infrastructure [246]. Wireless communication technologies used in a smart home are IEEE 802.11 based wireless LAN (Wi-Fi), IEEE 802.15.4 based ZigBee and IEEE 802.16 based WiMAX [227]. The upcoming 5G based IoT technology will be used as low latency communication technology for smart home [148]. In the IoT enabled smart infrastructure, two types of communication protocols are normally followed: Zigbee for the device to device communication and Wi-Fi for the device to AMI communication. Since two types of different protocols are being followed in same premises, there are chances of interference between them. As per a study carried out in [252], a distance of 8 m between ZigBee and Wi-Fi guarantee the reliable operation of Zigbee regardless of the offset frequency, while 8 MHz is a safest offset frequency for the minimum distance of 2 m. A brief comparison of all the three protocols based on operating frequency, data rate, operating range with their applications and limitations is presented in Table 2.1.

2.3 DSM Challenges

DSM implementation using load shifting techniques depends upon some key factors like load Profile of appliances, renewable energy generation, load categorization, dynamic pricing, and consumer categorization while reducing the electricity bills and ensuring the system stability. Therefore, within the given constraints and well-defined objectives, the DSM becomes a typical optimization problem. A lot of optimization techniques have been proposed for DSM which have their own merits and demerits. This section is devoted to discussing the major challenges in DSM as shown in Fig. 2.2.

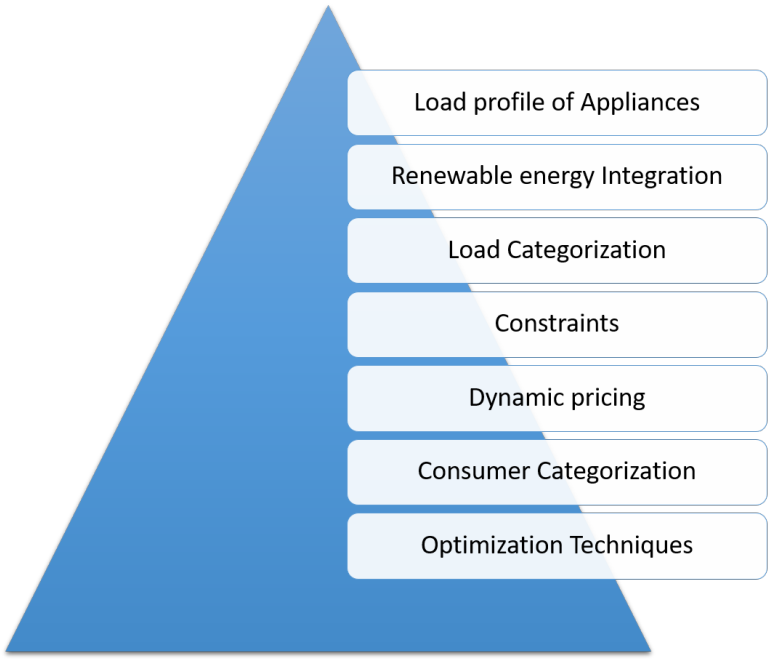

Figure 2.2: DSM Challenges

2.3.1 Load Profile of Smart Appliances

Smart appliances have inbuilt sensors for communication with the smart meter about their energy and power requirements. Energy consumption patterns of various smart home appliances give a key insight into consumer load pattern which may further be utilized for energy cost minimization and optimal resource management. It is also a critical component for developing accurate and efficient load management algorithms. A load profile of a smart home appliance indicates the energy consumption dependence with time from the start of operation to its end time. There are two different ways by which load profiles of appliances can be obtained: smart meters and survey of consumers.

Since the load profile of appliances greatly depends on the stochastic behavioral habits of consumers and external environment, developing a generalized DSM optimization algorithm that works for all types of consumers is highly challenging. It is also difficult to develop a generalized forecasting algorithm that can accurately predict the power consumption of different appliances for different consumers. Hence, the development of consumer-specific optimization algorithm considering their comfort preferences greatly depends on their appliances' load profile.

Table 2.2: Load Profile of Home Appliances

S.no	Appliance	Energy(KWh)	Power(KW)
1	Electric Stove	4.5	1.5
2	Clothes dryer	1	0.5
3	Vacuum cleaner	3	1.5
4	Refrigerator	2.5	0.125
5	Air Conditioner	6	1.5
6	Dishwasher	2	1
7	Heater	4	1
8	Water Heater	2	1
9	Pool Pump	4	2
10	PEV	10	2.5
11	Lightening	3	0.5
12	TV	1	0.5
13	PC	1.5	0.25
14	Ironing	2	1
15	Hair Dryer	1	1
16	Others	6	1.5

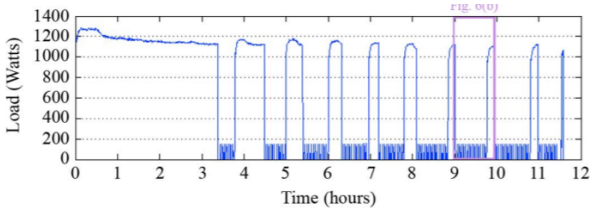

(a) Wall-AC

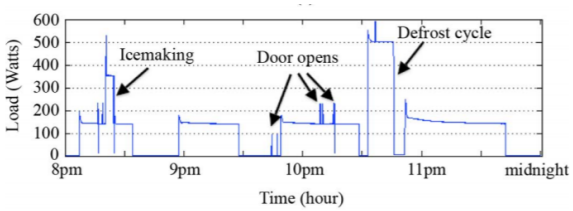

(b) Refrigerator

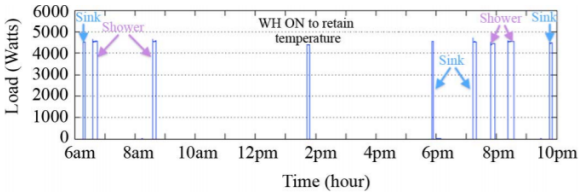

(c) Water-heater

Figure 2.3: Load Profile of TCL appliances

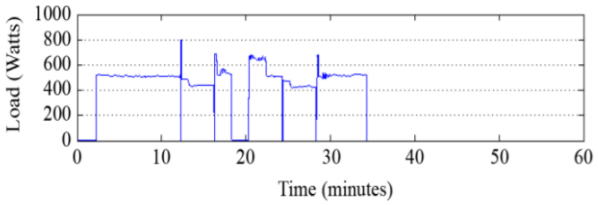

(a) Cloth-washer

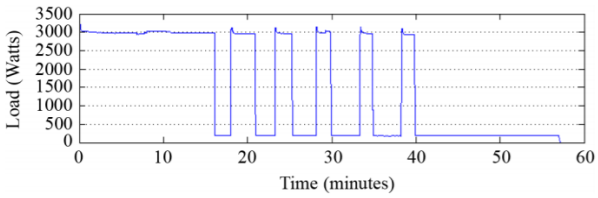

(b) Cloth-dryer

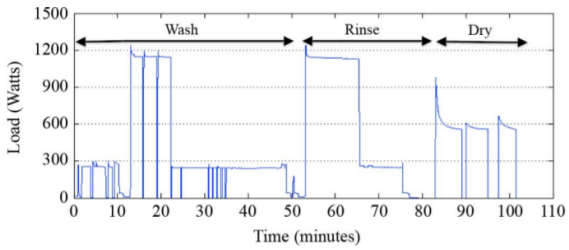

(c) Dishwasher

Figure 2.4: Load Profile of controllable appliances

2.3.2 Integration of Renewable Energy

Integration of distributed small scale renewable energy system in HEMS is the key to efficient scheduling optimization. Although promising, renewable energy is often intermittent and difficult to predict [52]. Offline storage control strategies such as BESS and rolling battery installed in EV with bi-directional power flow capability have been utilized to curtail the power fluctuations from RES. Moreover, the energy storage devices may also be very helpful in improving

the power imbalance, power quality, reliability and harmony between loads and distributed generated resources to have enhanced stability [253]. Besides these advantages, increased penetration of solar photo voltaic in HEMS pose great challenges in the management of electricity distribution networks. Intermittent generation may lead to difficulty in maintaining supply and demand, voltage and frequency stability such that over voltage conditions may lead to even power outages.

It is inevitable to note that the uncertainty of solar power and electricity tariff makes it difficult to schedule optimal residential energy demands. Several optimization algorithms based on heuristic optimization [146], two-stage robust optimization [135] and mixed-integer linear programming (MILP) [54] have been proposed to optimize the scheduling of distributed residential energy sources. Moreover, the bi-directional capability of electric vehicle (EV) as a battery energy storage unit has been explored for vehicle-to-home (V2H) and vehicle-to-grid (V2G) applications [54, 55].

2.3.3 Appliance Categorization

Different appliances have different characteristics, power requirements and operating modes. Grouping residential appliances in a suitable way based on consumer needs or behavior is important for the optimization of DSM. As per the reported studies, the authors have categorized the smart home appliances based on their behavior and operating characteristics. However, the same type of appliances has been categorized in a different way depending upon their research objectives. Table 2.3 presents the taxonomy of appliance categorization as per the various studies available in the literature. For the sake of understanding the different appliances as presented in Table 2.3 has been divided into five categories.

It can be inferred from Table 2.3 that home appliances based on their ability to participate in DR may be divided into three groups: Fixed loads, Controllable loads and Battery-assisted loads as shown in Fig. 2.5. The controllable loads can be further differentiated based on their thermal characteristics and are termed as non-thermostatically controllable (Non-TCLs) and thermostatically controllable (TCLs).

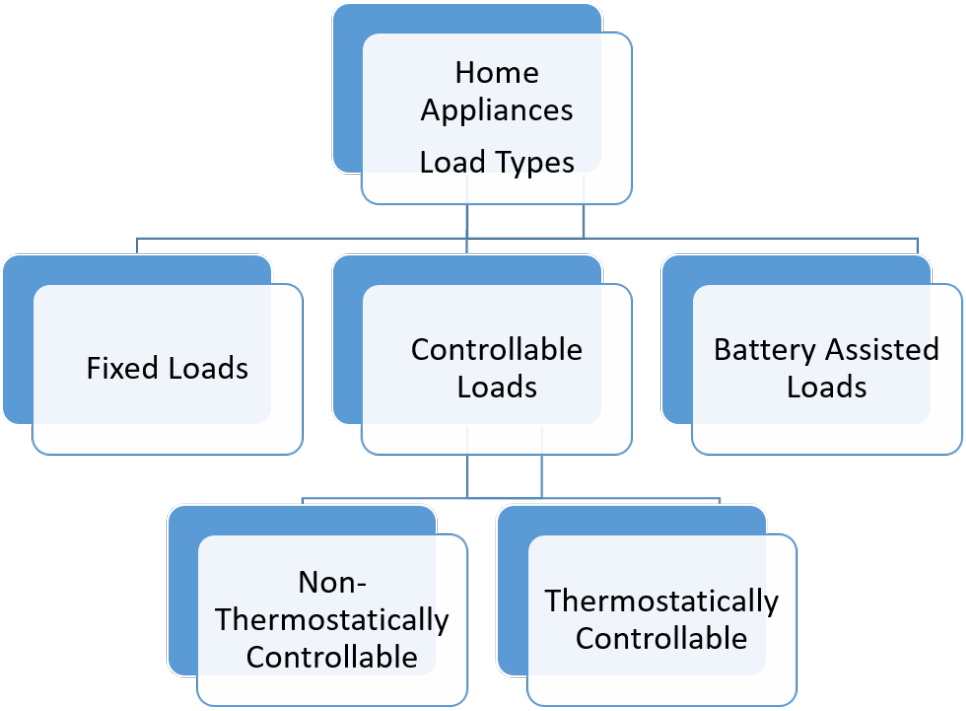

Figure 2.5: Load Categorization

2.3.3.1 Fixed Loads

These type of loads are primarily essential loads and does not participate in DR programs. The lights, fans, stove, TV, computer, etc fall in this category. Moreover, being a non-deferrable load, they cannot be rescheduled. These types of load contribute to nearly 28% of the electricity bill [239].

2.3.3.2 Controllable Loads

These loads are active participants of DSM programs. They can be further divided into two categories:

a) Non-Thermostatically Controllable (Non-TCL) These appliances are deferrable to a later period as most consumers do not need them immediately. Appliances such as dishwasher, clothes dryer, washing machine fall in this category.

b) Thermostatically Controllable (TCL): These type of appliances uses thermal storage (they can store heat in their thermal masses). By using their thermal inertia, these loads can be deferrable to near future periods without affecting consumer comfort. Mainly, the water heater

and HVAC system fall in this category. They almost contribute 60% of the electricity bill.

2.3.3.3 Battery Assisted Loads

These appliances consist of a battery as inbuilt energy storage. The EVs, BESS, vacuum cleaner, notebook PC and mobiles are typical examples of such type of loads. However, only the EV and BESS may significantly participate in DSM.

2.3.4 Constraints

The optimization problem of scheduling consists of many types of constraints. These constraints are both at the system level and appliance level. Constraints are addressed as follows:

2.3.4.1 Electrical Demand Supply Balance [217]:

The following equation demonstrates the electricity demand-supply balance at any hour considering power from grid and battery without considering load shifting and with consideration of shiftable and non-shiftable load demands. Without considering Load Shifting-

$$P_{grid}(h) - P_{batt}(h) = D_e(h) \tag{2.1}$$

Considering Load Shifting-

$$P_{grid}(h) - P_{batt}(h) = D_{nsh}(h) + \sum_{N_{sh}}^{n=1} D_{sh}^{n} \tag{2.2}$$

where P_{grid} is the power transferred between main grid and HEMS(kW), P_{batt} is the battery net output power(kW), $D_e(h)$ is the electrical demand at hour h(kWh), $D_{nsh}(h)$ is total power consumption of non-shift able loads at hour h(kW)and D_{sh}^{n} is the power consumption of nth shift able load at hour h (kW).

Table 2.3: Taxonomy for the Appliances Categorization

Appliances	**Category**	**Appliances Taxonomy**
Lights Stove Hair Dryer TV Computer	Category 1	Fixed Loads [263],[185] Non-Deferrable [22] Essential [136] General Appliances [154] Uncontrollable Loads [51], [174] Real-Time [21] Model-Based [92] Non-Reschedulable [9]
Dishwasher Dryer Washing Machine	Category 2	Deferrable Loads [263],[51] Non-Flexible Deferrable [22] Delay Sensitive Flexible [136] Wet Appliances [154] Schedulable [21],[221] Shift able [185] curtailable [15] Non-Interruptible [92] Type B (Soft Load) [222] Non-TCL [170] Reschedulable [9] Switching Controlled Loads [174]
HVAC Water Heater Space Heater	Category 3	Regulatable Loads [263] Flexible Deferrable [22] Delay Tolerant Flexible[136] Thermal Appliances [154] TCL [51],[170] Schedulable [21],[221], Shift able [185] [15] Interruptible Controllable [92] Reschedulable [9]
Refrigerator	Category 4	Type A (Hard Load) [222], Fixed Loads [15], Not Controlled (high Loads)[174]
EVs Vacuum Cleaner Notebook PC	Category 5	Battery Assisted [221] Type C (Soft Load)[222]

2.3.4.2 Temperature Constraint for TCLs [217]:

The energy scheduling for TCLs must be performed in such a way that the temperature (water in case of EWH and room in case of HVAC) should be maintained in the predetermined range

$$T^{\min}, T^{\max}$$

during the scheduling time window when the household is occupied.

EWH -

$$T_{outlet}^{\min} \leq T_{outlet}^{i} \leq T_{outlet}^{\max} \tag{2.3}$$

where $T_{outlet}^{\min}$, $T_{outlet}^{\max}$ are the minimum and maximum water outlet temperature in tank and T_{outlet}^{i} is the mixed water temperature in the tank at interval i.

HVAC-

$$T_{room}^{\min} \leq T_{room}^{i} \leq T_{room}^{\max} \tag{2.4}$$

where $T_{room}^{\min}$, $T_{room}^{\max}$ are the minimum and maximum room temperature and T_{room}^{i} is the room temperature at interval i.

2.3.4.3 Battery Constraints [240, 91]:

Battery level should be maintained within a certain range that is recommended by its manufacturer. Therefore, the following constraint is imposed-

$$SOC_{\min}(h) \leq SOC(h) \leq SOC_{\max}(h) \tag{2.5}$$

$$SOC(h) = E_{batt}^{h} / E_{batt}^{cap} \tag{2.6}$$

where $SOC_{\min}$ and $SOC_{\max}$ are the minimum and maximum State of charge of battery at hour h, E_{batt}^{cap} is the capacity of battery (KWH) and E_{batt}^{h} is the energy in battery at any hour. Battery maximum charging and discharging power limit can be represented as:

$$0 \leq \frac{P_{batt}^{ch}(h)}{\eta_{ch}} \leq P_{\max}^{ch} \tag{2.7}$$

$$0 \leq P_{batt}^{dch}(h) \cdot \eta_{ch} \leq P_{\max}^{dch} \tag{2.8}$$

where $P_{batt}^{ch}(h)$, P_{batt}^{dch} are battery's charging and discharging power, $P_{\max}^{ch}$, $P_{\max}^{dch}$ are the maximum battery's charging and discharging power and eta_{ch}, eta_{dch} are the battery's charge and discharge efficiency.

2.3.4.4 Charging and Discharging Constraints of EV [240]:

With Assumption that EVs can only be charged and discharged at home. Moreover, EVs are connected to home chargers as soon as they arrive home. Therefore, constraints on charging and discharging power applied to only time slots when an EV is parked at home as: For Charging-

$$0 \leq P_{ch}(h) \leq P_{\max}(h) \tag{2.9}$$

For Discharging-

$$0 \leq P_{dch}(h) \leq P_{\max}(h) \tag{2.10}$$

where P_{ch}, P_{dch} are the charging and discharging power of EV and $P_{\max}$ is the maximum power level of EV.

2.3.4.5 Grid Constraints [240]

The energy imported from the grid at each time slot must be must be upper bounded by some predetermined limit.

$$0 \leq P_{grid}(h) \leq P_{grid}^{\max}(h) \tag{2.11}$$

2.3.4.6 Phase Wise Energy requirement of Appliances [211]:

Since controllable appliances such as washing machine, dishwasher have different power requirement at each operation cycle. This constraint ensures each appliance operating cycle receives enough energy for its operation.

$$\sum_{k=1}^{m} p_{ij}^{k} = E_{ij,} \forall i, j \tag{2.12}$$

where p_{ij}^{k} is the energy assigned to energy phase*j* of appliance*i* during the whole period of time slot k and E_{ij} is the energy requirement for energy phase j in appliance i.

2.3.4.7 Power Safety [211]:

This constraint imposes an upper limit to the total energy assigned in any time slot should be always less than max energy from the grid.

$$\sum_{i=1}^{N} \sum_{j=1}^{m} p_{ij}^{h} \leq P_{grid}^{\max}(h), \forall i, j \tag{2.13}$$

where p_{ij}^{h} is the total energy required by all running appliances at hour h and $P_{grid}^{\max}$ is the maximum energy from grid at that hour.

2.3.4.8 Up Time Required to finish a task [217]:

When an appliance is turned on, it should not be turned off before the corresponding task is complete, e.g., dishwasher

$$\begin{aligned} &W_n(h) + W_n(h+1) + ... + W_n(h+TOP_n - 1) \geq \\ &(TOP_n - 1) \cdot (W_n(h-1) - W_n(h-2)), \forall h \in h_n \end{aligned} \tag{2.14}$$

where $W_n(h)$ is the operation state of n^{th} shift able load at hour h 1: on,0: off and TOP_n is the number of n^{th} shiftable load's time of operation.

2.3.4.9 Operation Ordering of Appliances [217, 171]:

it should be guaranteed that the appliances' operation ordering will be maintained. For example, a dryer should be operated after the washing machine has finished its duty. So, if the shiftable load m should be operated after shiftable load n then:

$$start_m \geq start_n + operating\_duration_n + gap \tag{2.15}$$

2.3.5 Dynamic Pricing

In recent times, the electricity market is going through a transition phase where the reduction of peak demand is one of the major objective while utilizing all the resources optimally. Several incentives have been introduced worldwide to motivate the customer by offering them several economic benefits and different electricity tariff at different load dependent intervals. Here, dynamic pricing is an inevitable component of the household energy scheduling problem, as it encourages the customer to shift their load from on-peak to off-peak period. Different pricing schemes have been employed to maintain a balance between demand and supply of energy as shown in Fig. 2.6.

2.3.5.1 Time of Use (ToU)

ToU is cost reflective electricity pricing scheme. It reflects the cost of producing electricity at different times of the day based on demand. ToU pricing is divided into three periods: on-peak, when both energy demand and cost are high; mid-peak when energy demand and cost are moderate, and off-peak when energy demand and cost are low [258].

As per the experience of ToU pricing scheme implemented in various countries such as Bangladesh [181], Irish [39], China [199], Malaysia [94], Taiwan [204] and Ontario [7]. It has been observed that ToU pricing strategy significantly affects the consumption pattern of residential consumers [267, 198].

2.3.5.2 Real Time Price (RTP)

RTP policy is dependent on the instant energy consumption of the consumer [48]. This kind of pricing scheme is very popular among the researchers as it offers enhanced economic and environmental benefits in comparison to ToU [164]. However, a real-time energy consumption with the varying cost is very challenging to implement as it requires customer active participation through bi-directional communication between consumer and service provider [38]. From the consumer perspective, it is very difficult to handle highly complex and voluminous data. On the other hand, it poses a great challenge to the service provider as the real time retail pricing affects the stability and volatility of power system [184].

2.3.5.3 Inclined Block Rate (IBR))

In IBR, the price is directly proportional to consumed power, i.e electricity price increases with increased power consumption beyond a certain limit. It is used to avoid load synchronization problems, i.e. the concentration of a large portion of energy consumption during low price hours. Here, it is pertinent to mention that in most of the cases, IBR policy is used in combination with either ToU or RTP. This is mainly done to take the benefit of both the pricing schemes.

2.3.5.4 Day-Ahead Pricing

The day-ahead market produces financially binding schedules for the generation and consumption of electricity one day ahead of the operating day [263]. In these markets, quotes for day-ahead delivery of electricity are submitted simultaneously for all hours in the next day [93]. The real-time market is usually more expensive and changes more sharply than the day-ahead market [128].

2.3.5.5 Critical Peak Pricing (CPP)

CPP is a pricing scheme similar to TOU; it provides two different prices between off-peak and peak periods to balance power demand in case it is extremely high compared with other power demand periods [109]. FCPP is declared only on days that are forecasted to have a very high power demand period, called a critical period (CP). This kind of pricing is normally used for bulk power consumers e.g heavy industrial and commercial loads. Here, customers are notified in advance of critical peak time-limited to several selected days throughout a year during which the tariffs are expected to be much higher than average.

2.3.6 Consumer Categorization

Table 2.4: Consumer Classification

Reference	Consumer Behavior		
[49]	**Selfish** (Individual utility maximizers)	**Altruistic** (Other users well-being maximizers)	**Welfare maximizers** (Whole system well-being maximizers
[156]	**Price Optimizers** (price prioritized over comfort)	**Price Sensitive** (tradeoff between comfort and price)	**Price Insensitive** (comfort prioritized over price)
[75]	**Eco Consumer** (minimum power demand from the grid)	**Average Consumer** (average power demand from the grid)	**Waste Consumer** (maximum power demand from the grid)
[85]	**Demand responsive** (responsive to changes in electricity pricing)	**Demand Unresponsive** (Do not respond to changes in electricity price)	

Consumer categorization is an imperative variable in the success of demand scheduling

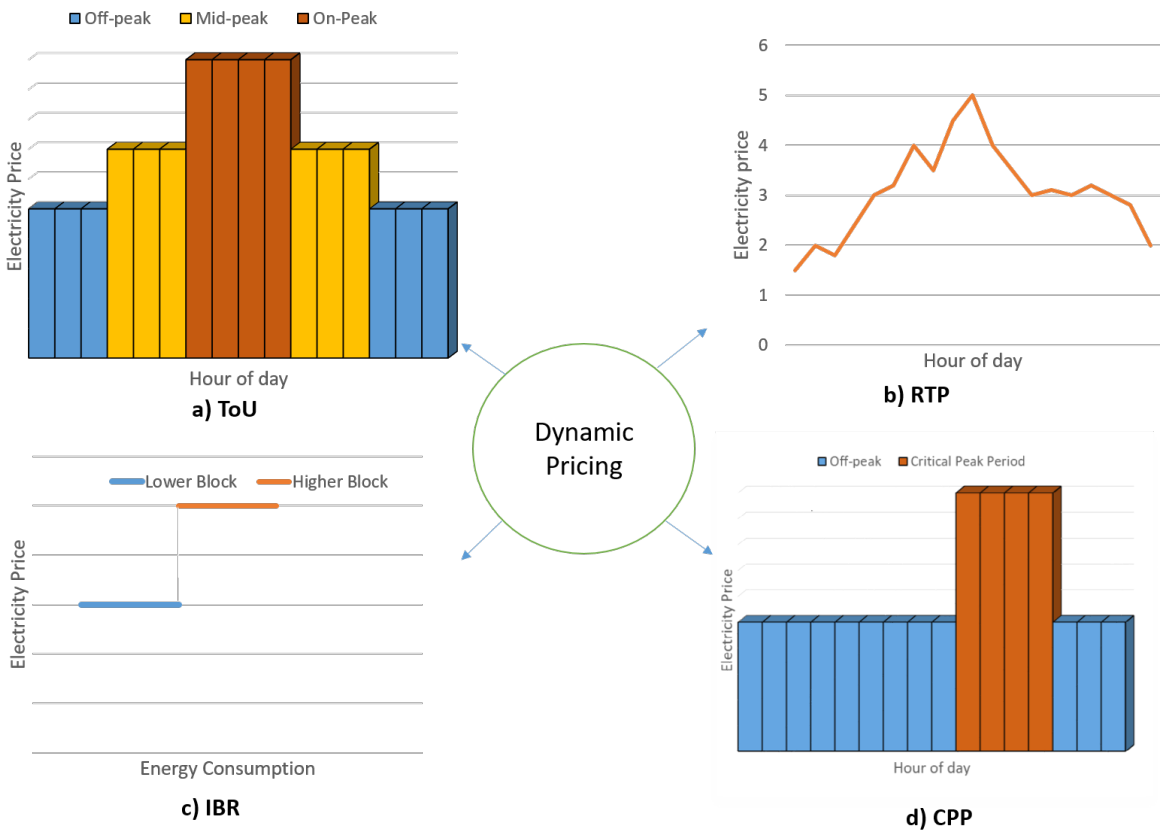

Figure 2.6: Dynamic Pricing Schemes

optimization. In order to make consumers active DR participants, their convenience should be guaranteed, by scheduling different appliances within their time and temperature limits. Consumers can be categorized based on 1) Behavior and 2) Demand. Consumer categorization based on their behavior is shown in Table 2.4.

2.3.7 Optimization Techniques

Optimized use of resources and assets enables users to efficiently manage energy consumption at home. Optimization is defined as the process of finding the conditions that give the maximum benefit or minimum cost of a process [213]. Optimization objective in published studies mainly focuses on reducing the peak-to-average ratio (PAR) in load demand and electricity cost of the consumer without disturbing the comfort. Additionally, maintaining the privacy of consumer data is an increasing need in the IoT era. Some researchers focus on a single objective while others provide solutions for solving multiple objectives, that make multi-objective optimization.

In this section, we review the various optimization techniques used in previous works. Based on the nature of expressions for the objective function and the constraints, the classification of optimization techniques is represented in Fig. 2.7.

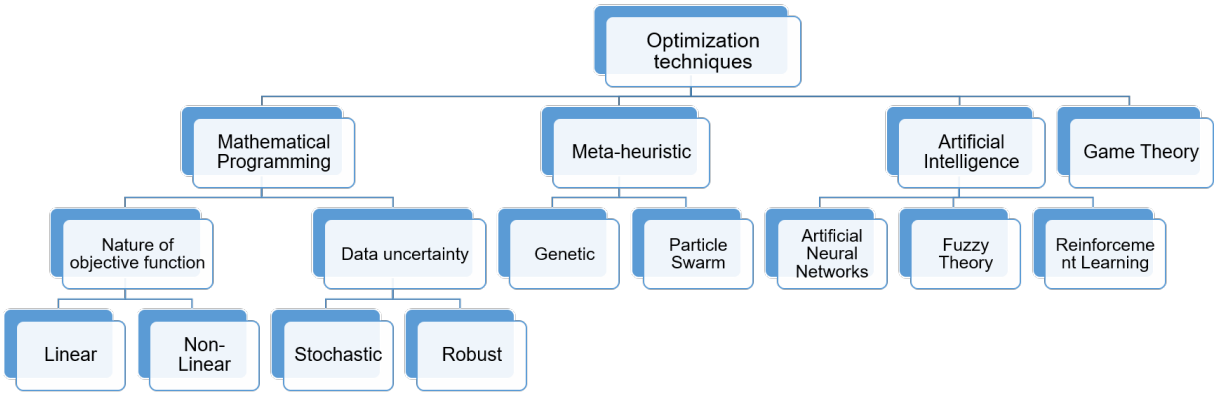

Figure 2.7: Classification of HEMS Optimization Techniques

2.3.7.1 Linear Programming

Linear Programming (LP) is an optimization technique in which objective function is represented by linear relationships of decision variables, subjected to linear inequality constraints [213]. Linear programming is said to be integer linear if all the decision variables are integers whereas Mixed-Integer Linear (MILP) if some but not all decision variables considered in problem formulation are integers. LP problem can be expressed in matrix form as:

$$minimize \qquad c^T x$$

$$Subject\ to \qquad Ax = b \qquad and \qquad x >= 0$$

where c^T, A and B are constant matrices. x is the variable (unknown).

LP optimization has been applied by many researchers for energy management optimization problems. According to the study in [38], it is the simplest technique and easily integrated into the energy management system (EMS) of the household for demand response problems.

MILP based model can be solved extremely fast and effectively using commercially available solvers such as CPLEX, Gurobi, Xpress and MATLAB. It can find global optimal solution of linear problems. It can be used to solve large and complex optimization problems. Despite these advantages, MILP formulations have some drawbacks. The non-linear constraints cannot be directly used in this model. Also, it suffers from the risk of high-dimensionality of the problem.

2.3.7.2 Non-Linear Programming

If any of the functions among objectives and constraints of the optimization problem is non-linear, the problem is called non-linear programming (NLP) problem. This is the most general form and used by many researchers in the past. The NLP optimization problem can be represented as:

$$minimize \qquad f(x)$$

$$Subject\ to \qquad g_i(x) \leq 0,\ for\ each\ i \in \{1,....,m\}$$

$$h_j(x) = 0,\ for\ each\ j \in \{1,....,p\}$$

$$x \in X$$

where n, m and p are positive integers. X is subset of R^n. f, $g_i(x)$ and $h_j(x)$ are real-valued functions on X, with at least one of them being non-linear.

The optimization problem of electricity load scheduling considering home appliances with different energy consumption and operation characteristics has been formulated as mixed integer non-linear programming (MINLP) in Ref. [183]. Generalized benders decomposition approach has been used to solve MINLP problem efficiently under ToU pricing scheme.

2.3.7.3 Stochastic Optimization

Stochastic optimization is a mathematical optimization technique that deals with maximizing or minimizing an objective function that deals with random variables or random constraints. To solve these types of problems, structural assumptions, such as limits on the size of decision and outcome spaces are required.

Stochastic optimization is intended to solve multi-objective decision-making problems under the presence of uncertainties and risks. However, they often cannot handle highly constrained optimization problems and do not offer bounds on the solution.

Stochastic optimization models have become an important paradigm in wide range of applications. Some of them are modelling renewable energy uncertainties [260], energy storage scheduling [112], traffic control [102], mobile GPS applications [24].

2.3.7.4 Robust Optimization

Both stochastic and robust optimization deals with the uncertainty of data. The difference between them lies in the fact that stochastic optimization assumes that the probability distribution of uncertain data is known/estimated. Robust optimization, on the other hand, optimizes the worst case that can occur and does have any such assumption and therefore more suitable for real-life optimization problems [73].

A distributed robust algorithm for monetary savings has been proposed in Ref. [261] for consumers with little computational complexity which provides flexibility to users as well as robust production price to the energy supplier.

The uncertain usage of manually operated appliances (MOAs) has been modeled as a robust optimization problem to avoid the risk of high electricity payment caused by MOAs' [45]. Robust modeling helps to consider the worst-case scenario to minimize the electricity cost of all home appliances using combined RTP-IBR. Computationally efficient inter generation projection evolutionary algorithm (IP-EA) has been utilized which is a nested heuristic algorithm with an inner GA and outer PSO algorithm.

Some of the examples of application areas of robust optimization includes modelling profit uncertainty of electric vehicles aggregators [10], optimum bidding strategy for compresses air

energy systems (CAES) [40], agriculture sector [244], optimization of solar-based Organic Rankine cycle (ORC) systems [173], Production scheduling [62].

Table 2.5: Main Features of Some Research works on DSM Optimization

Ref.	No# of appliances	Pricing Scheme	Technique	Cost Saving(%)	Load Categorization	RE Integration	User Comfort	Time Granularity
[139]	2604	Day-ahead	Heuristic-based algorithm	5% cost reduction	Y	N	Y	60 min
[164]	5	RTP	Stochastic optimization	Cost saving graph	Y	Y	Y	15 min
[9]	6	Day-ahead	Linear	36%	Y	N	N	15 min
[15]	11	RTP	MINLP	25%	Y	Y	Y	60 min
[170]	17	hourly	MILP	Different scenario analysis in different conditions	Y	Y	N	5 min
[171]	5 (shiftable)	ToU	MILP	11.3%	Y	N	Y	15 min

[193]	16	RTP+IBR	Stochastic Optimization	22% PAR reduction	Y	N	N	60 min
[156]	4	Hourly price	Probabilistic, Fuzzy and Genetic Algorithm	11.08 increase in profit of the retailer	Y	Y	N	60 min
[124]	10	Hourly	Linear programming	38%	N	N	N	60 min
[32]	6	RTP	Stochastic optimization	26.63%	Y	Y	N	5 min
[196]	5	ToU and RTP	Stochastic optimization	42%	Y	Y	Y	60 min
[155]	18	RTP	Robust Optimization	106.89 cents	Y	Y	N	60 min
[45]	14, no TCLs	RTP+IBR	Robust Optimization	9%	Y	N	N	12 min
[232]	6	RTP	Robust optimization	Comparison with another method	Y	N	Y	10 min

[192]	15	RTP-IBR	probability based algorithm	25.5%	Y	N	N	15 min
[149]	6	Day-ahead	Mathematical optimization using Dinkelbach method	11.60 increase in cost efficiency	N	Y	N	60 min
[144]	8	ToU	MINLP	34.71%	Y	N	Y	60 min
[229]	7	RTP	Stochastic Optimization	11%	Y	N	N	60 min
[235]	TCL	RTP	Fuzzy and PSO		Y	Y	Y	60 min
[97]	10	RTP	Genetic Binary PSO	36%	Y	N	N	1 day
[59]	5	ToU	Improved Enhanced Differential Evolution (iEDE) Algorithm	33%	Y	Y	Y	60 min
[69]	10	Day-ahead	Heuristic Forward-Backward Algorithm (F-BA)	18% to 25%	Y	Y	Y	60 min

[141]	9	CPP	Multi-objective mixed integer linear programming technique (MOMILP)	$138 yearly	Y	Y	N	30 min
[3]	10	RTP & ToU	Quadratic Binary PSO (QBPSO)	37.9%	Y	N	Y	10 min
[159]	7	ToU	Grey Wolf Optimization	16.8%	Y	Y	Y	12 min

2.3.7.5 Meta-heuristic

Meta-heuristic algorithms are heuristic and population-based soft computing algorithm which can find a global solution of NP-hard problems in a computationally efficient way by taking comparatively less execution time as compared to mathematical optimization solutions [163]. Many examples illustrated in literature focusing on meta-heuristic algorithms to solve the DR optimization problem.

The particle swarm optimizer (PSO) has been used in the central controller to optimize the set-point temperature of TCLs based on outdoor environmental information and customer preferences [235].

Uncertainties in electricity price and system loads are modeled as chance constraint optimization-based model in Ref. [91]. Gradient-based PSO and two-point estimate methods are employed to find optimum solutions.

The main advantages of meta-heuristic techniques are ease of implementation, handling non-linear or discontinuous objectives and constraints, solving high-computational complex problems. But the problems with using meta-heuristic algorithms are that they can converge prematurely and get stuck in a local minimum, particularly for complex problems. These algorithms are time-consuming for problems with large number of variables.

The diversified application areas of meta-heuristic algorithms include PV cell modeling and analysis [247], optimum sizing of hybrid RESs [11], sensors temperature prediction [118], scheduling charging of hybrid electric vehicles [13], software effort estimation [66].

2.3.7.6 Artificial Intelligence

The artificial intelligence is a field in which machines are trained to be intelligent and perform functions related to human intelligence [127]. Many researchers in the past used artificial intelligence for intelligent decision making, prediction, forecasting, and scheduling.

AI has ability to work with sparse data, parallel processing, making better decisions through learning, pattern recognition and solving non-linear functions with arbitrary complexity. It suffers from some disadvantages as well. Hardware with parallel processing power is required to run AI models. It can work with numerical values only. Validation and verification

Table 2.6: Different Optimization Objectives and Techniques Used with Price Variant

ObjectiveTechnique	Linear programming	Mixed integer Non-linear	Stochastic optimization	Robust optimization	Meta-Heuristic algorithm	AI-based algorithm	Game theory	Others
Cost minimization	[9][5] [170][2] [32][2] [222][3] [211][2] [17][8] [55][2]	[183][1]	[251][2] [229][2] [130][2]	[45][4] [261][2]	[156][5] [91][2] [176] [5]	[85][1] [111][2] [241][2]	[261][2] [224][6] [26][8] [194][8]	
Cost minimization and Comfort maximization		[15][2]	[164][2] [196][9] [255][2]	[232][5] [155][2] [232][2]	[235][2]	[29][8] [238][2] [178][1]	[245][8] [126][1]	[143][8]
PAR Reduction	[124][2]					[179][1]		
Cost minimization and PAR reduction	[250][8]		[193][4]	[135][2]	[139][5]	[75][1]	[208] [134][7] [223][8]	
Cost minimization and Privacy preserve		[249][1]					[20][8] [185][8]	

[1] ToU; [2] RTP; [3] IBR; [4] RTP+IBR; [5] Day ahead Price; [6] Price/unit enrgy(UTP); [7] RTP+ToU; [8] Price Function; [9] ToU+RTP+CPP.

of AI model require extensive testing with hardware.

The application of AI has made significant progress in many fields. Some of them are consumer comfort optimization [80], decentralize healthcare systems [138], AI-guided chatbots [14], recommendation systems [218] and Natural language processing [116].

2.3.7.7 Game Theory

Game theory for solving optimization problems in a distributed environment is recently gaining attention among researchers. This technique is mainly used in situations where selfish and rational consumers need to make decisions under uncertain environmental conditions [166]. Local energy trading (buying and selling of energy)in a smart grid environment is mainly implemented by the game playing approach [175].

A game model with real-time price for demand response in a household equipped with solar panels has been proposed by [214, 256]. Ref. [214] uses the model predictive control (MPC) based approach whereas Ref. [64] uses Stackelberg game approach for real-time price-based demand response. The Stackelberg game approach is used as a solution for energy trading problem to maximize the sum of benefits of all participant consumers [256]. This approach encourages active consumer participation in the demand response environment by incentivizing them. Energy trading between competing users in a distributed environment with the integration of renewable energy using game playing has been proposed in Ref. [194]. It reduces the effect of reverse power flow problem by encouraging users to consume their excess generation locally.

A fair and optimal billing mechanism among consumers has been proposed using game theory [20]. Also, a secure sum algorithm has been used to preserve the user's privacy in a distributed environment. A distributed privacy- friendly DSM has been proposed in Ref. [185], which overcome the problem of information leakage by sending a noisy version of the power demand profile.

Game Theory is a quantitative technique for solving problems where there is interdependence among decision makers and others' to arrive at optimal strategy. Hence, it can be used to decide the best strategy in competitive situations, therefore helps in rational decision making. However, Game theory becomes difficult to solve when there is increase in the number of players involved. Also, it does not tell about the winning strategy but uses only general rules of

logic. Uncertainty in the actual field is difficult to model using this technique.

Game theory has been extensively used in literature. The application areas include setting optimal selling price of micro grid [110], privacy preservation in IoT environment [182], Cyber-security and cloud computing [105], manage security issues in Block chain [137], production research and operational management [34].

2.3.8 Some brief comments related to the optimization techniques

From Table 2.5 and 2.6, it can be deduced that among mathematical programming techniques, most of the researchers have used MILP as nature of multi-objective optimization problem. The reason is, many commercially available solvers exist which can easily find the global optimal solution efficiently and quickly as compared to MINLP. Efficient linearization methods have been considered to avert the non-linear nature of the established model to a linear one. In the case of data uncertainty category, stochastic optimization has been mainly used to solve at most two objectives with the minimum number of constraints. On the contrary, robust optimization (RO) approaches have been widely used to find optimal and feasible solutions for uncertain scenarios such as uncertain usage of manually operated appliances (MOAs), user behavior uncertainty, market price uncertainty, renewable power generation uncertainty, etc. It has also been used to solve load scheduling problem considering many objectives and constraints. One common critique of RO is its over-conservative solutions, given that RO in its original formulation considers all potential deviations of the uncertain coefficients. The algorithms under meta-heuristic category have been mainly compared based on their convergence rate and accuracy of optimal solution where PSO and GA are found to be most popular. As per study in Ref. [81], a comparative study of GA and PSO in terms of solution quality and efficiency has been conducted. Algorithms are tested for 12 different bench-mark functions. Results show that the solution quality of both algorithms is 99% or more, with 99% confidence interval. However, in terms of efficiency, PSO is found to be better than GA. As per the study conducted by Ref [128] and [87], optimization-based DR algorithms appears to be more efficient than heuristic algorithms in terms of computational efficiency. From Fig. 2.8 it can be deduced that mathematical optimization is mostly used by researchers than all other algorithms from 2014 to till date. It has also been found that an optimal solution obtained using heuristic algorithm could be

local optimum solution, indicating a potential need for advanced algorithms that can guarantee a global optimum solution. Artificial intelligence based algorithms are primarily used for learning consumer behavior, market price trend, optimize battery charging requirements. Under this category, machine learning and deep learning algorithms have been proposed for forecasting of renewable energy yield, load demand and market price. On the other hand, fuzzy theory have been mainly employed to model uncertain characteristics of TCLs. As per study conducted in Ref. [109] artificial intelligence based forecasting models have greater ability to deal with non linearity of the input data. But, expensive hardware with parallel processing is required to use machine learning and deep learning techniques. Game theory based algorithms mainly used for energy trading in distributed environment. It has gained the most popularity in 2014 and still used by many researchers. However, this algorithm is difficult to implement in large network scenarios with many uncertainties.

Hence, depending upon the optimization problem, constraints involved, simulation scenarios appropriate category of optimization algorithm may be chosen.

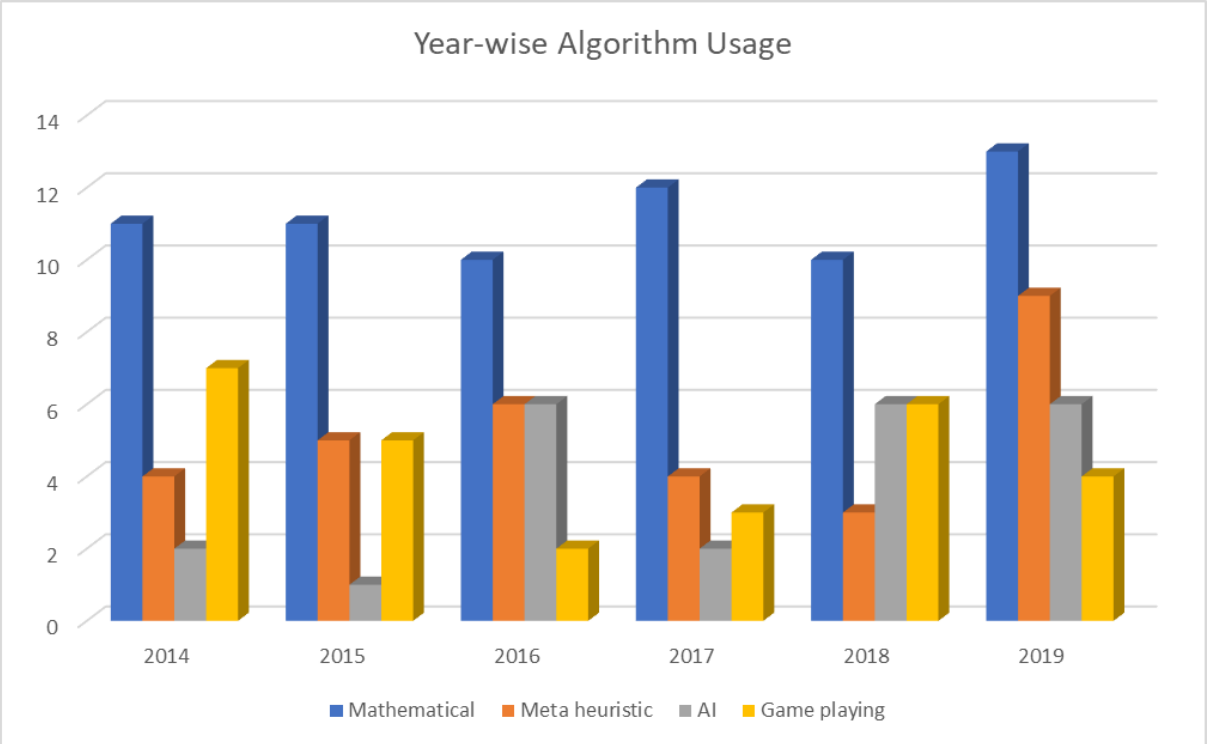

Figure 2.8: Year-wise usage of algorithms in all categories

2.4 DSM Implementation Challenges in distribution network

In this section, various issues related to DSM implementation with the distribution network are described in detail.

2.4.1 Grid Constraints

The DSM implementation raises the complexity of existing power systems operation and reliability because the appropriate performance of DSM requires monitoring distribution losses and voltage imbalance issues. Moreover, the integration and utilization of DG sources also responsible for the concern of voltage and frequency stability in the distribution network. Therefore, it has become crucial to investigate the impact of inappropriate load scheduling and DG sources integration on distribution system reliability while implementing DSM. The widespread use of RESs introduces new challenges to power systems such as finding their optimal location, voltage regulation, and other Power Quality (PQ) issues.

The optimization algorithm implementing the DSM must consider the network constraints (frequency and voltage disturbances) in the distribution network due to inappropriate scheduling of different types of loads. The optimal locations, sizing of DG, and other grid constraints must be taken into account while development of an appropriate optimization algorithm.

2.4.2 Incentivising Consumer Participation

Incentive based DR programs provide opportunities for consumers to reduce their energy consumption during peak demand periods and encourage energy self-sufficiency. The incentives are established by utilities, load serving entities, or regional grid operators. These incentives may be fixed (based on average costs) or time-varying. Diverse research has focused on developing optimal incentives or rewards for consumers participating in Incentive-based DR (IBDR) programs. A study in Ref. [140] evaluates the usefulness of two types of incentives on consumption behavior of the consumers. These two types of incentives are 1)Rebate and 2) Lucky

Draw, which were investigated for residential, industrial and commercial customers. It was found that, for residential customers, a 5% rebate can incentivize the customers as much as a lucky draw with $10 payouts. The rebate was found to be a more effective method for residential participation as compared to Lucky draw because of its low implementation cost.

However, despite many efforts in setting optimal incentives for benefit ting both service providers and consumers, some significant limitations remain. Considering the heterogeneity of real-world customers and their different consumption patterns, it is desirable to develop innovative incentive-based DR mechanisms for real-time demand response market. A scalable, flexible, adaptive, and easy to implement comprehensive algorithm is desirable rather than conventional techniques such as MILP or game theory which can describe consumers' response related to incentives.

2.4.3 Utility Policy and Regulatory frameworks

Utility Policies have a great impact on the rules for competition in the smart grid era. It directly affects the market structure for businesses and consumers to take part effectively in the energy market. It also plays a potential role in transforming energy demand. Researchers and policy-makers, need to develop a better understanding of how energy demand might be made governable, and revisions of non-energy policies to help steer long-term changes in energy demand [188]. Both utilities and regulatory bodies should reassess the way of providing services to consumers. New products and services need to be designed that minimize the transaction costs of exchange. Moreover, utilities should ensure that the network operates at all times within the specified limits as it is desirable for implementing constraint management. For some utilities, constraint management is implemented through either direct communication with potential providers or through an invitation to tenders to change their generation outputs. A flexible exchange strategy has been designed in Ref. [131] which ensures the network constraints are met with minimum power variation from customers. Nonetheless, efforts need to be made to eliminate the regulatory, business, and technology obstacles that many countries face, and to develop successful awareness initiatives to enhance DR's consumer acceptance. The author in Ref. [119] studies the current policy implication on balancing demand and supply using variable renewable energy sources (vRES) in the residential sector.

2.5 Conclusion & Future Work

This chapter reviews the major challenges involved in the optimization problem involving DSM using load shifting in IoT enabled HEMS. It also discusses the detailed architecture of IoT enabled HEMS. Different dimensions of stochastic and highly complex optimization problem of DSM in HEMS have been highlighted while including the load profile of appliances, RES integration, load categorization, constraints, dynamic pricing, consumer categorization, and optimization techniques.

Although DSM in the smart grid has been extensively studied, more research is imperative to solve this problem in real-time, using efficient communication techniques, accurate forecasting and optimization algorithms. Further, the uncertainties in the dynamics of energy consumption pattern of the consumer, his preferences, his response to dynamic real-time pricing and inaccuracy in the prediction of renewable energy make it a highly complex problem. Future research directions are suggested for the development of a more efficient multi-objective real-time optimization algorithm considering all the uncertainties and constraints.

Most of the researchers have focused on cost minimization, comfort maximization, PAR reduction, and preserving the consumers' privacy without considering the risk management. The risk management process is a critical issue that must be addressed. Therefore, it is recommended to consider the risk minimization as an additional objective to the problem formulation.

A detailed study regarding the categorization of different loads based on their operational behavior has been presented on case to case basis. However, the standardization of load categorization may greatly help in solving the optimization issue of DSM.

While it is possible to design a pricing mechanism, i.e., a control law that regulates the interaction of wholesale markets and retail consumers. In light of this, systematic analysis of the implications of different pricing mechanisms, inherent dynamics of the system induced by load-shifting and storage need to be considered. Further, the characterization of the fundamental trade-offs between volatility/robustness/reliability, economic efficiency, and environmental efficiency are important directions for future research.

Consumer participation using load shifting in the HEMS is made possible by implement-

ing distributed generation in HEMS environment. The accurate forecasting of the energy produced by such resources may help the consumer in the efficient management of their load and energy demand. However, planning an efficient HEMS power environment requires consideration of these resources at the design stage itself. Techniques for determining optimal sizing and accurate modeling of the PV panels, wind turbines, and battery storage are required for the optimal utilization of available resources.

Since different types of optimization algorithms have their pros and cons, its the responsibility of the developer to choose appropriate category and algorithm considering objectives, constraints, consumer load profile, price-type, simulation scenarios, hardware availability, etc. MILP is the most popular modeling technique among all others as it is easy to implement and computationally inexpensive. Researchers can work upon an ensemble of different categories to develop the most suitable algorithm having all required characteristics such as ease of use, computationally efficient, ability to model complex problems considering all types of constraints (linear and non-linear).

The appropriate DSM implementation should also take care of challenges related with the distribution network. The frequency and voltage stability issues, incentive management, and Government policy requirements should be taken into consideration. Researchers should focus on bi-directional implementation which includes appropriate locations of DGs at the residential site and Grid related concerns.

The increasing penetration of IoT enabled devices in the HEMS environment also poses a huge challenge in terms of handling voluminous data, its manipulation and its transfer over a communication network. Although, fog and edge cloud computing are becoming a promising problem solver, the issues related to security, reliability, compatibility and the interoperability of IoT devices require consideration. Therefore, there is a need to focus on the standardization of IoT devices to ensure efficiency and adequacy of the entire framework.

Chapter 3

Renewable Energy Forecasting using Deep Learning Model

3.1 Introduction

Increasing use of clean energy intensifies the development of more accurate and robust solar irradiance forecasting models. Many countries around the world have begun replacing fossil fuels with renewable energy sources due to their sustainable nature. 5% of the African and 2% of the Asian population have been estimated to access electricity through off-grid solar photovoltaic systems[162]. Solar power will account for 20% of all US electricity production by 2030, and photovoltaic utility capacity is expected to increase by 127 GW [2]. India plans to almost double its installed total capacity for renewable energy to 40% by 2030 [5]. Although the globally installed photovoltaic capacity (PV) is projected to exceed 8,519 GW by 2050, providing about 25% of the worldwide electricity. China, the world's leading photo voltaic installer, plans to produce 1300 GW of solar power by 2050 [4]. However, the intermittent nature of photovoltaic energy remains a great challenge, and accurate forecasting is required to

ensure reliable power grid operation.

The era of smart grids has required the adoption of photovoltaic energy in households to mitigate high market energy prices. Since solar PV power output is derived from solar irradiance, thus it generates greater interest in solar irradiance forecasting. Furthermore, it also helps optimize demand-supply management, better economic dispatch, peak shaving, energy arbitrage, energy market trading, and reducing uncertainty impact [30]. However, the stochastic and intermittent nature of solar irradiance makes it inherently challenging to predict accurately.

Due to the wide applications of solar forecasting, various methods have been proposed to solve the challenging problem. There are two types of forecasting methods proposed in the literature: Point forecasting and Probabilistic forecasting. Point forecasting methods only tell about the future predicted values of solar irradiance whereas probabilistic forecasting provides both expected values and probability distributions at forecasting time points. Point forecasting models can be classified as statistical and machine learning models. Statistical models include Auto-regressive Moving Average (ARMA) [98], Lasso [248], and Markov models [197, 101]. Machine learning models [230] include support vector machine (SVM) [262, 19, 61], feedforward neural network (FFNN) [12, 33, 216] and Recurrent Neural Network (RNN) [212].

Previously, statistical models were widely used for time series forecasting; but, with the advent of complexities in power systems and rapid increase of data volumes, deep learning (DL) techniques are outperforming statistical models. These techniques work by learning the stochastic dependency between the past and future with less computational cost.

In recent years, RNNs based on long-short-term memory (LSTM) [82] have become the de facto solution to deal with multivariate time series data. LSTMs are effective at exploiting long-range dependencies and handling nonlinear dynamics in time-series forecasting. In [6], LSTMs have been used to forecast PV power output at multi-horizon (1 hour, 1 day, 1 month) using PV power as the only input parameter on datasets of two cities in Egypt. The authors in [212] and [180] have also used the LSTM model for solar irradiance prediction using meteorological parameters as input to predict one hour and one month ahead solar irradiance, respectively. Hybrid Convolutional LSTM (CNN-LSTM) model has been deployed to predict PV power in [234] which outperforms LSTM in the next 5-minute prediction.

Recently, *A Vaswani* [228] proposed a Transformer deep learning model for sequence

modeling and has achieved great success. The benefit of using the self-attention approach on RNN models is three-fold: (i) *Memory*: since attention models dispense recurrence entirely, they have less memory requirements compared to recurrent models (LSTM), they can also make predictions using a very long sequence of past data, whereas LSTMs rely solely on short-term memory to make predictions; (ii) *O*ptimization: attention models are mathematically simpler than recurrent models; (iii) *Computation*: attention models are fully parallelizable, hence they accelerate learning during training and take less computation resources compared to recurrent models which are inherently sequential. The deep learning Transformer model has been implemented successfully in many areas such as translation, music, and image generation [42, 89, 169]. Some transformer-based, deep learning forecasting approaches for time-series forecasting have recently been proposed [129, 150]. However, most of the work based on the transformer model is limited to data sets of traffic, retail, and electricity.

To take into account the uncertainty associated with the forecast, a prediction interval around the forecast value must also be provided. This mitigates the risk associated with point forecasts by providing more information that would assist dispatchers in better decision-making. A few experiments on probabilistic forecasting have been carried out in recent years. In [30] a combined probabilistic forecasting method based on an improved Markov chain model has been proposed for probabilistic forecasting of PV power. However, this method involves a lot of complexity in modeling and may not be suitable for a large sample size. A probabilistic forecasting model based on joint probability distribution function (PDF) of irradiance has been proposed in Ref. [104]. The proposed model is predicted by numerical weather prediction (NWP) and its applications in the electric power trading market have been extensively studied. But the performance of NWP for solar radiation forecasting is highly variable when applied to different locations and not suitable for short-term forecasting [115]. A quantile regression-based probabilistic model for spatiotemporal PV forecasting has been presented in [8] for very short term horizons (0-6 h). It uses LASSO for probabilistic forecasting on real-world test cases with a high number of PV installations.

Therefore, the intermittency in solar irradiance and the complexity of mapping it with weather metrics make it a typical multivariate time series forecasting problem. The outstanding performance of the Transformer model and its capacity to comprehend complex links between weather metrics and solar irradiance intrigues us to use the model for multi-step ahead solar

forecasting. Also, quantile regression-based prediction interval modeling is used to calculate the corresponding lower and upper bound for each forecasted global horizontal index (GHI) value (point forecast).

The main innovations and contributions of this chapter are:

1. Leveraging the powerful learning ability of self-attention-based Transformer deep learning model for forecasting solar irradiance.

2. To combat the risk of prediction, the prediction intervals (50%, 90%, 95%) have been calculated for each predicted value using quantile regression.

3. Multi-horizon forecasting on all industry requested time horizons: Intra-hour, Hour-ahead, Day-ahead as stated by Kostylev and Pavlovski [115].

4. The proposed algorithm is applied to the data set available on the site of the National Renewable Energy Laboratory (NREL) and its performance is rigorously evaluated through various prediction parameters.

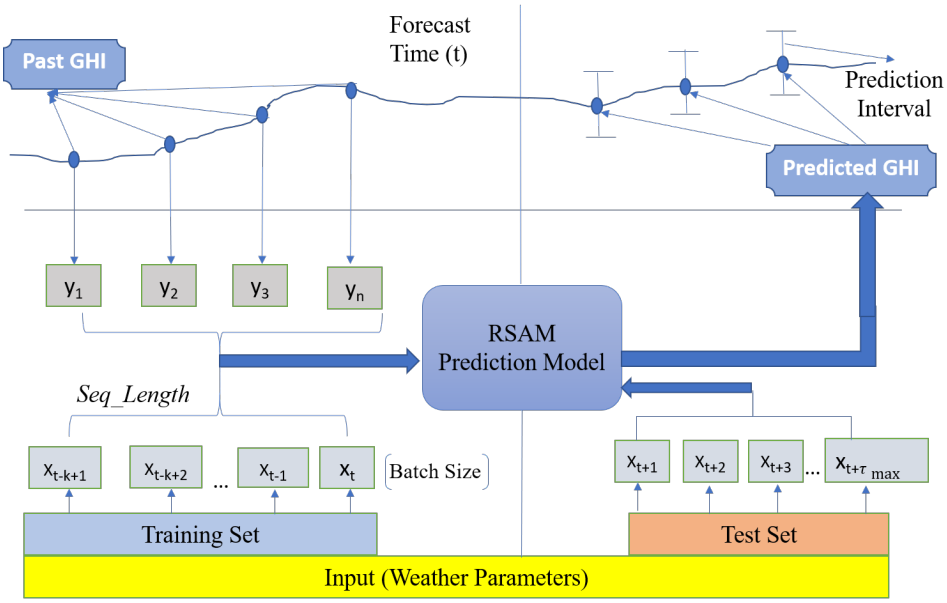

Figure 3.1: Illustration of Multi horizon forecasting with Point forecasting of GHI and their corresponding prediction intervals

3.2 Background

3.2.1 Problem Definition

The problem of solar irradiance forecasting can be depicted as multi-variate time series forecasting. The time series of GHI prediction depends on multiple weather parameters (such as temperature, humidity, clear sky index etc.). Therefore, this paper mainly deals with the robust multi-horizon forecasting of solar irradiance as depicted in Fig. 6.1. Let S be the set of unique entities in the data set considered. Formally, a sequence of time series $S = [s_1, s_2, \ldots\ldots\ldots, s_n]$ defines each element s_α in the data set with its associated features $X_{\alpha,t} \in$ and output $GHI_{\alpha,t} \in$ at each time step $t \in [1, T]$. Input features can be subdivided into two categories $X_{\alpha,t} = [o_{\alpha,t}, v_{\alpha,t}]$ i.e. observed inputs $o_{\alpha,t}$ which are measured at each time step (e.g. weather parameters) and $v_{\alpha,t}$ time-based vectors which are assumed to be predetermined (e.g. month, day-of-the-week at time t).

For multi-horizon forecasting, we are going to predict next τ time steps of GHI starting from forecast time t where $\tau \in \{1, 2 \ldots \tau_{max}\}$ and it can be represented by following conditional probability distribution:

$$p(GHI_{t+1:t+\tau} | GHI_{1:t}, X_{1:t}, \phi)$$

where ϕ denotes the learnable parameters.

To ensure the robustness of the model, prediction intervals are calculated as an indication of likely best and worst-case values that GHI can take as illustrated in Fig. 6.1. We use quantile regression to our multi-horizon forecasting (e.g. 50^{th}, 90^{th} and 95^{th} percentiles are calculated at each time step). The quantile forecast output can be represented as:

$$GHI(q, t, \tau) = f(q, \tau, GHI_{t-w:t}, o_{t-w:t}, v_{t-w:t+\tau})$$

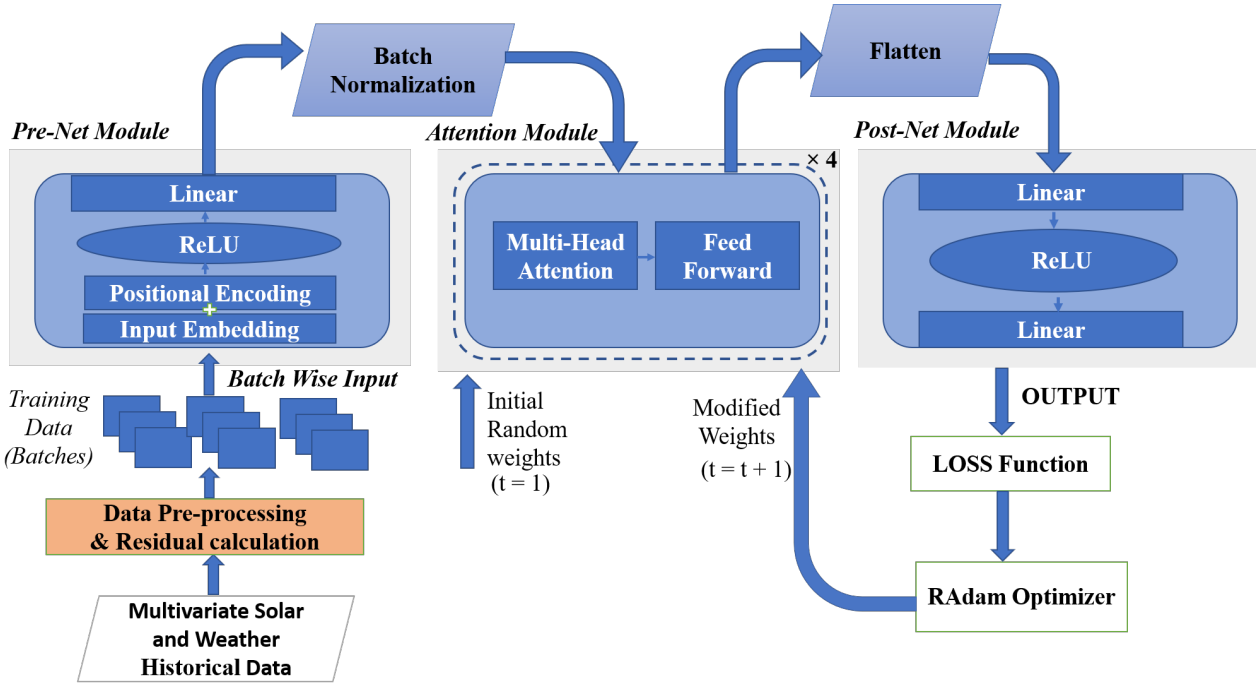

Figure 3.2: Training Phase of RSAM Model

where $GHI(q,t,\tau)$ is the predicted q^{th} sample quantile of the τ step ahead forecast at time t. The prediction model f incorporate all past information within a finite look-back window w, using GHI values and weather parameters (o) uptil forecast start time t and known temporal inputs (v) across entire range.

3.3 Solar Ir radiance Forecasting Model based on Self Attention

In this section, the proposed RSAM model has been presented, which utilizes the multi-head attention mechanism for multivariate solar time-series modeling and forecasting. The effectiveness of RNNs has been established in solar time series prediction problems. In this paper, we are interested in studying the efficacy of attention models for forecasting GHI values at various time horizons, dispensing recurrence entirely. The self-attention enables the transformer to capture both long and short-term dependencies, and different attention heads learn to focus on different aspects of temporal patterns. These advantages have made the transformer a good candidate for time series forecasting.

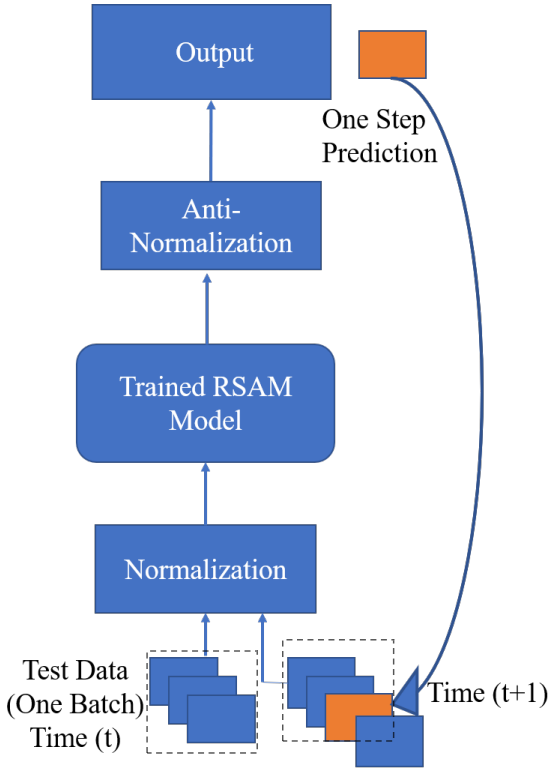

Figure 3.3: Testing Phase of RSAM Model

The modeling process of RSAM is divided into two steps: First, forecasting GHI values at different horizons (point forecasting); Second, determining the prediction interval for each GHI point prediction. In the first step, the historical weather parameters have been used to forecast solar irradiance at different time horizons using the transformer deep learning model. This step can be further divided into three phases: 1) Data preprocessing and residual calculations, 2) Model Training, and 3) Testing phase. In the second step, to enhance the robustness of our proposed model, prediction intervals have been calculated using quantile regression for each forecasted value.

3.3.1 Forecasting Model Architecture

The RSAM forecasting part uses self-attention based deep learning architecture because of its inherent advantages over recurrent models in terms of memory, computation resources, parallelizability, and simple implementation. The data preprocessing, training and testing phases of the RSAM model are illustrated in Fig. 3.2 and described as follows:

3.3.1.1 Data Preprocessing & residual calculation

Data preprocessing is used to remove the seasonal and temporal dependency on GHI values. Various types of residuals (year_residual, month_residual, day_residual, GHI_residual) are calculated over the training data, that encapsulate information relatively (relative to original data). These residuals represent yearly, monthly, daily, and time-of-day average deviation of GHI values from previous years, months, days, and time-of-day of the data set respectively. These residuals adjust the variability (bias) in GHI values and accelerate the learning process of the deep learning model. The following procedure describes this step in detail:

procedure DATA PREPROCESSING

y_r: *year_residual*

m_r: *month_residual*

d_r: *day_residual*

$GHI\_residual$: new (processed) GHI values

Require:

t: Time [year, month, day, hour, minute]

D: Training dataset indexed by 't'

Original GHI(t): GHI at time 't'

Ensure: $y\_r, m\_r, d\_r, GHI\_residual$

for all $t \in D$ **do**

$y\_r(t) = GHI(t) - Avg_D(GHI)$

end for

for all $t \in D$ **do**

$m\_r(t) = y\_r(t) - Avg(y\_r(t'))$ where

$t'[month] == t[month]$

end for

for all $t \in D$ **do**

$d\_r(t) = m\_r(t) - Avg(m\_r(t'))$ where

$t'[month, day] == t[month, day]$

end for

for all $t \in D$ **do**

$GHI\_residual(t) = d\_r(t) - Avg(d\_r(t'))$ where

$t'[month, day, hour, minute] == [month, day, hour, minute]$

end for

end procedure

After training of model gets completed, the testing phase predicts GHI values at different steps, these predicted GHI values again shifted to original GHI values by reversing the pre-processing steps using saved "yearly", "monthly" and "daily" residuals.

3.3.1.2 Training Phase

In this phase, training data is first divided into batches with a sequence length of m samples each. These batches are fed as input to the Pre-Net module. In the Pre-Net module, each sample is processed by input embedding to capture dependencies across different weather parameters and their effect on GHI. Similar to the embedding with words in NLP, here measurements at each time-step are mapped into a high-dimensional vector space to facilitate the actual sequence modeling [113]. To obtain d-dimensional embeddings for I measurements at each time step t, where $d > I$, the 1-D convolution layer has been employed which is parameterized by the kernel of size 1. To incorporate the information about the temporal order of the sequence in recurrence-free architectures, positional encoding is used. Using positional encoding, the sequence order information has been included by mapping time step t to the same randomized lookup table during both training and prediction. Here, the sequence order information is the information about the relative temporal position of measurements with respect to the predicted value. Hence, it allows the multi-head attention to learn the dependency of predicted values on the measurements based on their relative temporal position. The positional encoding is then added position-wise to the input embedding with the same dimension. Then, the data is processed using the Rectified Linear Unit (ReLU) activation function. Lastly, the linear layer is used to transform the dimensions of data to prepare it for input to the Attention module. Before sending data to the Attention module, each sample in data is normalized using the standard batch normalization procedure.

For sequence length m, the input to the attention module is the matrix having rows initialized with d-dimensional embeddings of the measurements at each position of the sequence $I^o \in^{m \times d}$. Multi-headed self-attention module iteratively compute representations I^t at step t for

all m positions in parallel using multi-headed dot-product self-attention. It works by calculating the attention score of each sample in the input sequence. To enhance accuracy in output prediction it gives high priority and weights to specific samples having a comparatively high attention score. Refer [228] for the detailed architecture of Transformer encoder. The first step in calculating self-attention is to generate three vector representations for each input sample. So, for each sample, a Query vector (Q), a Key vector (K), and a Value vector (V) are created by multiplying with their respective weight matrices as shown in equation 1. The weight matrices are first initialized with random weights and then optimized during the training process. In the proposed model Q, K, V all correspond to input embedding of the sequence (with positional encoding). In the second step, attention scores are calculated by taking the scaled dot product of the query vector with the transpose of the key vector of the respective sample. For node pair (a,b) from a to b in consecutive hidden layers of deep learning network with node $x_a, x_b \in^n$, all three vectors and score of their connection is calculated as follows:

$$Q_b = W^Q \cdot x_b, \;\; K_a = W^K \cdot x_a, \;\; V_a = W^V \cdot x_a \tag{3.1}$$

$$score = Q_b \cdot K_a^T \tag{3.2}$$

where

$$W^Q \in^{\frac{d \times d}{K}}, W^K \in^{\frac{d \times d}{K}}, W^V \in^{\frac{d \times d}{K}}$$

input sequence $I^0 \in^{m \times d}$, m is the sequence length and d represents dimensional embeddings.

These scores are then divided by the square root of the key vector dimension (K_{dim}) to obtain stable gradients. Then, the softmax operation is applied to normalize the scores so that they are all positive and add up to 1.

$$Attention(Q,K,V) = softmax \frac{score}{\sqrt{K_{dim}}} V \tag{3.3}$$

The next step is to multiply each vector value by the softmax score to maintain the values

of the sample, to focus on and to drown out inappropriate samples. Then, all weighted value vectors are summed up to produce the output of the self-attention layer at this position. In multihead self-attention (MHSA), the self-attention mechanism is replicated to multiple heads (h), allowing each head to attend different query, key, and value matrices. So, the output of the h heads of output dimension d_h are concatenated and projected to dimension d_{model} as follows:

$$MHSA(I^t) = Concat(head_1....head_h)W^o. \tag{3.4}$$

where W^o is the weight matrix of the learnable weights that is multiplied by the concatenated result of all heads to produce the final result of attention. The state I^t is assigned to queries, keys, and values with affine projections using learned parameter matrices:

$$head_\beta = Attention(I^t W_\beta^Q, I^t W_\beta^K, I^t W_\beta^V)$$

The proposed model adopt h = 4 parallel heads.

The output of the multi-head attention is passed to a fully connected feedforward network to obtain a vector representation for t. The purpose of the feed-forward network is to learn about context using information from surrounding samples. In the proposed model, the inner dimension of the feed-forward network is taken as 2048, the dimensionality of input and output of the transformer encoder (*d_model*) is 20, the value of the dimensional embeddings *(d)* is 32, and four stacked transformer encoders have been utilized.

The output data from the attention module is passed through a flatten layer which reshapes the input vector to have a shape that is equal to the number of elements contained in the vector. Concatenates all dimensions of the input vector into one output, as shown in equation 3.5:

$$(m, 1, d\_model) \rightarrow (m * d\_model) \tag{3.5}$$

The output from this layer is fed to the Post-Net module, which consists of a linear layer that is used to reshape the input to the output of size 512. Then again, the ReLU activation layer works on these 512 values. The output from the ReLU layer is fed to the next linear layer which transforms 512 size input to a single output. This output is combined as input for the next step

prediction until all training batches finish their execution. The mean square error (MSE) loss function between actual (y_i) and predicted $(\hat{y}_i)$ is used, which can be defined as:

$$\frac{1}{n}\sum_{i=1}^{n}(y_i - \hat{y}_i)^2 \tag{3.6}$$

Here, the Rectified Adam Optimizer (RAdam) [133] has been used with a learning rate of 0.001 to update the model weights. The network configuration details of the RSAM model are given in the Appendix Table **??**.

3.3.1.3 Testing Phase

Testing samples in the batches of sequence length 256 are first normalized according to *Batch Normalization* procedure described in the previous section. These normalized batches are then fed to a trained RSAM model to predict the GHI at the time step t. To provide a robust estimation of modeling parameters, we perform walk-forward validation. This methodology involves moving along the time series one time step at a time by applying a moving window to available time-series data. The forecast value of the trained RSAM model is stored or evaluated against the actual value. Then, the next time step $t+1$ includes this actual expected value from the test set for the forecast in the next time step $t+2$ by moving the window one step. The procedure is repeated until the end of the data is reached. The testing process is illustrated in Fig. 3.3. For multi-horizon forecasting, the window size is equal to the horizon interval. For example, for 12 hours ahead forecasting, the next 12 forecasted values (sliding window size = 12) are used in input for next time step predictions.

3.3.2 Multihorizon Forecast Interval Prediction

Since GHI point predictions are subject to high uncertainty, it is equally important to measure the potential prediction error for many commercial applications. At each time step, quantile forecasts are predicted at 50, 90, and 95 percentile. This is achieved by training the model by

jointly minimizing the quantile loss terms summed across all quantile outputs [**?**]:

$$L(\omega, W) = \sum_{y_t \in \omega} \sum_{q \in Q} \sum_{\tau=1}^{\tau_{max}} \frac{QL\{y_t, \hat{y}\{q, t-\tau, \tau), q\}}{N\tau_{max}}, \tag{3.7}$$

$$QL(y, \hat{y}, q) = q(y - \hat{y}) + (1-q)(\hat{y} - y) \tag{3.8}$$

where ω is the domain of training data containing N samples, W represents weights of the RSAM model, $q = \{0.50, 0.90, 0.95\}$ is the output quantile value. $\hat{y}$ is the predicted GHI from the model and y is the observed GHI.

Normalized quantile losses are evaluated across the entire forecasting horizon during testing phase [90].

$$q - risk = \frac{2 \sum_{y_t \in \hat{\omega}} \sum_{\tau=1}^{\tau_{max}} QL(y_t, \hat{y}(q, t-\tau, \tau), q)}{\sum_{y_t \in \hat{\omega}} \sum_{\tau=1}^{\tau_{max}} |y_t|} \tag{3.9}$$

where $\hat{\omega}$ is the domain of the test samples. Quantile forecasts are generated using linear transformation of the output from the transformer model:

$$\hat{y}(q, t, \tau) = W_q \hat{\phi}(t, \tau) + b_q \tag{3.10}$$

where $\hat{\phi}(t, \tau)$ is the trained RSAM model, $W_q \in^{1 \times l}$, where $l = 2 \times \tau$ and $b_q \in$ are linear coefficients for the specified quantile q. Note that forecasts are only generated for horizons in the future i.e. $\tau \in \{1 .... \tau_{max}\}$. The quantile output is obtained using equation 10, consisting upper and lower limits for all quantiles. The one-step ahead quantile forecasts output are of the form:

$$lower - limit[\hat{y}_{t+1}(0.5), \hat{y}_{t+1}(0.9), \hat{y}_{t+1}(0.95)]$$

$$upper-limit[\hat{y}_{t+1}(0.5),\hat{y}_{t+1}(0.1),\hat{y}_{t+1}(0.05)]$$

where the lower limit denotes the lower bound values on the 50, 90 and 95 quantiles and the upper limit denotes the upper bound values on the 50, 90, and 95 quantiles. For the forecast in 1 step, 2 step and 12 steps ahead, the number of output values is 6, 12 and 72, respectively.

3.4 Experiment Details

To validate the proposed RSAM model and its ability to improve the solar irradiance forecasting accuracy, two experiments have been conducted. First, the point forecast results at different intervals have been compared with reference forecast methods; Second, prediction intervals are calculated to make the model robust.

3.4.1 Dataset

The US Department of Energy, the National Renewable Energy Laboratory (NREL), has made solar resource maps and related environmental data available from the US and other international locations [1]. The experiments reported in this paper are based on two locations, namely Hotevilla (Arizona) and Jammu and Kashmir (India). The details of these data sets and the input parameters used are presented in the Appendix Table A2.

In addition to the weather parameters mentioned in Table A2, time-series contain some known temporal features (Year, Month, Day, Hour, Minute). Additionally, residual features (year_residual, month_residual, day_residual, GHI_residual) calculated at the pre-processing step have been added to the feature space of the proposed model. Therefore, 18 features for Hotevilla (Arizona) and 15 features for Jammu and Kashmir (India) serve as input to all models under consideration. Solar radiations values at night hours have been removed based on filtering method i.e. row-data for which solar zenith angle is greater than 80° [120]. Only hours of the

day that are between 5:00 am and 7:30 pm is included.

3.4.2 Performance Criteria

The commonly used error metrics are: the Root Mean Square Error (RMSE), Mean Absolute Error (MAE), and Mean Bias Error (MBE) [84, 37, 41]. The definition of these error metrics is given in the appendix table A1. To substantiate the quality of the forecasts, we also include a new metric: the forecast skill proposed by [37] is given by

$$Forecast\_skill = 1 - \frac{Model_{RMSE}}{Smart\_Persistence_{RMSE}} \tag{3.11}$$

where $Model_{RMSE}$ denotes the RMSE of each forecasting method and $Smart\_Persistence_{RMSE}$, is the RMSE of the smart persistence model. Further, a higher forecast skill score shows improvement in forecasting.

3.4.3 Reference forecast methods and model tuning

1) Smart Persistence Algorithm: An improved variation of persistence model, which considers sky conditions, will remain constant over time (instead of irradiance itself). The expected value of GHI at horizon τ can be calculated as [106]:

$$GHI_{SmartPersistence}(t+\tau) = CSI(t) \times GHI_{clearsky}(t+\tau) \tag{3.12}$$

where $CSI(t)$ is the clear-sky index correction factor, defined as:

$$CSI(t) = \frac{GHI(t)}{GHI_{clearsky}(t)} \tag{3.13}$$

$GHI_{clearsky}$ is the GHI value under cloudless conditions, which is generated by a clear-sky model. The technique proposed by [172] has been utilized to implement the clear-sky model. The smart persistence algorithm is used as a baseline algorithm for our proposed work.

2) Long Short Term Memory (LSTM): It is a recurrent neural network model that has recently gained attention in solar forecasting. The architecture of the LSTM consists of one input layer having features depending upon the dataset (15 for India and 18 for Hotevilla). The number of hidden neurons was set to be 32. The output layer with a linear activation function had one neuron. Maximum epochs were set to be 50, optimizer used is Adam and the learning rate is 0.01.

3) Attention based LSTM (A-LSTM): It is an enhanced version of the basic LSTM where the attention mechanism has been incorporated into the LSTM model. The LSTM hidden layer output at each time-step has been fed to the additional attention layer which calculates attention score or weights. The attention layer produces attention_score_matrix (*att_score*) based on the hidden vectors, $H_v \in^{\kappa \times T}$ where $H_v = [h_{v1}, h_{v2}, ...h_{vT}]$ produced by LSTM given by following equations 14 and 15:

$$M = tanh([W_h H_v]) \tag{3.14}$$

$$att\_score = softmax(g^T M) \tag{3.15}$$

where $W_h \in^{\kappa \times \kappa}$, $g \in^{\kappa}$ are parameter vectors, and g^T is a transpose. κ denotes the size of hidden layers in the LSTM network. The number of hidden neurons was set to be 32 with one hidden layer. The output layer with a linear activation function had one neuron. Maximum epochs were set to be 50, optimizer used is Adam and the learning rate is 0.01.

4) Convolutional Neural Network-LSTM (CNN-LSTM): It is a hybrid model combining convolution and the LSTM model. The architecture of the CNN-LSTM algorithm consists of three convolutional 1D (Conv1D) layers followed by the Maxpool layer, again one more Conv1D layer. This layer is followed by the LSTM layer with one hidden layer of 32 neurons. The output layer with a linear activation function had one output neuron. The model is trained batchwise with a sequence length of 256. Maximum epochs were set to be 50, optimizer used is Adam and the learning rate is 0.01.

5) Attention-based CNN-LSTM (A-CNN-LSTM): In this model, an additional attention layer has been embedded to the existing CNN-LSTM model to implement self-attention mech-

anism. The attention scores are calculated in same way as described in the equations 14 and 15. Since attention layer specifically give more weights to the time-steps and features affecting output, it provides better performance against just CNN-LSTM. This model has same configuration as CNN-LSTM with extra attention layer. The maximum epochs were set to 50, the optimizer used is Adam, and the learning rate is 0.01.

Hyperparameter tuning plays a significant role in every deep learning model that is implemented. To identify the suitable setting for algorithmic hyper parameters, grid search has been utilized. Appendix Table A5 contains the candidate parameter settings and optimal parameters. These deep learning models have been trained with TITAN RTX GPU using Python 3.6 with Pytorch library on a computer system with Intel-Core-i7 CPU.

3.5 Results and Analysis

3.5.1 Point Forecasting Analysis

Table 3.1 summarizes the forecasting results for our proposed model, which uses only weather parameters as input. On average, the RMSE of Smart-Persistence, LSTM, A-LSTM, CNN-LSTM, A-CNN-LSTM and RSAM is 96.23, 63.21, 59.88, 55.93, 54.56 and 52.45, respectively on India data set. In Hotevilla, the average RMSE of Smart-Persistence, LSTM, A-LSTM, CNN-LSTM, A-CNN-LSTM, and RSAM is 116.02, 135, 82.18, 73.07, 70.13, and 64.87, respectively. The results in both locations indicate the superiority of RSAM in forecasting solar irradiance on multiple horizons. In J&K (India) one-step ahead prediction, the RSAM model achieves the lowest RMSE (50.82 W/m^2) and MAE (26.23 W/m^2) values as compared to Hotevilla, Arizona. The relatively small deviation shown by MBE values of the RSAM model results in a good unbiased prediction. The forecast skills displayed in Table 3.1 show consistently higher scores for the RSAM model over all other comparable models. Using the attention mechanism with sequential models (A-LSTM and A-CNN-LSTM), the models are showing better performance as compared to the baseline models because attention has the benefit of reducing the maximum path length between long range dependencies of the input and the target value; but still the sequential nature of RNN models hinders while working with large data sets

having multivariate time series. Therefore, the RSAM model, which is based on a non-recurrent and parallel sequence-to-sequence transformer model, can handle the large length input of multiple time series together effectively.

For visualization, taking the (horizon = 1 step, 2 steps, 12 steps) as an example, the prediction result of RSAM and other comparative models in the Hotevilla and India data sets are shown in Figs. **??**, **??** and 3.4. On analyzing these results, it can be observed that RSAM generally fits the actual data much better than other comparable models and this validates the fact that the RSAM has better prediction performance. As the time horizon expands, the superiority of RSAM becomes more noticeable. The main reason for the better performance of the RSAM model compared to other comparative models is that it can handle the large length input of multiple time series together effectively. For the 12-steps ahead prediction, RSAM obtains 61.20%, 54.57% forecast skill on Hotevilla and India, respectively.

3.5.2 Seasonal Variation analysis

For season-wise performance analysis, the three seasons considered for the Hotevilla (Arizona) are Summer (June to August), Winter (December to February), and Spring (February to May). For India, these seasons are Summer (March to May), Monsoon (June to September), and Winter (November to February). Table 3.2 and 3.3 provides a detailed seasonal analysis of all algorithms using different accuracy metrics at all intervals on India and Hotevilla, respectively. It can be seen from Table 3.2 that the RMSE values are less during winter, moderate in summer, and worst during the monsoon season. This is due to low GHI values during the winter season and variable sky conditions during the monsoon. The higher forecast skill in the monsoon is due to the large difference in the RMSE values between smart persistence and RSAM. Similarly, in Table 3.3 the results for the Hotevilla data set have been presented where it can be easily observed that RSAM shows better forecasting accuracy on all the seasons as compared to other reference algorithms. The RMSE values are least during winters, moderate in the spring season, and highest during summers. This is mainly due to moderate GHI values and less variation in the spring season than summers. In a season-wise analysis as well, RSAM performs better on India data set as compared to Hotevilla.

Table 3.1: Results of four evaluation metrics of the RSAM model and other comparative models

	RMSE (W/m^2)			**MAE** (W/m^2)			**MBE** (W/m^2)			**Forecast Skill** (%)		
	1-step	2-step	12-step	1-step	2-step	12-step	1-step	2-step	12-step	1-step	2-step	12-step
SITE 1:HOTEVILLA												
Smart Persistence	61.54	96.47	190.05	40.78	55.98	90.7	-2.5	16.4	12.43	-	-	-
LSTM	72.38	162.30	170.32	57.06	50.84	139.03	16.75	10.89	2.42	-17.61	-68.23	10.38
A-LSTM	65.72	84.50	96.32	39.97	48.56	56.27	4.16	5.87	-2.65	-6.79	12.40	49.31
CNN-LSTM	61.10	74.87	83.26	40.30	44.70	55.40	-9.17	-7.59	-5.35	0.7	22.39	56.19
A-CNN-LSTM	58.98	70.64	80.77	36.12	44.11	51.67	2.87	-3.98	-2.95	4.1	26.77	57.50
RSAM	**55.60**	**65.29**	**73.73**	**30.32**	**43.83**	**49.20**	**-0.63**	**1.01**	**-2.35**	**9.65**	**32.32**	**61.20**
SITE 2: INDIA												
Smart Persistence	66.20	100.76	121.73	40.98	65.2	74.5	4.2	3.08	7.43	-	-	-
LSTM	57.03	65.28	67.32	31.41	34.47	35.01	-1.33	-4.64	3.07	13.85	35.21	44.69
A-LSTM	55.38	61.50	62.77	29.89	32.98	33.38	2.11	1.42	3.65	16.34	38.96	48.43
CNN-LSTM	51.19	57.95	58.67	29.76	30.40	28.70	0.96	-1.11	-4.82	22.67	42.48	51.80
A-CNN-LSTM	51.00	54.23	58.47	27.53	28.25	27.98	1.82	-1.54	3.05	22.96	46.17	51.96
RSAM	**50.82**	**51.25**	**55.30**	**26.23**	**27.96**	**27.40**	**-0.13**	**0.04**	**2.92**	**23.23**	**49.13**	**54.57**

1

3.5.3 Quantile Interval analysis

The ability to accurately and meaningfully measure the risk associated with a forecast plays an important role in energy risk management. To estimate the risk of q, we use q = 0.5, 0.1 and 0.05 (i.e. $1-q$ = 0.5, 0.9 and 0.95) to access the prediction intervals of 50%, 90% and 95%, respectively. For the worst-case scenario, i.e., 12-step ahead forecasting, the q-risk value comes out to be 0.229 and 0.236 for India and Hotevilla, respectively. Individually, the P50 loss is 0.333 in India and 0.35 in Hotevilla. P95 loss is 0.19 and 0.276 on India and Hotevilla respectively. The least q-loss value is at P90 which is 0.17 and 0.255 on India and Hotevilla

Table 3.2: Season-wise results of four evaluation metrics of the RSAM model and other comparative models on INDIA

	RMSE (W/m^2)			**MAE** (W/m^2)			**MBE** (W/m^2)			**Forecast Skill** (%)		
	1-step	2-step	12-step	1-step	2-step	12-step	1-step	2-step	12-step	1-step	2-step	12-step
SUMMER												
Smart Persistence	68.89	86.59	106.17	27.69	34.87	70.4	4.78	-1.2	3.90	-	-	-
LSTM	60.82	64.42	70.65	29.46	33.37	35.51	6.64	-2.15	1.64	11.71	25.60	33.45
A-LSTM	58.82	61.22	68.70	28.90	30.23	32.75	3.87	2.10	3.64	14.61	29.29	35.29
CNN-LSTM	55.61	57.13	58.55	27.49	28.43	28.74	**1.9**	-1.23	2.67	19.27	34.02	44.85
A-CNN-LSTM	54.47	56.32	57.92	27.10	27.94	28.05	2.3	**-1.18**	1.53	20.93	34.95	45.44
RSAM	**53.45**	**54.02**	**55.47**	**26.93**	**27.03**	**27.84**	-3.24	1.35	**-1.14**	**22.41**	**37.61**	**47.75**
WINTER												
Smart Persistence	57.70	66.50	98.59	26.98	48.0	67.7	4.14	6.36	10.05	-	-	-
LSTM	52.25	58.61	62.21	26.27	28.57	31.31	4.71	5.50	6.69	9.44	11.86	36.90
A-LSTM	51.73	55.20	58.73	26.11	27.52	29.88	3.91	4.41	7.71	10.34	16.99	40.43
CNN-LSTM	51.01	54.45	56.36	24.42	26.72	27.62	3.47	4.75	**5.09**	11.59	18.12	42.83
A-CNN-LSTM	51.00	52.74	56.00	24.70	25.49	26.21	2.85	3.08	8.95	11.61	20.69	43.19
RSAM	**50.9**	**51.45**	**53.50**	**24.39**	**24.56**	**25.82**	**1.08**	**2.24**	5.18	**11.78**	**22.63**	**45.73**
MONSOON												
Smart Persistence	72.69	95.60	134.20	38.9	46.7	83.6	11.4	15.9	13.2	-	-	-
LSTM	68.85	72.91	78.83	35.89	41.88	43.55	6.33	12.04	6.76	5.28	23.73	41.25
A-LSTM	64.72	70.28	75.49	32.79	36.95	39.64	10.48	12.00	8.20	10.96	26.48	43.74
CNN-LSTM	60.05	62.80	68.35	30.05	31.45	32.06	13.61	12.58	9.8	17.38	34.30	49.06
A-CNN-LSTM	58.68	60.54	68.13	29.76	30.88	31.49	8.98	10.38	9.12	19.51	36.67	49.23
RSAM	**55.58**	**56.88**	**60.49**	**27.88**	**28.05**	**30.02**	**6.24**	**8.53**	**5.46**	**23.53**	**40.50**	**54.92**

Table 3.3: Season-wise results of four evaluation metrics of the RSAM model and other comparative models on HOTEVILLA

	RMSE (W/m^2)			**MAE** (W/m^2)			**MBE** (W/m^2)			**Forecast Skill** (%)		
	1-step	2-step	12-step	1-step	2-step	12-step	1-step	2-step	12-step	1-step	2-step	12-step
SUMMER												
Smart Persistence	84.28	118.70	198.65	46.26	72.73	109.84	-6.9	**0.16**	-3.52	-	-	-
LSTM	88.72	160.23	188.02	48.32	67.33	83.14	7.26	8.76	9.78	-5.26	-34.98	5.35
A-LSTM	75.91	92.44	110.62	38.83	53.45	66.72	5.31	6.74	6.77	9.93	22.12	44.31
CNN-LSTM	70.15	86.64	91.80	35.01	41.93	54.14	4.69	4.96	6.70	16.76	27.00	53.78
A-CNN-LSTM	66.87	80.30	89.63	32.56	42.00	54.00	2.55	2.87	4.26	20.65	32.35	54.88
RSAM	**60.85**	**70.72**	**84.12**	**24.88**	**41.75**	**52.49**	**1.33**	2.6	**2.6**	**27.80**	**40.42**	**57.65**
WINTER												
Smart Persistence	64.25	75.24	99.81	39.2	46.04	64.8	5.25	7.61	8.15	-	-	-
LSTM	65.97	78.29	100.90	36.14	43.65	54.75	6.05	8.80	5.90	-2.67	-4.05	-1.09
A-LSTM	63.78	73.42	80.21	40.24	42.71	50.76	5.98	9.76	3.81	0.73	6.22	19.63
CNN-LSTM	60.04	66.12	73.09	30.63	32.43	42.33	3.91	8.97	2.39	6.24	12.12	26.77
A-CNN-LSTM	56.81	59.76	70.29	31.65	33.60	42.50	3.69	3.90	5.26	11.57	20.57	29.57
RSAM	**52.59**	**56.25**	**62.48**	**25.73**	**27.74**	**31.71**	**0.59**	**2.23**	**1.88**	**18.14**	**25.23**	**37.40**
SPRING												
Smart Persistence	71.63	98.73	156.2	41.7	60.3	93.88	6.4	6.19	10.8	-	-	-
LSTM	70.52	96.07	135.96	44.28	55.81	73.46	5.63	5.93	8.32	1.54	2.69	12.84
A-LSTM	66.75	80.44	94.65	40.32	44.89	55.55	4.87	5.01	6.80	6.81	18.52	39.40
CNN-LSTM	63.00	70.16	86.33	32.73	35.97	42.02	4.0	4.54	7.64	12.04	28.93	44.66
A-CNN-LSTM	60.68	65.49	85.23	31.56	32.59	42.55	3.45	3.99	5.39	15.28	33.66	45.43
RSAM	**58.90**	**62.33**	**76.29**	**29.47**	**31.10**	**42.01**	**2.51**	**2.53**	**4.34**	**17.77**	**36.86**	**51.09**

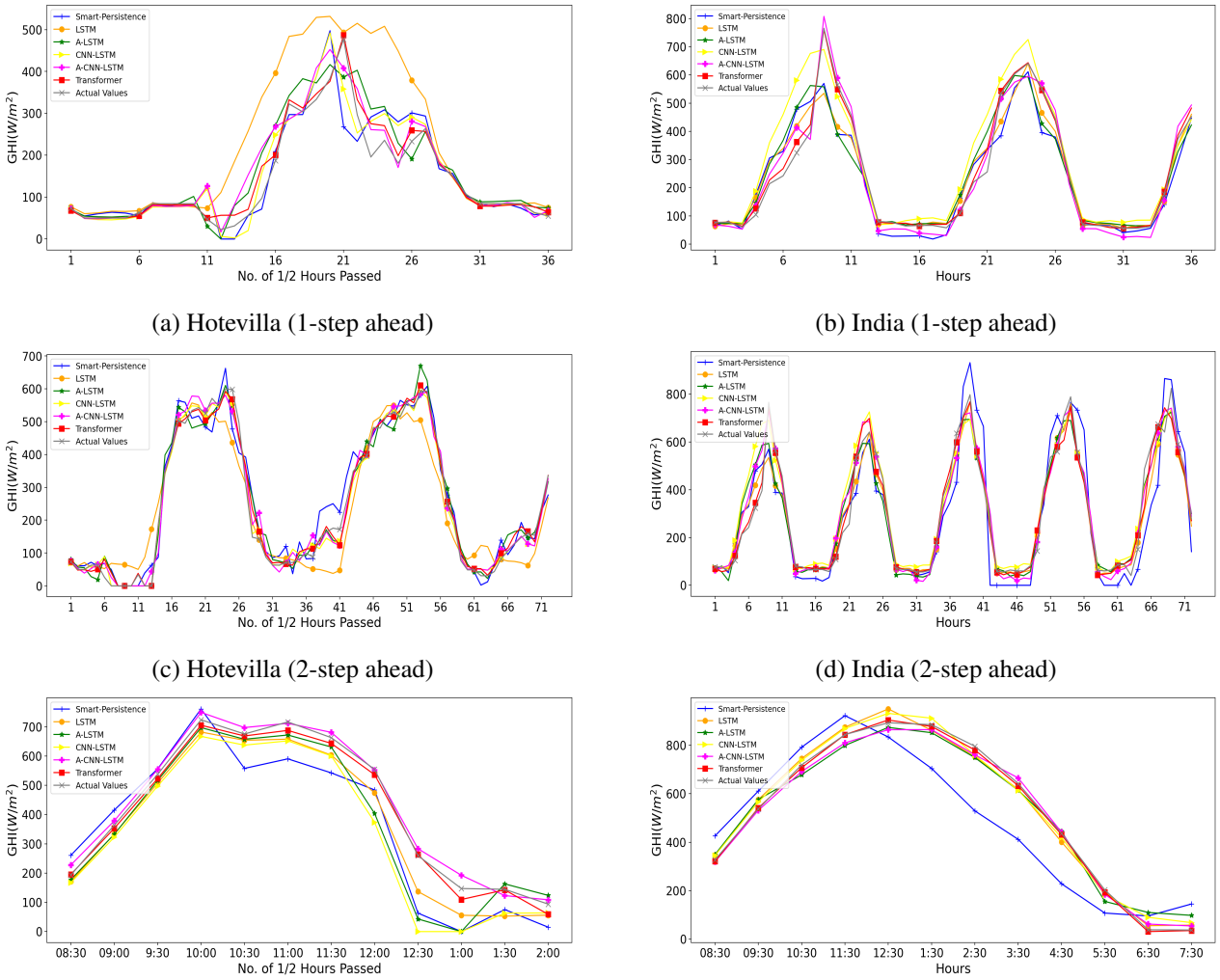

(a) Hotevilla (1-step ahead)

(b) India (1-step ahead)

(c) Hotevilla (2-step ahead)

(d) India (2-step ahead)

(e) Hotevilla (12-step ahead)

(f) India (12-step ahead)

Figure 3.4: 1,2 and 12 step ahead predictions on Hotevilla and India

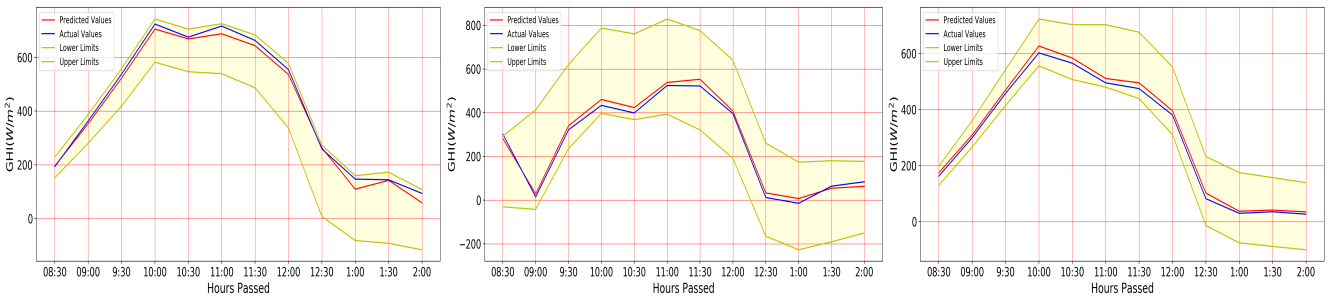

(a) Clear-sky (1 January, 2018)

(b) Supercool (13 Febraury, 2018)

(c) Overlapping (12 December, 2017)

Figure 3.5: Illustration of 12-step ahead forecasts with 90% prediction intervals for three cloud types in Hotevilla

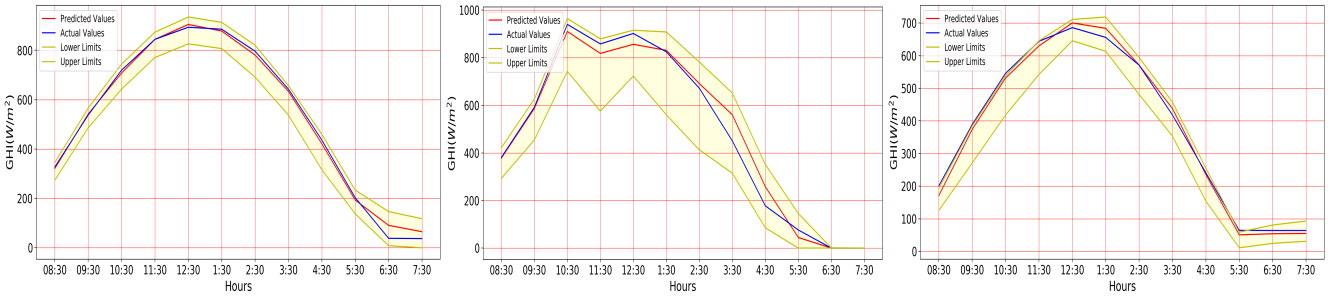

(a) Summer (12 March, 2014) (b) Rainy (12 August, 2014) (c) Winter (6 January, 2014)

Figure 3.6: Illustration of 12-step ahead forecasts with 90% prediction intervals for three cloud types in India

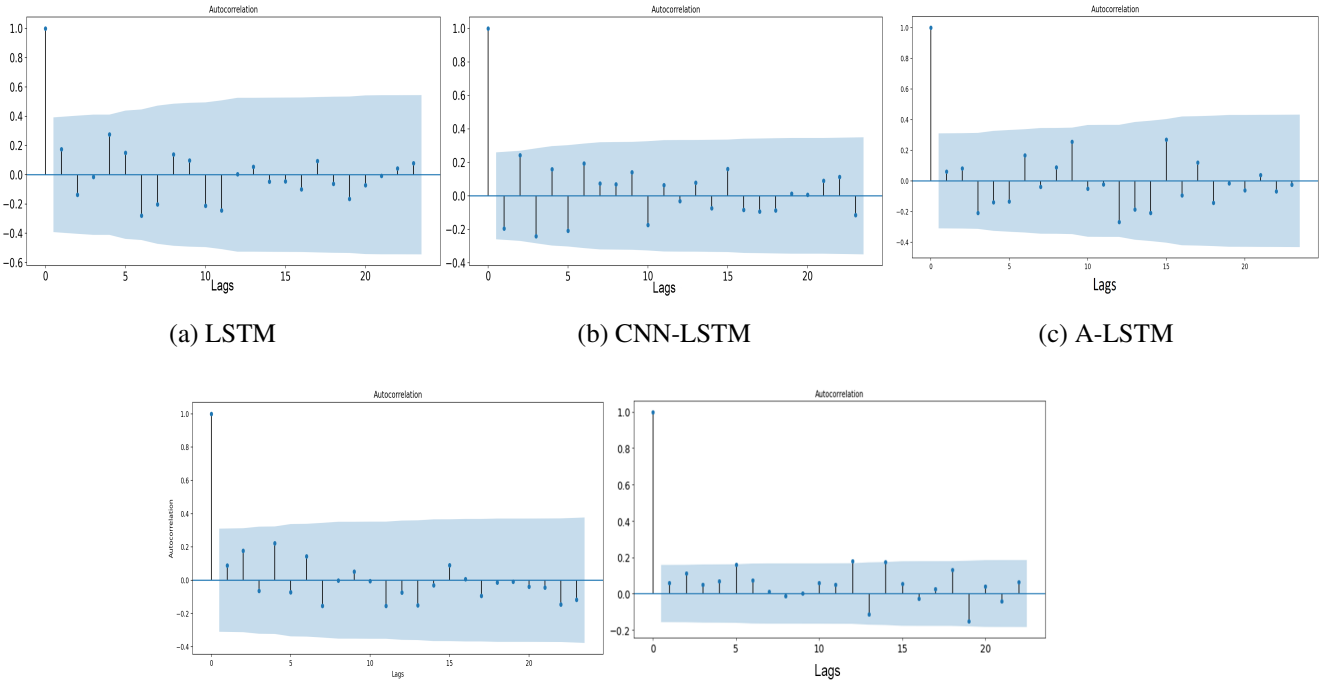

(a) LSTM (b) CNN-LSTM (c) A-LSTM

(d) A-CNN-LSTM (e) RSAM

Figure 3.7: ACF plots

respectively. Figs. 3.5 and 3.6 represent the graph of 12-step ahead predictions with three different cloud types on both data sets with a prediction interval of 90%. It can be seen from the graphs that prediction risk is almost covered by the width of the interval. Also, the weather in Hotevilla is more fluctuating than in India; hence, it has a wider interval width and the same also applies for a rainy day in India as depicted by Fig. 3.6 (b).

3.5.4 Training time analysis

RSAM shows an overwhelming advantage of deep learning approaches in terms of time usage. Compared with the comparative models LSTM, CNN-LSTM, A-LSTM, and A-CNN-LSTM which takes 0.8, 0.13 , 0.28, 0.40 seconds per step respectively. RSAM takes 0.0054 seconds per step as the expense of each time step.The time per step for RSAM is the lowest because it avoids the recurrent data-folding training cycle. In terms of computational complexity, the training and testing complexity of LSTM/ CNN-LSTM is $m \times \eta^2 \times \kappa$ while for attention-based LSTM/CNN-LSTM it is $m^2 \times \eta^2 \times \kappa$. For the self-attention-based transformer model (RSAM), complexity is reduced to $m^2 \times \eta \times \kappa$. Here, m is sequence length, κ denotes number of layers in the deep neural network and η denotes number of neurons at each layer.

3.5.5 White noise test of residuals

The differences between the expected and observed values (residuals) must be unpredictable. In other words, no explanatory / prediction information should be contained in the error. Residuals are useful in testing whether a model has captured all of the structure, and the only error left is the random fluctuations in the time series that cannot be modeled. A good forecasting method will yield residuals with the following properties: (a) Adjacent residuals should not be correlated with each other (auto correlation). (b) For unbiased forecasting, the residuals should have zero mean. The auto correlation function (ACF) is the correlation of the residuals (as a time series) with its own lags. Fig. 3.7 represents the ACF of the residuals of LSTM, CNN-LSTM, Attention-LSTM, Attention-CNN-LSTM, and RSAM, respectively. The blue area indicates the values for the ACF are within 95% confidence interval for lags > 0. It can be seen that in the LSTM ACF plot there is a residual pattern between lag 4 and lag 11 that is significantly visible. Similarly, in CNN-LSTM ACF-plot there exists a residual pattern between lag 1 and lag 6. These patterns indicate that residual autocorrelation is not random and these models have not completely captured the structure of time-series. In the A-LSTM model, there is a small pattern between lag 15 and lag 18. Similarly, for A-CNN-LSTM, there is small pattern between lag 3 and lag 5. This shows that attention-based LSTM and CNN-LSTM capture structure of

time-series better than just LSTM and CNN-LSTM, respectively. The RSAM model stratifies the aforementioned two conditions (no pattern and mean converges to almost 0), thus can get better forecasting results while capturing the structure of time-series.

3.6 Conclusion

In the proposed work, a robust multi-step solar irradiance prediction model has been developed that uses Transformer deep learning model for point forecasting and quantile regression for interval prediction. The actual GHI value may deviate from the forecast and, hence, knowing the likelihood can help consumers with hedging risks. A multi-step forecast together with precise prediction interval is essential for real-time smart grid operations. Through a rigorous analysis of the results, it has been validated that the proposed model exhibits the best performance accuracy with the least training time as compared to recurrent deep learning models (LSTM and CNN-LSTM). For the NREL data set of two different sites with different climatic conditions, the proposed RSAM model shows better performance both annually and season-wise. In India, RSAM is 58.89%, 18.60%, 13.22%, 6.42%, and 3.94% more accurate (annually) than Smart-Persistence, LSTM, Attention-LSTM, CNN-LSTM, and Attention-CNN-LSTM, respectively, in terms of RMSE.

Chapter 4

Appliance Power forecasting for Consumer behavior Learning

4.1 Introduction

In the smart grid era, demand response (DR) programs are considered an increasingly valuable resource option for the problem of energy demand imbalance, which is always a concern for power grid operators [71]. Load shifting regulates load flow and reduces energy cost by rescheduling consumers' energy consumption patterns during peak hours in response to dynamic prices or financial incentives. In this regard, appliance-level power forecasting can help residential consumers respond effectively to DR programs. Accurate load forecasts of individual consumers will determine flexibility in demand and will make them aware of their energy usage, allowing them to better manage their usage costs. In addition, it can help utilities identify promising consumers to participate in DR programs in the power shortage scenario.

Until now, power forecasting has been performed at the house and sub-metering level. With the advent of IoT, fine-grained load data for domestic appliances are readily available,

allowing predictions at the appliance level. Appliance-by-appliance consumption information will enable consumers to improve their energy efficiency. It also provides home energy automation systems to either directly control appliances or give the consumers recommendations about the period, resulting in lower energy costs for the usage of appliances based on the learned user's behavioral habits from historical data. Therefore, it determines the flexibility of the appliances to participate in DR programs. It showed that appliance-level energy usage information could help residents save up to 12% in energy costs instead of receiving conventional monthly details at the whole building level [56].

Brown et al. [23] incorporated individual energy profiles to implement automated energy management based on consumers' occupancy and behavior. Since appliance-level energy requirements depend upon the number of residents, their occupation, action, outside weather, location, etc., determining a single algorithm that forecasts appliance power while capturing different consumers' behavioral patterns is challenging. However, the approaches and discussions on this subject are still in the primitive stage and not mature enough because of the high volatility of the residential load profiles.

Most previous studies are based on short-term load forecasting at the building level or aggregate level [177], [50]. Recently, different approaches have been suggested for accurate load forecasting of individual residential customers.

Artificial intelligence (AI) techniques support demand side flexibility (DSF), which helps consumers play an active role in demand change programs [35]. Today, deep learning has become one of the most popular techniques for time series forecasting [242]. Unlike shallow learning, deep learning typically involves stacking multiple layers of the neural network and relying on stochastic optimization to solve complex problems [225]. The Long Short-Term Memory network (LSTM) and Gated Recurrent Unit network (GRU) are usually more potent than traditional RNN as reported in some load forecasting tasks [117].

The LSTM deep learning model is used for short-term load forecasting at individual customer levels in the smart grid [114],[206]. A simple back-propagation neural network compared to LSTM has been used to predict short-term household power [114]. In [206] a pooling-based LSTM strategy is used which utilizes multiple data from the smart meters' load profile for forecasting purposes. A combination of convolutional neural network (CNN) and bidirectional LSTM (Bi-LSTM) has been utilized to predict household electric energy consumption (EECP)

[123],[226]. A hybrid CNN-GRU model to predict short-term electricity consumption in residential buildings by learning both spatial and temporal features of multi-variate time-series [190]. A transfer learning concept and a cluster-based strategy have been utilized to train an LSTM-based electricity forecasting model [122]. However, these models are not suitable for real-time implementation. A two-dimensional (2D) CNN using recurrence plots has been implemented for load forecasting of individual residential customers [205]. However, this technique works specifically for time-series that repeat their states.

Many researchers focus on probabilistic forecasting models for short-term and household-level power forecasting. A short-term probabilistic density power forecasting model based on deep learning and quantile regression has been proposed in [77]. However, the multi-layer perceptron (MLP) based deep learning technique is not suitable for large and complex data sets. Probabilistic household-level load forecasting has been reported using LSTM deep neural network [237] and hidden Markov model [99]. Most of the forecasting approaches used in these literary works focus on individual household-level smart meter data. In contrast, the power forecasting at the appliance level in real-time is much more sparse.

It is widely acknowledged that an ensemble of multiple deep learning models can boost prediction efficiency and has greater generalization skills than individual models [72],[25]. The goal of combining multiple models is to obtain a more accurate estimate than the one obtained by a single model as the errors in aggregating diverse model predictions can be easily compensated. Various successful methods have been proposed to improve load prediction accuracy by integrating several models.

It is well known that a boosting-based ensemble is more effective in handling the time series data set based on long-range dependencies. An ensemble method for short-term load forecasts based on the hybrid LGBM-XGB-MLP model has been proposed in [152]. However, the extreme learning machine (ELM) based architecture is a two-layer neural network that cannot handle the long-term dependencies and volatility of the appliance's power series. A hybrid deep neural network with a fuzzy clustering approach has been utilized in [207] for hourly load forecasting. Here, the fuzzy approach is used to group the data into multiple subsets, further taken as input to the deep neural network model.

The CNN-LSTM model has been used in [25] for predicting energy consumption at the residential level. The results indicate that CNN-LSTM performs better than LSTM for indi-

vidual household load forecasting. A deep ensemble model for probabilistic load forecasting has been developed for individual customers [26,27]. The quantile strategy combined with the LASSO technique has been utilized [26], whereas the deep residual network (ResNet) has been reported for forecasting day ahead [27]. However, the neural network-based deep learning model is still a better choice. But probabilistic forecast being non-linear and non-convex, is not suitable for real-time DR programs.

The proposed work will significantly help in the development of a scheduling optimization algorithm for the response to real-time demand. The consumer behavior aspects can be determined only by their appliances' power usage pattern and related association. The scheduling algorithm using load shift shifts controllable appliances to later intervals to minimize electricity costs without violating consumer comfort. Learning consumer behavior helps to maintain his comfort, which means determining the earliest start time and finish time of various appliances and their power requirements at different time slots.

The association mining further enhances behavioral learning by providing information to the algorithm about which appliance should preferably run after the currently running appliance (in case many appliances are ready to run). Association mining helps to provide supervised information to the scheduling algorithm to preferably run the next appliance associated with the currently running appliance. In this way, the proposed work is essential for developing consumer-oriented scheduling appliances for demand response implementation.

Since the data set of household appliance power consumption is noisy and real, no individual forecasting model can be generalized to all consumers. The energy forecasting domain demands more robustness, higher prediction accuracy, and generalization ability for real-world implementation. Therefore, an ensemble model combining RNNs and gradient boosting tree capabilities for superior prediction performance has been developed and applied for appliance-level forecasting. Hybrid Convolutional LSTM (CNN-LSTM) deep learning models are used as base learners for the XG-Boost algorithm.

The main innovations and contributions of this work includes:

1. Development of a multistage ensemble deep learning model with powerful learning ability for appliance-level power forecasting.

2. A 5-minute prediction time horizon has been considered for the appliance level power

forecasting, which is more suitable for real-time demand response programs.

3. Mining of appliance-appliance associations using the Dynamic item set counting (DIC) algorithm to determine which appliances frequently occur together.

4. The performance of the proposed model has been rigorously evaluated on publicly available data sets, namely GREEND and UK-DALE.

4.2 Forecasting Model Architecture

A deep learning-based ensemble model has been developed to capture appliances' stochastic power usage at 5-minute intervals. The multistage boosting ensemble technique elevates the base model's predictive strength by covering large data space and minimizing the error rather than those obtained by individual models.

The hybrid deep learning Convolutional LSTM (CNN-LSTM) has been utilized as the first stage of our Ensemble model. The three CNN-LSTM model outputs are stacked together and fed to the boosting stage for the final forecasted value. XGBoost, namely eXtreme Gradient Boosting, combines trees in a boosting manner and currently provides state-of-the-art performance amongst several prediction challenges. XGBoost allows parallel programming without significant loss of accuracy.

The ensemble model prediction step can be divided into two phases: 1) Model Training and 2) Testing. The training and testing phases have been illustrated in Fig. 4.1 and 4.2 respectively, and described as follows:

4.2.1 Training Phase

In this phase, the ensemble model is initialized with random weights, and these weights get updated with each training cycle.

Input Data - Training data is divided into batches with a sequence length (k) of 128 samples. These batches (n = 128) are fed as input to the convolution-1D layer. The sequence of

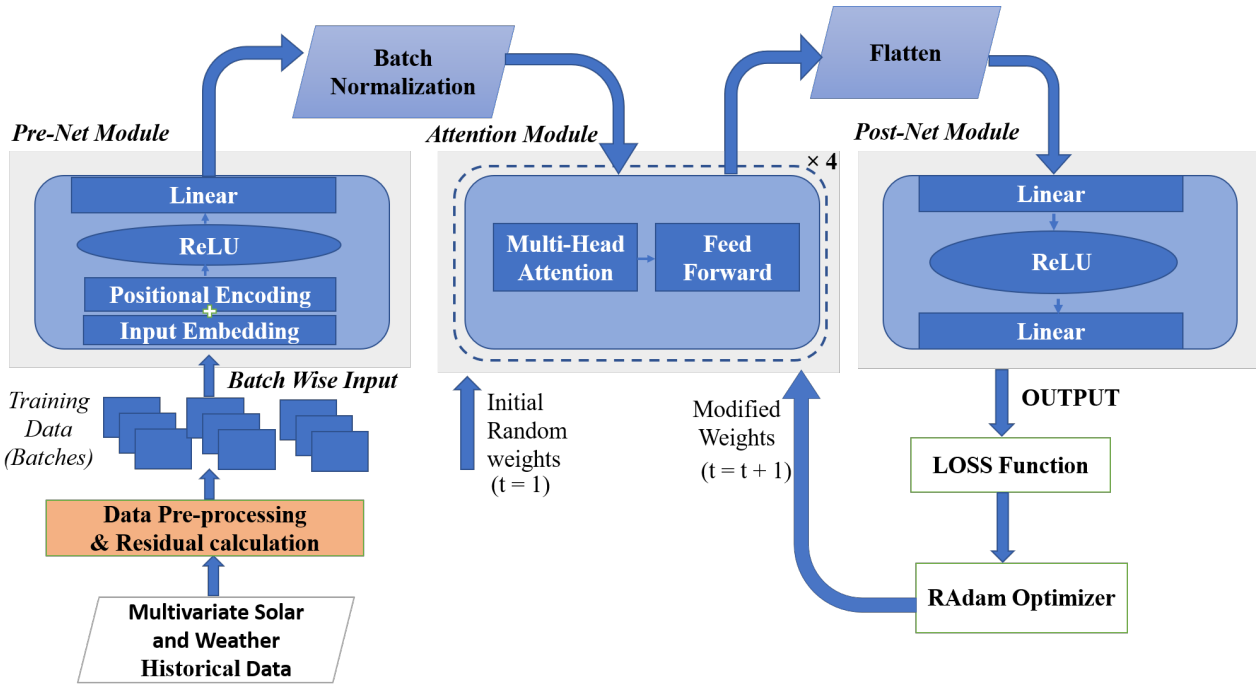

Figure 4.1: Training Phase of proposed Ensemble Model

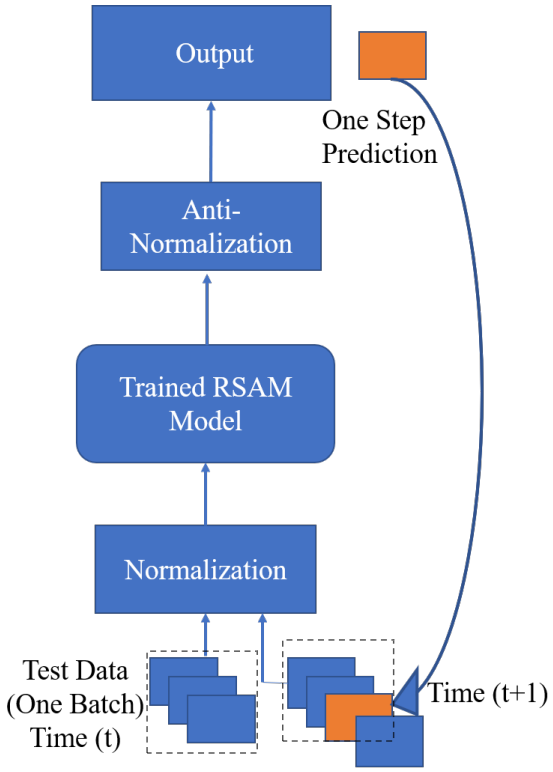

Figure 4.2: Testing Phase of proposed Ensemble Model

training examples can be represented as $(x_1, y_1), (x_2, y_2), ...(x_{128}, y_{128})$ with $x_t \in^{n \times k}$ and $y_t \in^n$ for $1 \leq t \leq 128$. x_t denotes input for univariate time-series and y_t denotes output.

Convolution layers - These layers can learn from the raw time-series data directly without scaling or differencing and deriving interesting features from the shorter (fixed-length) sequence of the total time-series dataset. Two layers of Conv-1D have been utilized to give the model a fair chance of learning features from the long noisy input data. The first layer with 64 parallel feature maps and a kernel size of 3 takes the input shape 128×1 and produces the output shape of 126×64. This layer is used to learn basic features. The second Conv-1D layer with same configuration has been utilized to learn more complex features. The output shape of this layer is 124×64. The output of the convolution layer can be expressed as [266]:

$$C_r(t) = f(\sum_{i=1}^{l} \sum_{j=1}^{k} x(i + s(t-1), j)\omega_r(i, j) + b(r)) \tag{4.1}$$

where $x \in^{n \times k}$ denotes the input time series or the output of the preceding layer, s denotes the convolution stride, $C_r(t)$ refers to the t^{th} component of the r^{th} feature map, $\omega_r \in^{l \times k}$ and $b(r)$ refers to the weights and bias of the r^{th} convolution filter. This filter connects the j^{th} feature map of layer $l-1$ with the i^{th} feature map of layer l.

Max Pool Layer - The pooling layer reduces the learned characteristics to 1/4 of their size and consolidates them into the critical elements. It prevents overfitting of learned features by taking the maximum value within the window region. With the pool size set to 2, the output shape of this layer is 62×64. This layer output can be expressed as:

$$P_r(t) = max(C_r((t-1)l+1), C_r((t-1)l+2), ..., C_r(tl)) \tag{4.2}$$

Flatten Layer - It reduces the feature maps to a single one-dimensional vector. The output shape after this layer is a vector containing 3968 (62×64) values. This layer is followed by a repeat vector layer, which converts current 2D vector of shape (none, 3968) into 3D vector with shape (none, 1, 3968) to make it suitable to input to next LSTM layer.

LSTM Layer - The LSTM gating architecture is computationally efficient than traditional RNNs. The selective read, write, and forget procedure followed in LSTM avoids explosive and

vanishing gradient problems [83].

At each time step t, for input x_t, each memory cell c_t is updated and a hidden state h_t is generated as output according to the following equations [74]:

$$\begin{aligned} i_t &= \sigma(W_{xi}x_t + W_{hi}x_{t-1} + b_i), \\ f_t &= \sigma(W_{xf}x_t + W_{hf}x_{t-1} + b_f), \\ o_t &= \sigma(W_{xo}x_t + W_{ho}x_{t-1} + b_o), \\ c_t &= f_t \oplus c_{t-1} + i_t \oplus \phi(W_{xc}x_t + W_{hc}h_{t-1} + b_c), \\ h_t &= o_t \oplus \phi c_t, \end{aligned} \tag{4.3}$$

In the proposed model, an LSTM layer with 100 neurons has been utilized. The output vector from this layer is of shape (none, 1, 200).

Dense Layer - It is a fully connected layer used to reduce the vector's size. The proposed model uses two dense layers. The first dense layer reduces the vector size of (none, 1, 200) to (none, 1, 100). The second dense layer is the output layer, producing a single output of the CNN-LSTM forecast with output shape (none, 1, 1).

XGBoost - XGBoost, namely, eXtreme Gradient Boosting, is an integrated learning method that uses decision trees and random forests to make predictions. It uses boosted decision trees to obtain final predictions using base learners. However, a gradient decent algorithm is used to reduce the errors effectively. If $F = \{F_1, F_2, F_3, ...F_m\}$ are the set of base learners. The final prediction can be given by

$$\hat{y}_i = \sum_{t=1}^{m} F_t(x_i) \tag{4.4}$$

where $\{x_1, x_2, x_3, ...x_m\}$ are data points. The loss function of XGBoost on t^{th} iteration [31]:

$$L^t = \sum_{i=1}^{n} l(y_i, \hat{y_i}^{(t-1)} + f_t(x_i)) + \lambda f_t \tag{4.5}$$

where L^t denotes the loss in the t^{th} iteration. l is based on the loss function of the former

$t-1$ tree, y_i is the label of x_i, λ denotes regularization parameter, f_t represents t^{th} tree output, $l(y_i, \hat{y}_i)$ is the training loss of x_i, $\hat{y}_i^{(t-1)}$ represents the prediction of the combination of all the tree models.

The second-order expansion of Taylor is performed on the above equation to obtain the final loss and may be represented as:

$$LOSS = -\frac{1}{2}\sum_{j=1}^{T} w_j + \gamma T \tag{4.6}$$

where w_j is the prediction for node j which can be expressed by following equation:

$$w_j = -\frac{G_i}{H_i + \lambda} \tag{4.7}$$

where G_i is $\sum_{i \in I_j} g_i$ and H_i is $\sum_{i \in I_j} h_i$. Here, g_i and h_i are the first order and second order derivative loss of predictions at previous iterations, respectively. Also, I_j denotes the set of instances belonging to node j. The smaller value of *LOSS* denotes the better structure of tree.

For the XGBoost module, the proposed ensemble model utilizes 45 estimators with the learning rate set to 0.1. The depth of tree is taken as 5. The fraction of columns to be randomly sampled for each tree, denoted by the parameter col_sample by the tree, is set to 0.3. The objective function of regressor is set to be linear.

In the proposed ensemble forecasting method, the hybrid structure of CNN-LSTM handles the dynamics and non-stationarities of real-world time series accurately. The output of three discrete CNN-LSTM models is stacked together and fed to the XGBoost model. In this way, the prediction performance gets further boosted, and better prediction results have been achieved.

For the m number of CNN-LSTM models in an ensemble, the forecast result for time series with observations n,$(y^1, y^2 ...., y^n)$, is given by

$$\hat{y}^t = \sum_{i=1}^{m} w_m \hat{y}_m^t \qquad for \;\; t = 1, ..., n. \tag{4.8}$$

where $\hat{y}_m^t$ denotes the forecast output (at the t^{th} time stamp) obtained using the m^{th} CNN-LSTM model and w_m is the associated weight. Each weight w_m is assigned to the forecast output of the corresponding CNN-LSTM models. Also, $0 \leq w_m \leq 1$ and $\sum_{i=1}^{m} w_m = 1$.

4.2.2 Testing Phase

Testing samples in the batches of sequence length 128 are fed to a trained ensemble model to predict power at time step t. To provide a robust estimation of modeling parameters, walk-forward validation has been performed. This methodology involves moving along the time series one step by applying a moving window to available time-series data. The forecast value of the trained ensemble model is evaluated against the actual value. The next time step t + 1 includes this actual expected value of the test set for the forecast on the next time step t + 2 by further moving the next window. The procedure is repeated until the end of test data is reached. The testing process is illustrated in Fig. **??**(b).

4.2.3 Appliances' Association Rules Extraction

The frequently associated appliances are extracted using dynamic item set counting (DIC), a variant of the Apriori algorithm. This algorithm incorporates the dynamic change (addition and deletion) of appliances power us-age in the database. It means it can incorporate the changing behavioral aspect of occupants well. With this approach, a small portion of the database is extracted at each iteration, which reduces the memory overhead and improves efficiency compared to Apriori.

This algorithm uses a support-confidence framework to extract association rules and generating frequent item sets of appliances, i.e. the set of appliances that often run together. The correlation rule can be expressed as

$$X \implies Y[Support, Confidence, Correlation] \tag{4.9}$$

where the correlation can be measured using Lift metric that provides more insight into support-

confidence relationship. where

$$Lift(X,Y) = \frac{Confidence(X \implies Y)}{Support(Y)} \tag{4.10}$$

4.3 Experiment Details

4.3.1 Data set

The experimental study has been carried out using two popular open-access data sets for evaluating the performance of the proposed ensemble model, namely, GREEND and UK-Dale. The GREEND dataset contains appliance-wise data of eight different houses in Italy and Austria. We utilize the data of house number 2, which is an apartment with one floor in Klagenfurt (AT). The residents are a young couple, spending most of the daylight time at work during weekdays and mostly being home in the evenings and weekends. The data collection module's plugs kit consists of a Zigbee network having nine sensing outlets, each collecting active power measurements from the connected load.

The UK-DALE (UK Domestic Appliance Level Electricity) data set records the power consumption of five UK houses, appliance-wise and the whole house as well. We have used 8 appliances of house number 1 for our experiment. The detailed description of both data sets is described in Table 4.1.

4.3.2 Data Preprocessing

The GREEND data set's null values are replaced with the most frequent power value for each appliance. Then, the 1-second data is resampled to 5 minutes by taking the average of 300 samples for each appliance. Similarly, for the UK-dale dataset, the 6-second data samples per appliance are resampled into 5 minutes by taking an average of 50 samples. The duration of 5 minutes is chosen as it is appropriate for load shifting under a real-time environment using real-time pricing (RTP) schemes. In addition, the chosen horizon incorporates the minimum

Table 4.1: Data sets Information

	GREEND [160]	**UK-DALE** [108]
Location	Austria, Italy	UK
Duration	1 year and 4 months	5 year and 5 months
House	2	1
Resolution	1 Hz	6 sec
Total Samples (5 min)	1,34,933	4,68,836
Training Samples (5 min)	1,00,481	2,81,327
Validation Samples (5 min)	8,612	37,501
Testing Samples (5 min)	34,452	1,87,509
Training Set	15-02-2014 to 21-03-2015	09-11-2012 to 15-07-2015
Testing Set	21-03-2015 to 29-06-2015	15-07-2015 to 26-04-2017

operating duration of smart household appliances. Then, the resampled data are divided into training and testing as an 80 to 20 ratio. Out of 80% training data, again, 20% is used for validation purposes and select appropriate hyperparameters. Table 4.1 contains details on the number of data samples in training, testing, and validation for both data sets. The training data are divided into batches of sequence length 128 to be used as input to the ensemble model. Similarly, the test data is also divided into batches with a sequence length of 128 to predict the power output of the trained ensemble model.

4.3.3 Performance Criteria

Two standard evaluation metrics measure the ensemble model's forecasting performance: Root Mean Square Error (RMSE) and Mean Absolute Error (MAE). These are described as follows:

$$RMSE = \sqrt{\frac{1}{N}\sum_{i=1}^{N} e_i^2} \tag{4.11}$$

$$MAE = \frac{1}{N}\sum_{i=1}^{N} |e_i| \tag{4.12}$$

where

$$e_i = Power_{forecast,i} - Power_{actual,i}$$

is known as forecast error. $Power_{forecast,i}$ is the forecast power of the i^{th} sample and $Power_{actual,i}$ is the actual power of the i^{th} sample. N is the number of samples used for measuring accuracy.

4.3.4 Reference forecast methods and model tuning

1) **Feed-forward neural network (FFNN)** - This is the basic form of the neural network used for regression problems. It uses two hidden layers with 64 neurons each and the ReLU activation function. The sequence length is set to 128. The mean square error (MSE) is used as a loss function where the RMS prop optimizer has been incorporated. The model has been run for 20 epochs.

2) **Long-short term memory (LSTM)** - This belongs to the family of recurrent neural networks (RNNs) that has recently gained attention for time series forecasting. The LSTM architecture consists of one input layer with ten hidden neurons used with the ReLU activation function. This layer is followed by one dense layer. Adam optimizer has been utilized to update the weights and reduce errors in the model. The model has been run for 20 epochs with batch size and sequence length of 128 samples.

3) **Convolutional-LSTM (CNN-LSTM)** is a hybrid model that combines the convolutional and LSTM models. The architecture of the CNN-LSTM algorithm consists of two convolutional 1D (Conv1D) layers with kernel size 3 and 64 filters. This layer is followed by the Maxpool layer with pool size 2 and the LSTM layer with 200 hidden neurons. The output layer with a linear activation function consists of one output neuron. The model is trained batch-wise with a sequence length of 128, maximum epochs 20 and learning rate 0.01 with Adam optimizer.

4) **Convolutional-XGBoost (CNN-XGBoost)** - It is a multistage ensemble model having three CNN models and XGBoost. The outputs from all CNN models are stacked together and fed to the XGBoost regressor. Each CNN model has two convolutional layers having 64 filters, kernel size is 3 with ReLu activation. Two dense layers at the end to change the output size to 512 and 1, respectively. Then, the outputs are stacked, and the XG-Boost regressor boosts the output to generate the final power prediction. The configuration of XG-Boost has been taken as the proposed model for a fair comparison.

All the reference forecast methods have been tuned to the best possible hyper-parameters for one-step ahead forecasts. The grid search method has been utilized to tune the hyper-parameters of the proposed model. The table corresponding to hyper-parameter tuning is presented in the Appendix A5. These deep learning models have been trained with TITAN RTX GPU using Python 3.6 with Keras 2.2.4 library on a computer system with Intel Core-i7 CPU.

4.4 Results and Analysis

The results in Tables 4.2 and 4.3 demonstrate the effectiveness of the ensemble deep learning model in improving forecast performance (in terms of both RMSE and MAE) against all reference models on the GREEND dataset. We can categorize GREEND appliances as fixed appliances (microwave, water kettle, radio, dryer, kitchenware, and bedside light), controllable appliances (dishwasher and washing machine), thermostatically controllable (TCL) (Fridge). For fixed appliances, the average RMSE of FFNN, LSTM, CNN-LSTM, CNN-XGBoost and the proposed model is 15.93, 15.28, 14.03, 12.41 and 9.032, respectively. For controllable appliances, on average, the RMSE of FFNN, LSTM, CNN-LSTM, CNN-XGBoost and Ours is

30.085, 48.015, 35.65, 33.13, and 27.885, respectively. There is only one TCL appliance in GREEND whose RMSE and MAE can be seen from Tables 4.2 and 4.3, respectively.

For the UK-Dale dataset, all the appliances come under the fixed category except boiler which is a TCL appliance. Tables 4.4 and 4.5 show the outstanding performance of the ensemble model over all other reference models. Here, the average RMSE of fixed appliances of FFNN, LSTM, CNN-LSTM, CNN-XGBoost, and Ours is 5.34, 4.45, 4.42, 3.80, and 2.63, respectively. The average MAE of fixed appliances of FFNN, LSTM, CNN-LSTM, CNN-XGBoost, and Ours is 1.91, 2.44, 1.50, 1.28, and 0.82, respectively.

For visualization, the prediction results of the Ensemble model and other comparative models on all GREEND appliances are shown in Fig.4.3. Similarly, the prediction results of all appliances in the UK-Dale dataset are shown in Fig.4.4. On analyzing these results, the ensemble model generally fits the actual data much better than other comparable models, which validates the fact that the proposed ensemble model has better prediction performance.

Results indicate that the multi-stage CNN-LSTM XGBoost ensemble performs slightly better on the UK-Dale data set than the GREEND dataset in terms of both RMSE and MAE. This is due to periodicity observed in appliance usage in the UK-Dale data set. For the GREEND data set, in terms of RMSE, the proposed model performance for controllable appliances is 7.5%, 53.05%, 24.46%, 17.21% better than FFNN, LSTM, CNN-LSTM and CNN-XGBoost, respectively. Similarly, for fixed appliances, the proposed model is 55.28%, 51.41%, 43.36%, 31.52% superior to FFNN, LSTM, CNN-LSTM, CNN-XGBoost, respectively. For the UK-Dale dataset, on fixed appliances, the performance of the proposed model beats FFNN, LSTM, CNN-LSTM, and CNN-XGBoost by 68%, 51.41%, 50.78%, 36.39%, respectively. The proposed model of the TCL appliance shows a lower RMSE of 29.69 on UK-Dale than 43.49 on GREEND. The working code of the proposed work can be found here [201].

The proposed model performs better than all other comparative models because the combination of CNN and LSTM allows the LSTM layer to extract patterns and sequential dependencies in the time series. In contrast, the CNN layer, through dilated convolutions methods and filters, further improves this process. This approach mainly helps in granular level forecasting (5 min in our case). The benefit of this model is that the model can support very long input sequences that can be read as blocks or sub sequences by the CNN model, then pieced together by the LSTM model. Further, the performance has been enhanced by using the XG-

Boost tree, which boosts the performance of its base models by providing high preference to poorly estimated samples over well-estimated samples.

Table 4.2: Comparison of the proposed Ensemble model with reference forecasting models on GREEND data set with respect to RMSE (W/m^2)

	FFNN	LSTM	CNN-LSTM	CNN-XG	**OURS**
Fridge	56.62	66.88	47.36	45.78	**43.49**
Dishwasher	6.23	7.45	6.22	5.95	**4.15**
Microwave	17.16	16.67	15.07	14.86	**12.98**
Water-kettle	61.68	59.76	56.27	48.76	**35.55**
Washing Machine	53.94	88.58	65.08	60.32	**51.62**
Radio	4.31	6.83	4.25	3.91	**2.61**
Dryer	5.56	1.16	1.14	1.11	**1.09**
Kitchenware	4.90	5.32	3.75	2.75	**0.77**
Bedside light	1.98	1.94	3.73	3.11	**1.19**

4.4.1 Appliances Association Analysis

For GREEND dataset, the strong association rules are exhibit by four appliances: radio, bedside light, dishwasher, and microwave. Table 4.6 shows the association rules, with support, confidence, and lift parameters with $min\_sup >= 0.2$. Further, the energy consumption curves of these appliances as represented in Fig. 4.5, compliments these association rules discovered and proves their simultaneous usage by the consumer. Similarly, associations rules are generated for UK-Dale appliances as well, as presented in Table 4.7. These associations results determine occupants' behavioral traits. For example, a radio is used at the bedside light, depicting the occupant listens to the radio with the bedside light switched on. Moreover, for other occupants of the UK-Dale house, there is a strong association found in the usage of kettle, toaster, and

Table 4.3: Comparision of the proposed Ensemble model with reference forecasting models on GREEND data set with respect to MAE (W/m^2)

	FFNN	LSTM	CNN-LSTM	CNN-XG	**OURS**
Fridge	24.79	51.06	28.75	26.32	**22.33**
Dishwasher	3.18	3.66	4.95	3.06	**2.04**
Microwave	8.09	7.23	4.89	3.98	**2.86**
Water-kettle	22.00	29.68	11.67	11.02	**10.72**
Washing Machine	14.35	23.93	15.94	13.56	**11.97**
Radio	0.96	2.19	1.33	0.93	**0.66**
Dryer	1.33	0.83	0.82	0.73	**0.60**
Kitchenware	3.23	3.10	2.76	1.85	**0.62**
Bedside light	0.16	0.19	0.15	0.14	**0.13**

kitchen light. It means that the occupant likes to use a kettle and toaster while in the kitchen.

4.4.2 Training Time Analysis

In terms of training time, the FFNN model takes 7 seconds per epoch, the LSTM model takes 600 seconds per epoch, CNN-LSTM takes 401 seconds per epoch, CNN-XGBoost takes 700 seconds per epoch, and the proposed model takes 800 seconds per epoch. Its better performance can compensate for the more significant training time of the proposed model. The 800 seconds per epoch are taken during training the model. Once the model is trained, it gives comparable performance to other reference models for real-time prediction.

Table 4.4: Comparision of the proposed Ensemble model with reference forecasting models on UK-Dale data set with respect to RMSE (W/m^2)

	FFNN	LSTM	CNN-LSTM	CNN-XG	**OURS**
Boiler	35.19	48.80	32.24	31.06	**29.69**
Thermal pump	0.78	1.43	0.86	0.80	**0.73**
Laptop	3.29	2.64	0.96	0.90	**0.88**
TV	4.50	5.67	4.41	3.79	**2.88**
LED Lamp	0.42	0.77	0.43	0.38	**0.34**
Kitchen Light	13.63	13.48	14.18	12.65	**10.39**
Kettle	6.10	6.21	6.12	4.61	**0.55**
Toaster	8.70	15.55	4.00	3.53	**2.69**

Table 4.5: Comparision of the proposed Ensemble model with reference forecasting models on UK-Dale data set with respect to MAE (W/m^2)

	FFNN	LSTM	CNN-LSTM	CNN-XG	**OURS**
Boiler	14.62	21.54	12.26	12.00	**10.94**
Thermal pump	0.29	0.70	0.49	0.38	**0.25**
Laptop	1.73	0.45	1.39	1.00	**0.40**
TV	2.12	2.19	2.20	2.04	**1.57**
LED Lamp	0.21	0.37	0.13	0.11	**0.01**
Kitchen Light	3.04	3.36	3.06	2.69	**1.86**
Kettle	0.39	0.39	0.87	0.74	**0.35**
Toaster	5.64	9.67	2.37	2.05	**1.35**

Table 4.6: Association Rules on GREEND equipments

S.no.	Association Rule	Support	Confidence	Lift
1.	Radio $\Longrightarrow$ Bedside light	0.16	0.89	1.2
2.	Dishwasher $\Longrightarrow$ Microwave	0.21	0.93	1.5
3.	Microwave $\Longrightarrow$ Dishwasher	0.24	0.92	1.4
4.	Bedside light $\Longrightarrow$ Radio	0.12	0.80	1.3

Table 4.7: Association Rules on UK_DALE equipments

S.no.	Association Rule	Support	Confidence	Lift
1.	Kettle, Toaster $\Longrightarrow$ Kitchen Light	0.20	0.90	1.6
2.	Kitchen Light $\Longrightarrow$ Toaster	0.18	0.80	1.1
3.	Solar Pump $\Longrightarrow$ Boiler	0.13	0.75	1.1
4.	Toaster $\Longrightarrow$ Laptop	0.15	0.78	1.2
5.	Kitchen Light $\Longrightarrow$ Kettle	0.19	0.92	1.5

4.5 Conclusion

Appliance-level power prediction is quite challenging due to the volatility and behavioral habits of individual consumers. An Ensemble deep learning model has been developed to capture the stochastic dynamics of appliances' power time-series data. It utilizes two powerful algorithms' inherent advantages: a deep learning-based CNN-LSTM and tree-based Xtreme Gradient Boosting (XG-Boost) for performance enhancement. The prediction is carried out at a 5-minute time horizon, which is best suited for load shifting under real-time pricing schemes. In addition, the dynamic item set counting (DIC) algorithm has been used to determine which appliances are often used together. Rigorous experimental analysis on two open-source data

sets (GREEND and UK-Dale) verifies the Ensemble model's outstanding performance in terms of RMSE and MAE accuracy metrics. The percentage decrease in RMSE of the proposed ensemble model in the GREEND data set is 32.18%, 49.54%, 27.73%, and 19.43% compared to FFNN, LSTM, CNN-LSTM and CNN-XGBoost, respectively. For the UK-Dale data set, the RMSE of the proposed Ensemble model is 40.58%, 65.09%, 27.17%, and 18.15%, lesser than FFNN, LSTM, CNN-LSTM, and CNN-XGBoost, respectively.

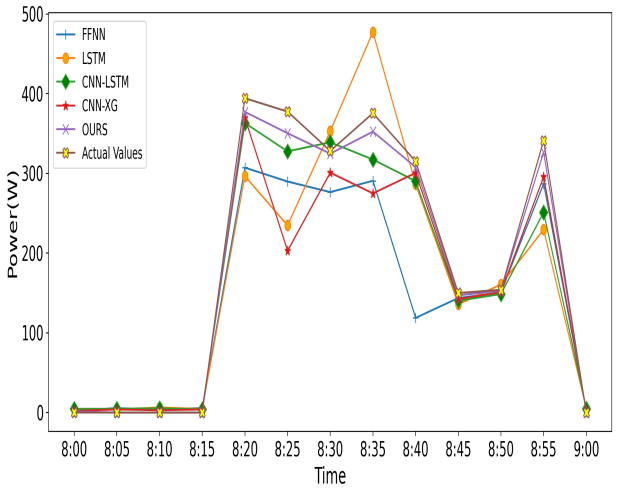

(a) Fridge

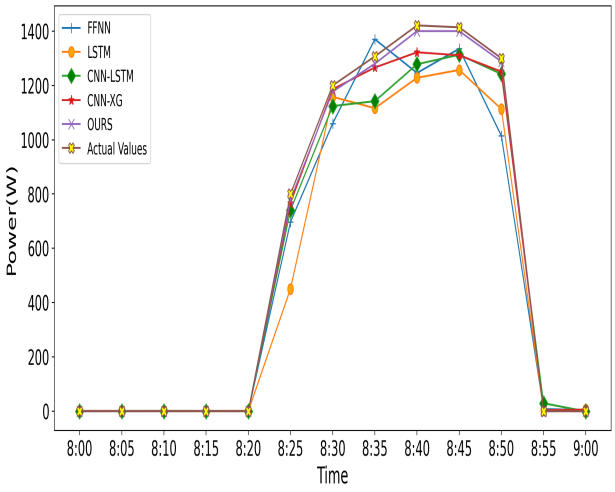

(b) Dishwasher

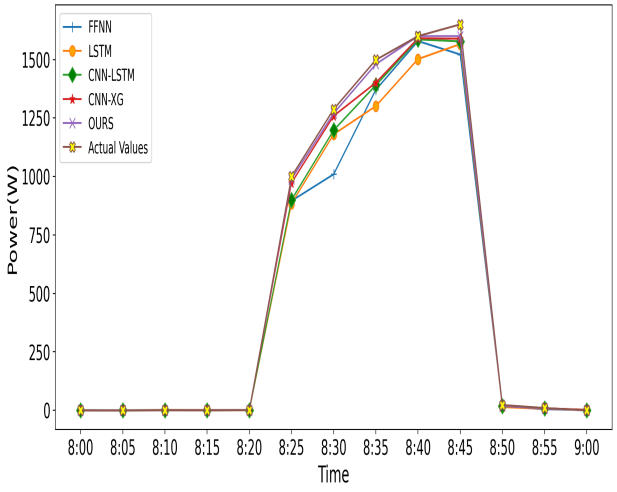

(c) Microwave

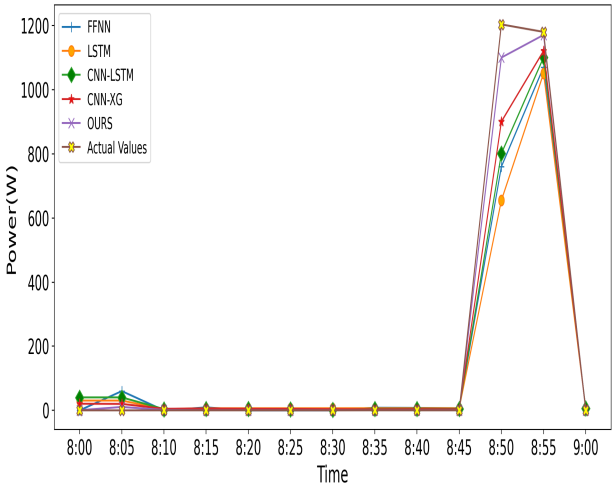

(d) Water-kettle

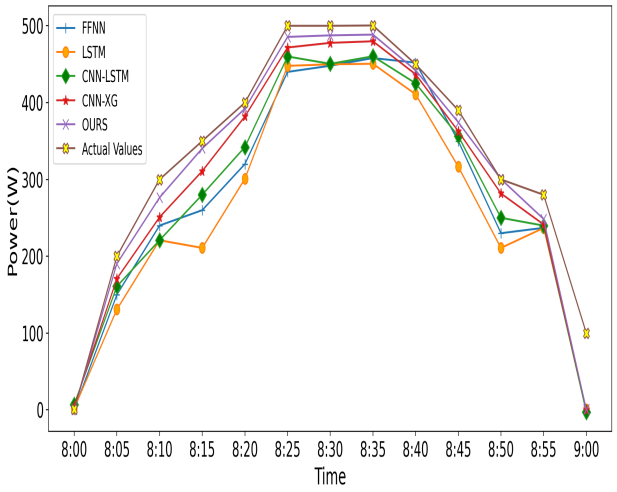

(e) Washing Machine

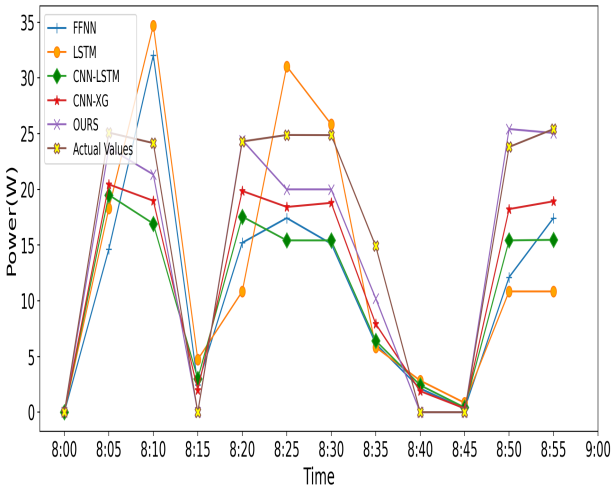

(f) Radio

Figure 4.3: Appliance-wise power forecasting using Ensemble model on GREEND appliances

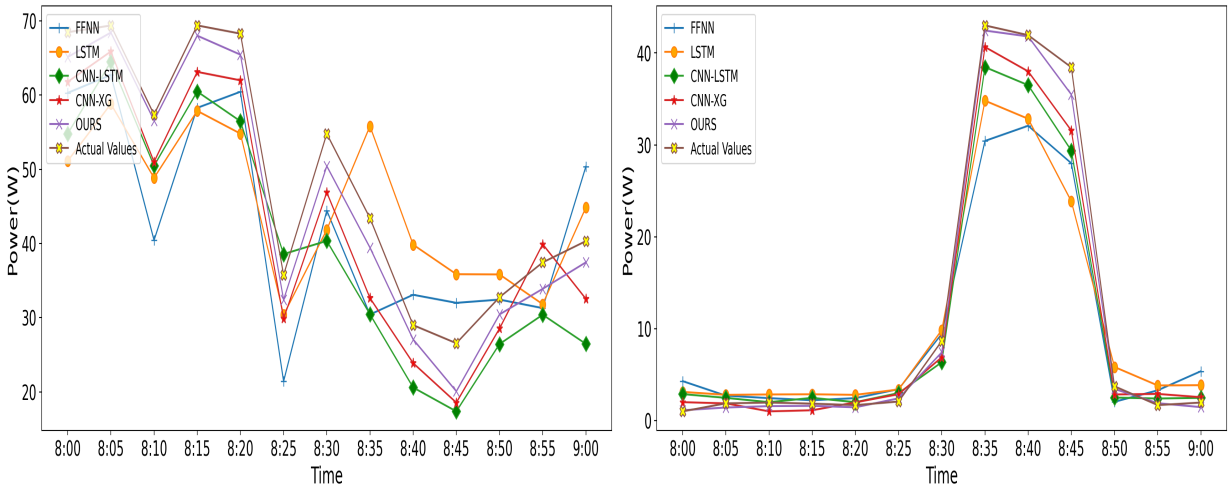

(a) Boiler

(b) Solar pump

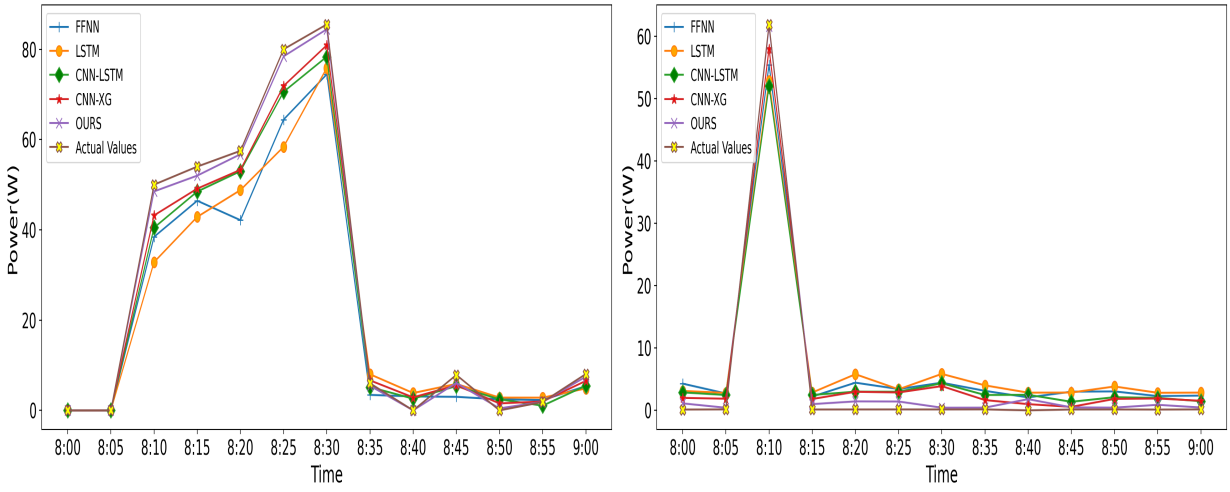

(c) Laptop

(d) Kitchen Light

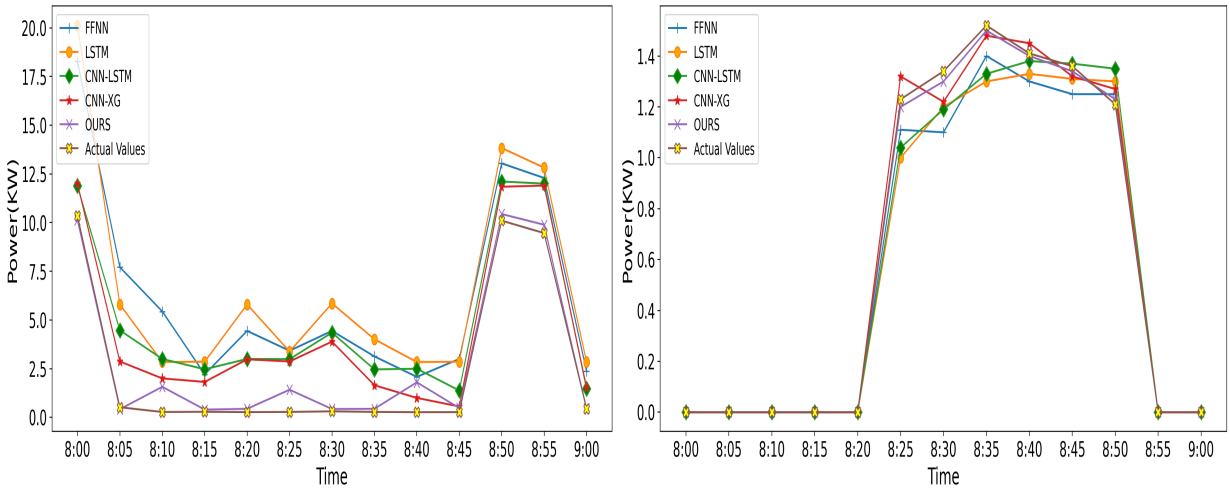

(e) Kettle

(f) Toaster

Figure 4.4: Appliance-wise power forecasting using Ensemble model on UK-Dale appliances

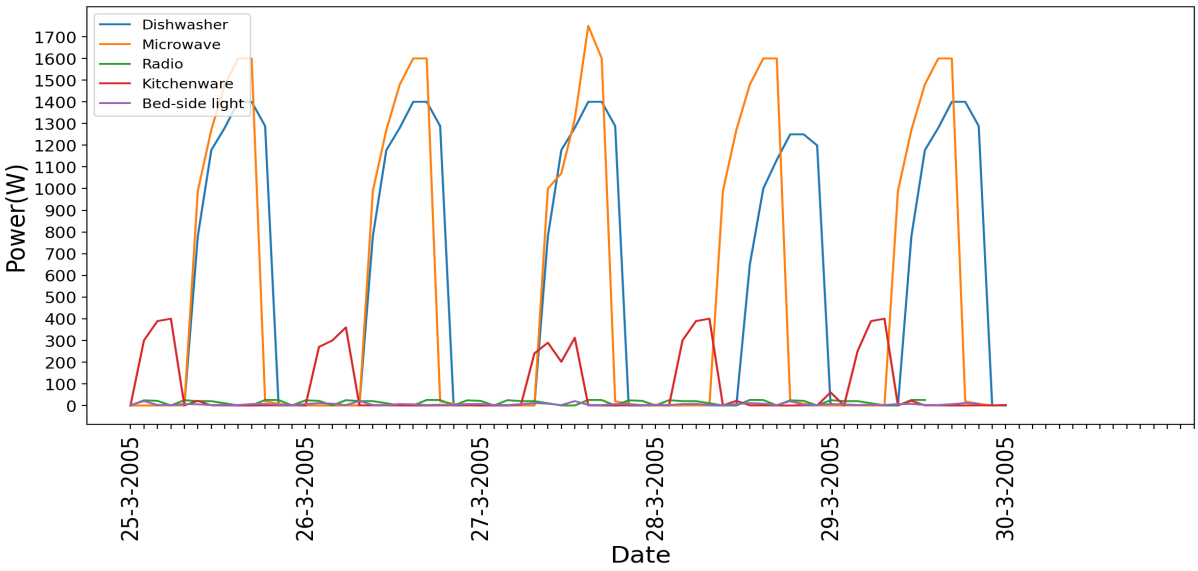

Figure 4.5: Associations represented by Energy curves

Chapter 5

A Real-Time Automated Scheduling Algorithm with PV Integration for Smart Home Prosumers

5.1 Introduction

Household energy consumption is often a noticeable problem, as it accounts for about 35 % of the total consumption of all activities [107]. Research conducted in [57] showed that 15% of energy savings could be achieved by shifting the load of controllable appliances in the household. With the advent of the smart grid, household consumers are actively participating in energy management through demand response programs. Consumers are now becoming Prosumers, i.e., consuming energy from the grid and producing and sharing energy with the grid. Moreover, there is direct communication with the grid using IoT-enabled devices [259]. The smart home of Prosumers consists of intelligent appliances, advanced metering infrastructure (AMI), smart thermostat, smart plugs, and wireless communication infrastructure. The schedul-

ing optimization problem for Prosumers mainly deals with minimizing their energy cost without affecting their comfort. In HEMS, the stochastic scheduling optimization problem involves arbitrary dynamics of consumer demand, renewable energy, consumer behavior, and electricity price.

The HEMS for demand response (DR) applications has been substantially studied by the researchers. The DR programs can be incentive-based or price-based. Incentive-based programs give reward to consumers for their participation in distributing load from on-peak to off-peak hours. On the other hand, price-based programs involve different price signals to provide monetary savings to the consumers. Different types of price signals include real-time price (RTP), time-of-use (ToU), inclined block rate (IBR), critical peak pricing (CPP), and day-ahead pricing [203]. Price-based programs are the main focus of researchers in the field of DR programs for home energy management system (HEMS). The optimization algorithms proposed by researchers in previous studies based on ToU pricing [126, 171], RTP price [155, 86], Combined RTP and IBR [45], CPP [141, 147], Day-ahead price [68, 165, 79].

Our previous work in [202] comprehensively discusses the various challenges associated with solving the complex optimization problem of load shifting in IoT-enabled DSM. The various optimization techniques can be classified into four broad categories: mathematical programming, meta-heuristics, artificial intelligence (AI), and game theory. Mathematical programming involving mixed-integer linear programming (MILP) and non-linear programming (MINLP) is most popular among researchers. Many current commercially available solvers can find the optimal global solution easily, effectively, and quickly. MILP based model has been used to minimize energy and water use and CO_2 emission besides monetization for the householder [53], cost minimization using RTP pricing [70], smart thermostat combined with scheduling of home appliances [46]. However, MILP based model cannot work on non-linear constraints directly.

Moreover, it suffers from the risk of the problem being high-dimensional. The meta-heuristic algorithms have been mainly compared based on their convergence rate and accuracy of optimal solution where particle swarm optimization (PSO) [91, 60] and genetic algorithm (GA) [156, 145] is found to be most popular. It has also been found that the heuristic algorithm could get stuck in local optima while finding optimal solution suggesting a possible need for advanced algorithms that can ensure a global complete and optimal solution.

Researchers mainly use AI-based techniques for intelligent decision making, prediction, forecasting, and scheduling. The Reinforcement Learning (RL) architecture has been utilized to optimally monitor entire-building Heating, ventilation, and air conditioning (HVAC) systems for energy savings and thermal comfort [18, 189], and for learning consumers' dissatisfaction [243]. However, to run AI models, it is requisite to have expensive hardware with comparable processing power. AI models often work with only numerical values. Moreover, extensive testing with hardware is needed for validation and verification. The game theory methodology is used primarily to make decisions under unpredictable environmental circumstances, i.e., local energy trading [175] involving selfish and rational consumers. However, the increase in the number of players makes the use of game theory complex and challenging. Also, it uses only general rules of logic without telling about the winning strategy. Using this approach, uncertainty in the real field is difficult to model.

The previous studies mainly focus on the development of scheduling algorithm alone, without really implementing in real-time scenario i.e., controlling home appliances by developing smart plugs. Moreover, a subset of home appliances was taken into account without considering their intermediate operation cycles.

In this study, IoT-enabled smart plugs integrated with cloud infrastructure have been designed to store load profiles of appliances and control their operation from the cloud. Moreover, an efficient scheduling algorithm is developed considering integrated PV resources, maximum possible appliances, different operating cycles of appliances, various types of other constraints in the presence of different price signals. The scheduling algorithm runs on the cloud with a duration of 5-min for real-time DR implementation and autonomously sends control signals to appliances. Extensive simulations and results demonstrate that the proposed framework greatly minimizes the consumers' electricity cost without any change in consumption pattern.

5.2 Overview of automated IoT based energy management

An automated energy management system consists of three main components: IoT-based Node-MCU hardware equipped with sensors and various relays, adafruit cloud, and scheduler algorithm. The Node-MCU ESP8266 device has been used to measure the power of various home

appliances and control the appliances by changing their operating state. The adafruit cloud is used to store the measured power of different types of equipments and run the scheduler algorithm. The scheduler algorithm solves the problem of multi-objective optimization, i.e., decreasing electricity cost and PAR (peak to average ratio) of the consumer while maintaining comfort.

The framework of IoT-enabled automated scheduler has been shown in Fig. 5.1. The power measurements from various types of home appliances (fixed, thermostatically controllable (TCL), and non-thermostatically controllable (non-TCL)) are measured by sensors embedded in Node-MCU, then MQTT publish protocol is used to send the measurement values to Adafruit cloud. The data collection script is run on the cloud, which creates the load profile of each appliance according to the measured values. The automated scheduler algorithm is a software program that takes multiple inputs and decides the schedule of all appliances for a day in 5 min slots. The inputs of the scheduler consist of 1) Load profile of all home appliances, 2) Photo-voltaic (PV) unit output for a day, 3) Pricing scheme (RTP, ToU, CPP), 4) various other constraints which should be satisfied for correct scheduling. The scheduling algorithm is based on the dynamic least slack-time-based algorithm, which depends on the price-data, outputs a schedule that uses the PV power at peak prices, and stores the extra PV power in the battery for future use. The output of the scheduler is the schedule of all appliances for a day in 5-minute slots, which reduces the electricity cost while running all appliances according to the consumer's comfortable timings. The scheduling decisions of the algorithm are published on the Adafruit cloud using a data-publish script. Using the MQTT download packet, the scheduling decisions are downloaded into the Node-MCU device, which wirelessly controls (On/Off) the home appliances according to schedule.

5.2.1 Load Profile of Smart Appliances

Table 5.1 [155] represents typical load specifications of different types of appliances. Appliances can be categorized into two types: electrical controllable (ECL) and thermostatically controllable (TCL). The table specifies the earliest start time (EST) and latest finish time (LFT) of all appliances. The window is the difference between LFT and EST, which tells about the maximum duration an appliance can be delayed. Since some appliances operate in different

Table 5.1:

Load specification of Home Appliances [155]

S.no	Appliance	Type	Pow (KW)	Duration (h)	EST (h)	LFT (h)	Window (h)
1	Washing machine	ECL	1.7	2	8	11	3
2	Dish washer	ECL	1.6	1	8	16	8
3	Dryer	ECL	2.4	1	12	17	5
4	Microwave	ECL	1.6	1	6	8	2
5	Oven	ECL	2.4	2	14	18	4
6	Cooker hood	ECL	0.25	1	16	18	2
7.	Refrigerator	TCL	0.185	24	0	24	24
8	Water Heater	TCL	1.6	24	0	24	24
9	AC	TCL	1.35	12	12	24	12
10	TV	ECL	0.24	6	18	24	6
11	Desktop	ECL	0.4	2	20	24	10
12	Iron	ECL	2.5	1.5	5	15	10
13	Laptop	ECL	0.2	5	18	24	6
14	Vaccum cleaner	ECL	2.3	1.5	7	18	11
15	Sensors	ECL	0.03	24	0	24	24
16	Radio Player	ECL	0.22	1.5	6	8	2
17	Illumination	ECL	0.6	6	17	24	7
18	Others	ECL	3.5	4	0	24	24

Table 5.2:

Different Types of Prices [195]

Case	Non-peak	Peak (9-12 AM)	Critical Peak (6-8 PM)
Base case	Tarriff: 0.05 /kWh		
ToU	0.049 /kWh	0.08 /kWh	0.16 /kWh
CPP	0.08 /kWh		0.118 /kWh
RTP	0.048, 0.045, 0.043, 0.043, 0.044, 0.046, 0.054, 0.064		
	0.081, 0.080, 0.070, 0.060, 0.053, 0.052, 0.054, 0.059, 0.067		
	0.093, 0.091, 0.083, 0.060, 0.054, 0.053, 0.050 /kWh		

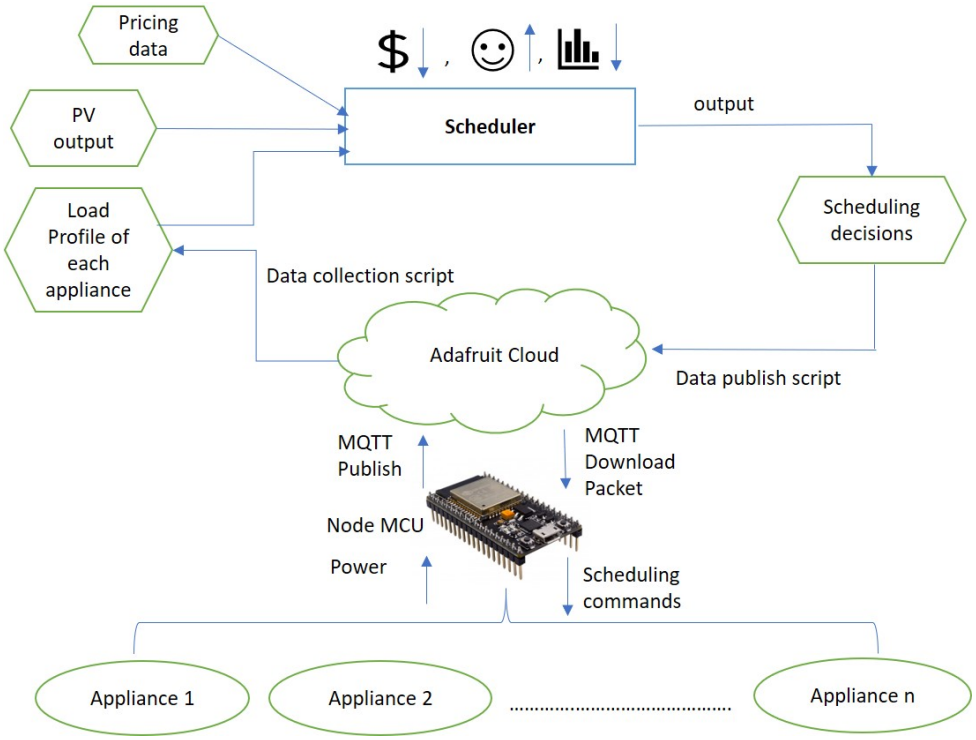

Figure 5.1: Framework of the IoT enabled automated scheduler

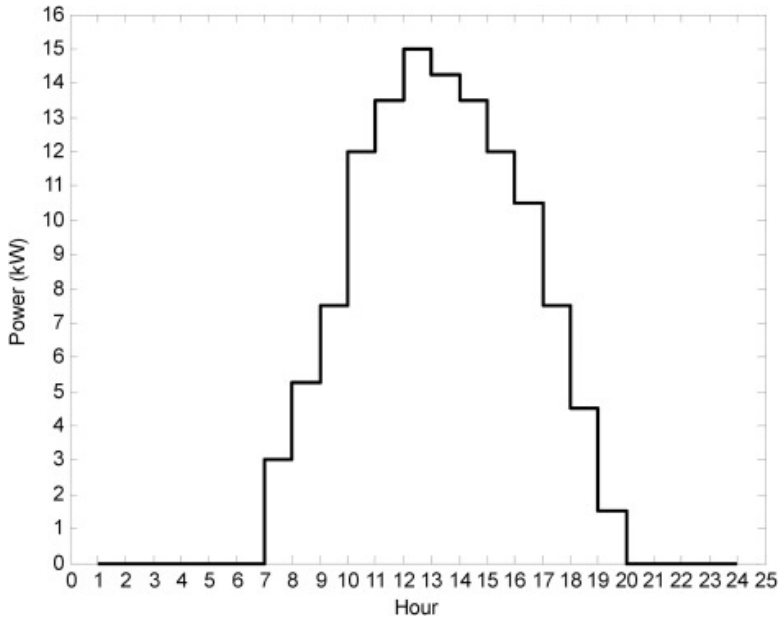

Figure 5.2: Typical PV output

phases, consuming different power in each phase; therefore, each phase has been considered individually. The different operating phases with power requirements and operational time of controllable appliances have been described in different tables. The operating phases of con-

trollable appliances namely, dishwasher, washing machine, and dryer has been described in Table A6[210], Table A7[210], and Table A8[210] respectively. While designing the scheduling algorithm, these appliances operating cycles have been taken into account for efficiency purposes.

5.2.2 Integration of Renewable Energy

The power generated by the PV source at each time slot t can be represented as $P_{PV}(t)$ where $t \in \{1,2,...,24\}$. The typical PV output taken for this study is presented in Fig. 5.2. The 24 hour PV power can be forecasted for designing more efficient and real-time scheduling. Our previous work [200] on forecasting solar irradiance (GHI) can be used to forecast robust GHI at any location.

5.2.3 Constraints

The scheduling optimization problem discussed in the literature includes several constraints. Such constraints are both at the level of the system and the level of the appliance. Constraints will be discussed as follows:

5.2.3.1 Balancing Electrical Demand Supply

The demand supply balance is the major concern for the grid operators which is directly affected by consumer behavior. Without considering Load Shifting-

$$P_{grid}(h) - P_{batt}(h) = D_p(h) \tag{5.1}$$

Considering Load Shifting-

$$P_{grid}(h) - P_{batt}(h) = D_{ns}(h) + \sum_{N_{sh}}^{n=1} D_{sh}^{n} \tag{5.2}$$

5.2.3.2 Maintaining temperature for TCLs [88]

Within scheduling time window, the temperature range of TCLs (EWH and HVAC) should be maintained in preset range $T^{\min}, T^{\max}$ provided the household occupancy.

HVAC-

$$T_{room}^{\min} \leq T_{room}^{i} \leq T_{room}^{\max} \tag{5.3}$$

EWH -

$$T_{out}^{\min} \leq T_{out}^{i} \leq T_{out}^{\max} \tag{5.4}$$

5.2.3.3 Battery related Constraints [91]

The state of charge (SOC) of the battery should be preserved within a predetermined range for its efficient and long use. Hence, the following constraint is needed -

$$Batt\_SOC_{\min}(h) \leq Batt\_SOC(h) \leq Batt\_SOC_{\max}(h) \tag{5.5}$$

$$Batt\_SOC(h) = Batt\_E(h)/Batt^{cap} \tag{5.6}$$

Battery maximum charging and discharging power limit can be represented as:

$$0 \leq \frac{P_{batt}^{ch}(h)}{\delta_{ch}} \leq P_{\max}^{ch} \tag{5.7}$$

$$0 \leq P_{batt}^{dch}(h) \cdot \delta_{ch} \leq P_{\max}^{dch} \tag{5.8}$$

5.2.3.4 Grid Constraints

At any time slot, the energy provided by the grid should be non-negative and bounded by upper limit.

$$0 \leq P_{grid}(h) \leq P_{grid}^{\max}(h) \tag{5.9}$$

5.2.3.5 Phase Wise Energy requirement of Appliances

The controllable appliances (washing-machine, dishwasher, dryer) should receives enough power for their particular operating cycle.

$$\sum_{k=1}^{m} p_{ij}^{k} = E_{ij,} \forall i, j \tag{5.10}$$

5.2.3.6 Power Limit Constraint

At a given time slot, the total power used by all operating devices should always be less than the maximum energy from the grid.

$$\sum_{i=1}^{N} \sum_{j=1}^{m} p_{ij}^{h} \leq P_{grid}^{\max}(h), \forall i, j \tag{5.11}$$

5.2.3.7 Operating Cycle Constraint

A running appliance cannot be turned off at a given time slot until the corresponding operating cycle is completed, e.g., dishwasher

$$\begin{aligned} &W_n(h) + W_n(h+1) + ... + W_n(h+TOC_n - 1) \geq \\ &(TOC_n - 1) \cdot (W_n(h-1) - W_n(h-2)), \forall h \in h_n \end{aligned} \tag{5.12}$$

5.2.3.8 Operation Ordering of Appliances

The ordering of appliances should be preserved. A dryer can, for example, be run after the washing machine has done its task. Therefore, if the shiftable load is handled after a shiftable load, then:

$$\begin{aligned} &W_m(h+TOC_n) + W_m(h+1+TOC_n) + ... \\ &+W_m(h+TOC_n+TOC_m) \geq (TOC_m - 1) \\ &\cdot (W_n(h-1) - W_n(h-2)), \forall h \in h_n \end{aligned} \tag{5.13}$$

5.3 Problem Formulation

5.3.1 Energy Consumption Model

Table 5.1 indicates all appliances can be categorized into ECLs and TCLs. The ECL appliances can be further categorized into fixed and controllable depending upon their flexibility for participating in the scheduling algorithm. The fixed appliances are also known as must-run because their operation cannot be delayed further. In contrast, the controllable appliances (dishwasher, washing machine) can be shifted (fully or operation cycle) for a run at later intervals.

The total energy consumed at each time slot t by all types of appliances can be calculated

by the following equation:

$$P_{total}(t) = P_{Fixed}(t) + P_{Controllable}(t) + P_{TCLs}(t) \tag{5.14}$$

5.3.2 Energy Cost Model

The cost of energy is calculated by multiplying energy consumed by appliances with the price at that period.

$$C = \sum_{t=1}^{T} (Pow_{total}(t) \times price_t) \tag{5.15}$$

$$C = \sum_{t=1}^{T} \sum_{i=1}^{N} Pow_i \times price_t \times K_{i,t}^{opt} \times lt \tag{5.16}$$

where T is total number of periods in scheduling cycle, lt is length of each time period, N is total number of appliances, Pow_i stands for rated power of i^th appliance, $price_t$ is electricity price in period t, $K_{i,t}^{opt}$ is operation status of i^{th} appliance after optimization. Different types of electric tariffs exist for defining energy pricing over a day such as Time of use (ToU), Day-ahead price (DAP), Real-time price (RTP), Critical peak pricing (CPP).

5.3.3 Inconvenience

Consumer inconvenience is directly related to advance or delay in the appliance running behavior. The length of advance or delay time can be calculated using the following equation:

$$I = \sum_{i=1}^{N} \sum_{t=1}^{T} (K_{i,t}^{opt} - K_{i,t}^{b}) \tag{5.17}$$

where $K_{i,t}^{b}$ stands for baseline on/off status.

The objective function for scheduling algorithm will be minimizing both energy cost and inconvenience. Also, peak to average (PAR) value should be as least as possible for an optimal scheduling decision.

$$Obj = min(C) + min(I) + min(PAR) \tag{5.18}$$

5.4 Proposed Automated Scheduling Algorithm

The multi-objective scheduling optimization problem of minimizing the electricity cost of consumers and PAR (peak-to-average ratio) with maximum comfort is highly complex. An automated and dynamic algorithm has been developed using modified least slack time to solve the stochastic problem involving so many constraints, different categories of appliances, stochastic PV output, and different pricing scenarios.

Four different types of lists are created, namely, $task\_list$ containing all the appliances to be scheduled, $PV - power$ containing output power of the PV source at different times of the day, $price\_list$ storing price information at different durations of the day, $ready\_list$ storing appliances which are ready to run at a particular instant. The different parameters considered for each appliance are maintained in a separate data structure. These lists can be represented as follows:

$$task\_list = \{appliance_1, appliance_2, ...appliance_n\}$$

where for each appliance, its data structure contains following information:

$$\begin{aligned} appliance\_struct = \{&id, appliance\_type, earliest\_start\_time,\\ &latest\_finish\_time, total\_duration, pow\_rq,\\ &no\_of\_operating\_cycles, slack\_time\} \end{aligned}$$

$PV - power = P_{PV}(t)$ where $t \in \{1, 2, ..., 24\}$

$price\_list = price_t$ where $t \in \{1, 2, ..., 24\}$

If multiple appliances are ready to run at some instant t then *ready_list* is initialized with all ready appliances in order of their priority (highest priority first). The priority of all ready appliances has been calculated using the dynamic slack time algorithm.

5.4.1 Appliance' State Change Procedure

The state of an appliance based on the time taken by its operating cycles has been described in this section.

Assuming the particular operating cycle of appliance takes n time slots. The operating state of appliance A at a time slot t:

$$\chi_t^A = (r_t^A, d_t^A)$$

where r_t^A denotes number of remaining operating cycles of appliance A, d_t^A indicates the number of time-slots for appliance A operation can be delayed and $\chi_t^A \in \{0,1\}$ indicates whether appliance A has been scheduled to run at timeslot t.

The state of appliance A at time $t+1$, (χ_{t+1}^A)depends upon its current state χ_t^A, $appliance\_type$ and operating decision made by scheduling algorithm by taking price and PV power at time t into consideration.

procedure SCHEDULING ALGORITHM

n: Number of appliances in *ready_list*

Pow_i: Power required to run appliance i

Pwr: Total power consumption of accepted requests from the grid (initialized with 0)

Pwr_max: Maximum power consumption threshold

$price_{max}$: Maximum price threshold

Require:

initialize *ready_list* as R with n appliances

Ensure: 24-hour schedule of all appliances with 5 min time slots

for $t \in \{1,2,...,288\}$ **do**

for each appliance $A_i \in R$ **do**

if ($price_t \geq price_{max}$) AND ($Batt\_SOC(t) \geq Batt\_SOC_{min}$) **then**

Run appliance A_i

change state(A_i)= running

Remove A_i from R

$Batt\_SOC(t) = Batt\_SOC(t) - Pow(A_i)$

else if $price_t \leq price_{max}$ **then**

Run appliance A_i

change state(A_i)= running

Remove A_i from R

$Pwr = Pwr + Pow(A_i)$

else if $SOC_{battery} \leq SOC_{min}$ & $P_{PV}(t) \geq 0$ **then**

change battery state to charging

else

change state (A_i)= waiting

end if

end for

end for

for all $A_i \in$ waiting state **do**

if $latest\_finish\_time(A_i) - t \geq 0$ **then**

$slack(A_i)++$

else

run appliance A_i

$Pwr = Pwr + Pow(A_i)$

end if

end for

end procedure

The slack time parameter of all the appliances gets updated at every time slot according to the following parameter:

slack(or priority) = remaining time to $latest\_finish\_time(A_i)$ - remaining execution time.

The above scheduling algorithm runs the appliance if the price at a particular time slot is less than the threshold price or if sufficient power is available in the battery to run the appliance

(when prices are higher). At the peak time of day (11 am - 3 pm), the PV power is used to charge the battery so that it can be used to run appliances in the late evening and night time. The consumer comfort is maintained using the slack parameter, which takes care of the latest finish time of the appliance and increases the appliance's priority accordingly.

The scheduling algorithm has been run and executed using Python on Anaconda platform. The code of algorithm can be found in [201].

5.5 Case Study

In this section, simulation studies are carried out to verify the effectiveness of the proposed algorithm. Eighteen different types of appliances are considered as mentioned in Table 5.1. There are three TCLs and fifteen different ECLs devices. There are some controllable devices with different operating cycles: washing machine, dishwasher, and dryer. TCLs devices can be controlled by shifting their temperature as their operation cannot be delayed for comfort maintenance. The load shifting decision greatly depends on the pricing scheme. All the different pricing schemes are utilized for simulation purpose.

As illustrated in Table 5.2, the base case uses a fixed rate tariff for electricity. The tariff is equivalent to the average of the RTP hourly rates. As a result, the base case accurately represents the function of the HEM mechanism without taking into account any demand response program (DRP). In TOU case, the off-peak tariff is 50% lower than the peak tariff, while the critical peak tariff is 50% higher than the off-peak tariff. A CPP scenario is also considered, in which a high electricity rate (e.g., 118 /KWh) is applied to consumption during critical peak hours.

It is assumed that the household contains a PV source of 5KW, while the impact of varying PV size is also analyzed. Increasing the size of PV and battery directly affects the cost reduction. The generation of a mentioned PV system has been forecasted based on solar irradiance available at a particular location. We utilized the forecasted GHI as per our previous work [200] to calculate the power produced by PV systems of varying sizes. Providing the least upper bound and greatest lower bound on forecasted values provides the robust forecasting estimate that effectively handles the stochastic nature of solar irradiance. The typical PV power output at location India as per Fig 5.2 has been utilized for simulation purposes.

The load profiles of different types of appliances have been recorded for two months at an interval of 5 minutes. The self-developed low-cost smart plug has been used for this purpose. The recorded load profiles are stored on Adafruit Cloud. Then, from these load profiles, the earliest start time and latest finish time of all appliances have been extracted, which is used as input to the scheduling algorithm running on the cloud. The consumer comfort-oriented scheduling algorithm checks the various constraints, the state of various appliances, current price, and send signals (on/off) to the smart plug, the operating instructions of the appliance according to their priority and power requirement.

The proposed algorithm adjusts itself according to specific consumer behavior i.e. the power consumption pattern of the appliances. For example, the smart plugs initially record the power requirement of various smart home appliances for two months. The current scheduling decisions are based on the consumer behavioral habits extracted from this data. A different deep learning algorithm has been utilized for this purpose. The behavioral habits may change with time, seasons, and various other factors reflected in the power consumption data obtained on the cloud. The changes in the operation pattern of various appliances are continuously tracked, which provides the changes in the load profile of each appliance to the scheduling algorithm. Hence, the scheduling algorithm decisions change/adapt to the change in the behavior of the consumer.

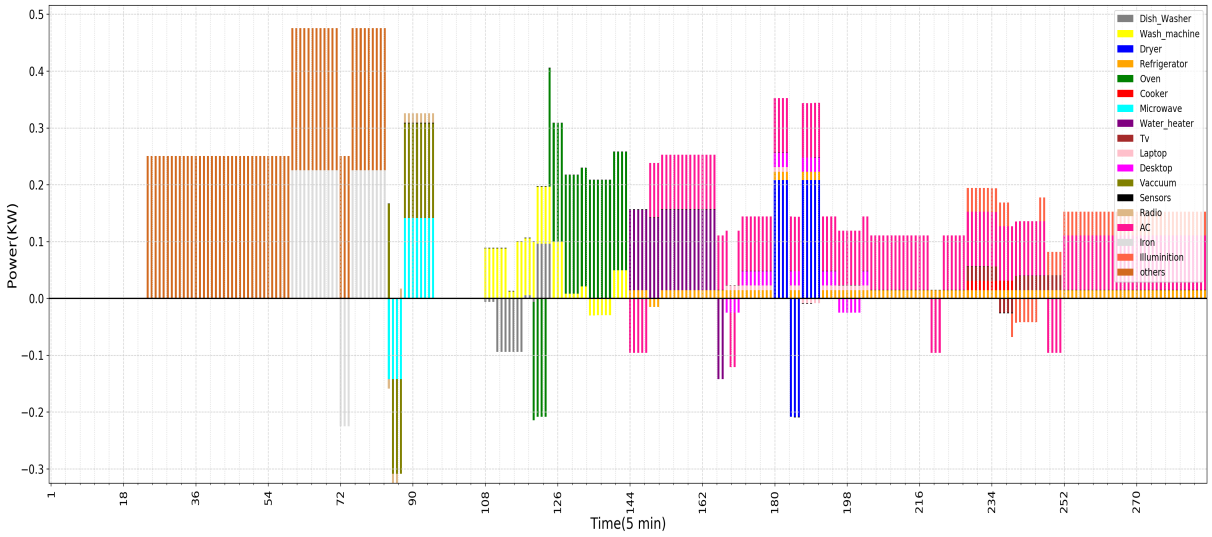

Figure 5.3: 24 hour (5-min slots) schedule of all appliances with RTP pricing scheme

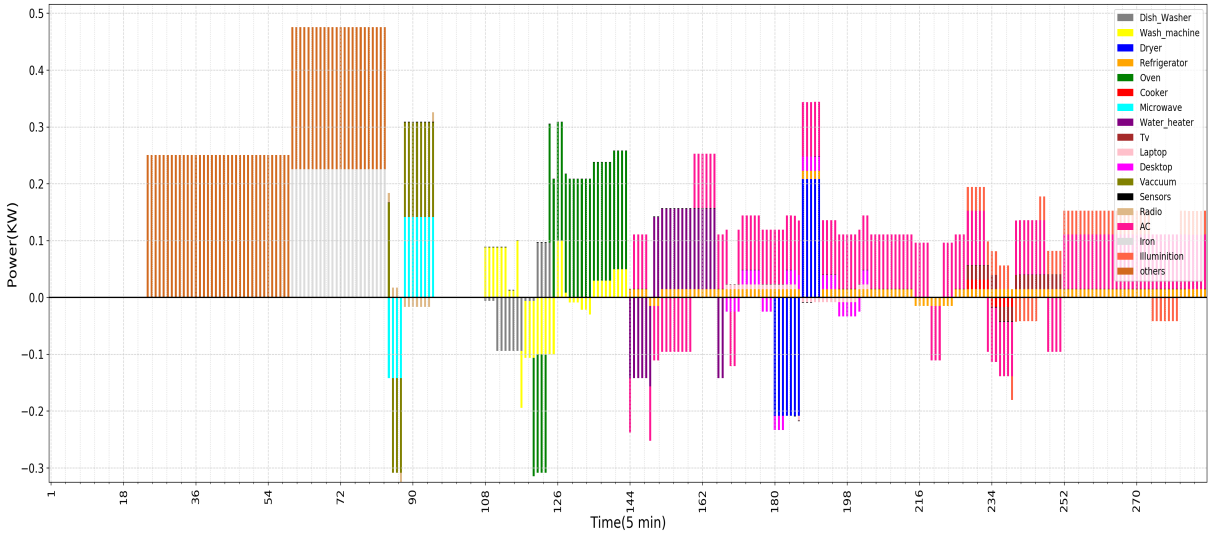

Figure 5.4: 24 hour (5-min slots) schedule of all appliances with ToU pricing scheme

5.6 Results and Analysis

5.6.1 Cost Reduction Analysis

The reduction in the electricity consumption cost can be analyzed using different pricing schemes for consumers using PV sources at their homes. It can be seen from Fig. 5.3, all the 18 different types of appliances mentioned in Table 5.1 are scheduled for a day using the RTP pricing scheme at 5 min interval. The proposed autonomous scheduling system sends operating instructions to each appliance using an IoT device according to the schedule obtained using the scheduling algorithm. Using a PV source of 5KW and a battery of 5KW, our proposed scheduling algorithm results in a cost-saving of up to 40% under the RTP pricing scheme. it can be seen that some appliances are running together at the same time-consuming energy from the grid. The negative power taken by appliances represents running using PV resource or battery thereby reducing the electricity bill. The PAR reduction has been automatically achieved since appliances' operation has been shifted to later periods at peak pricing. Under the time of use (ToU) pricing scheme as depicted in Fig.5.4, the cost-saving achieved comparable to the base case is up to 45%. Moreover, under the critical peak pricing (CPP) scheme, up to 48% cost saving has been achieved.

It can be observed from Fig. 5.4 that during peak hours (9 to 11 am) when the electricity price is at the higher side, our algorithm uses a battery to run many appliances depending on the availability of SOC. Meanwhile, since the availability of PV power is typically high from 9 am to 3 pm, it's a good time to charge the battery and use it to run ready appliances at peak period to minimize the PAR and electricity cost. Similarly, at the critical peak time (6 pm to 8 pm), the electricity price is highest. Again, the ready appliances are operated using a battery following the constraints mentioned in equations 5.5 and 5.6. At a non-peak period, around 6 am to 8 am, the energy from the grid is utilized to operate appliances; hence the peak in electricity consumption from grid can be seen at that time. In this way, 45% cost saving has been achieved as compared to the base case.

The sudden price increase can be observed in the RTP pricing scheme from 8 am (0.081) to 10 am (0.070). The scheduling graph in Fig.5.3 shows the negative and positive power consumption for some appliances from 9 am to 10 am (108 - 120 slots). It means that the algorithm utilizes a battery to run a current operating cycle of the dishwasher Table A6 and grid power for the washing machine Table A7. The SOC of the battery is not sufficient to run both the appliances concurrently as it is utilized at night. Again from 5 pm to 7 pm, the price is highest, the available SOC of battery has been utilized to operate ready appliances. For some appliances, the operation has been delayed depending on the high price and low SOC availability. The priority of each delayed appliance is increased to run it on urgent mode when its latest finish time comes nearer. In this way, 40% cost reduction is achieved using in RTP case.

5.6.2 Appliances Flexibility Analysis for DR

The house DR potential greatly depends on the flexibility of smart appliances. The 'flexibility' of appliance 'A' can be calculated as $Pow(A) \times window(A)$. Here, the window of appliance refers to the difference between latest finish time (LFT) and earliest start time (EST) of the appliance. There are 18 different types of appliances are considered in this study. Their operation time determines the behavioral habits of the consumer. The flexibility of various appliances has been represented in Fig. 5.6. The TCL appliance 'AC' shows greater flexibility as the consumer starts using it at noon and continues its use up to the night. It is easy to maintain comfortable

room temperature by changing its setpoint to some extent. Around 9 am, the consumer concurrently operates multiple controllable appliances. The dishwasher, washing machine, and oven tend to be operated together. It increases the DR potential as they can be operated by running them in intervals, according to the power required by their different operating cycles. In the afternoon, the flexibility of the house is quite poor because only one appliance (dryer) is in use together with a long operation time appliance (AC).

Because of the power use and the owners' habits, the versatility of appliances belonging to the same category but for different users can greatly vary. However, there is an exception in the case of refrigerators that operate all day for most consumers. The implication is that, unlike refrigerators, it would be impractical to build a single user behavior model for such appliances.

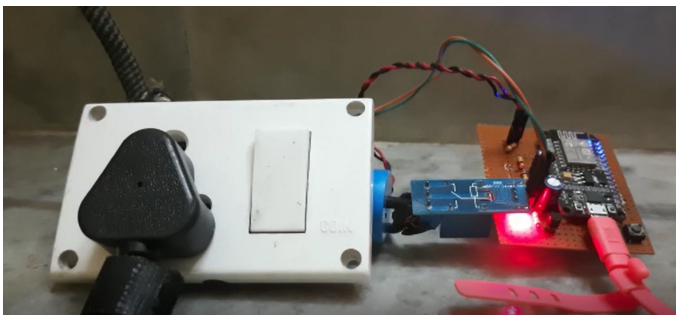

Figure 5.5: Smart Plug

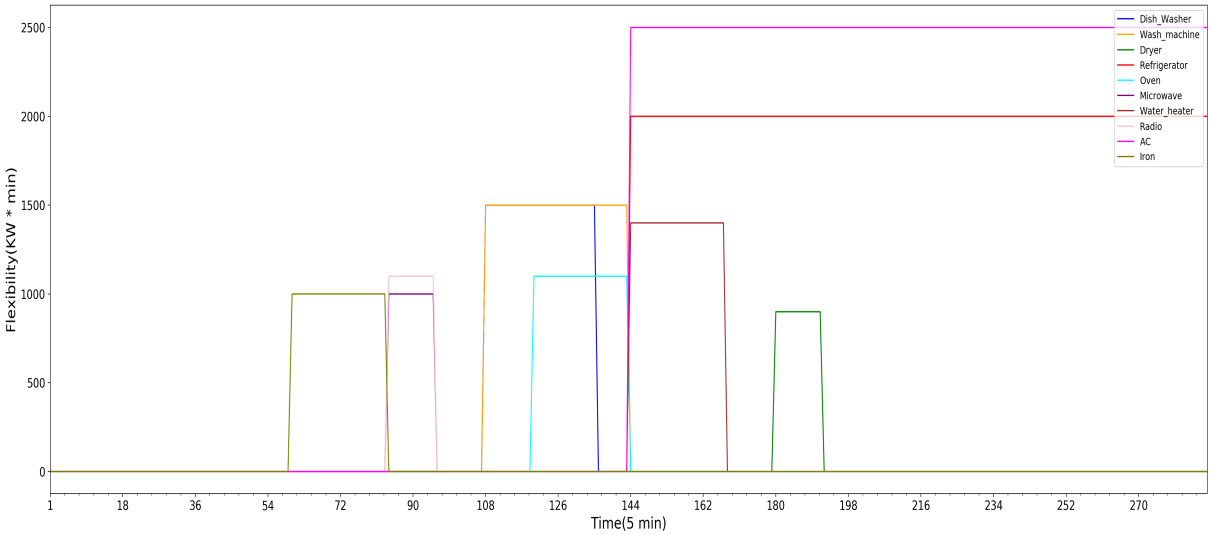

Figure 5.6: Flexibility of various appliances

5.6.3 Consumer Comfort Analysis

The multi-objective optimization targets both electricity cost reduction without affecting consumer comfortable operation timing of appliances'. All the appliances, including their operation cycles, have been scheduled by setting their priority according to their latest finish time as per Table 5.1. The scheduling algorithm design takes the utmost care of preparing all appliances within their time window. There is no comfort violation observed while appliances have been scheduled with different types of pricing schemes. However, the flexibility of appliances plays a significant role here. Greater the size of the time window of appliances 5.1 implies greater flexibility and greater comfort to the consumer.

The decisions of the proposed automated scheduling algorithm are based on many different parameters and constraints. The cost-saving relies heavily on the availability of PV power and consumer power usage patterns. Learning the behavioral pattern of consumers significantly helps the algorithm adapt to the new operation time of appliances'.

The smart plug developed for saving load profiles of different appliances can be seen in Fig. 5.5. In this figure, the smart plug is attached to the laptop charger, recording the power requirement to the cloud and sending scheduling decisions (on/off) at any instant to the device as well.

5.7 Conclusion & Future Work

This chapter describes an autonomous load shifting model for prosumers under a real-time environment by considering uncertainties of user behavior, PV output, various other constraints. The bottom-up approach deals with the design and development of a complete cost minimization solution for prosumers. The load profiles of all home appliances are gathered using self-created smart plugs based on IoT architecture. The least slack time-based scheduling algorithm that runs on the cloud schedules all home appliances, reducing electricity cost without consumer annoyance. Various types of constraints and different operating cycles of appliances have been taken into account for real-time implementation. Moreover, the flexibility of various appliances

to participate in the DR program proves the user behavior uncertainty. The average cost saving on different pricing schemes RTP, ToU, CPP is 40%, 45%, 48%, respectively. This performance has been recorded by strictly maintaining consumer behavioral habits.

Chapter 6

Graphical Computational Model for Smart Grid Reliability Assessment

6.1 Introduction

The power system is one of the most important infrastructures or critical infrastructure (CI), as it is reliant on almost all other infrastructures [67]. The reliability of information and communication technology (ICT) plays a major role in the smooth functioning of the smart grid. The smart grid is the smarter version of the power grid that involves the combination of traditional power grid and new ICT. Therefore, to construct a cyber physical system (CPS), that is, a smart grid, ICT is a crucial addition to conventional power system modules, allowing for improved flexibility and functionality. Although ICT systems improve functionality, they also lead to failures, such as unseen failures in protection systems, as seen in recent power outages. It also brings with it new challenges, including cyber attacks.

The functionalities of cyber components have been assumed perfectly reliable in the conventional reliability assessment phase. For conventional power grids where there was only

minimal cyber-physical interdependence, this assumption might be rational. However, modern power grid reliability is more reliant on the availability of cyber-enabled functions with the growing deployment of cyber infrastructure. To achieve more practical results, it is important to include cyber malfunctions in the assessment of power system reliability. The impact of cyber malfunctions on the reliability of composite power systems is investigated in this subject, which is referred to as "cyber-physical reliability" [78].

The efficiency of the power distribution system is calculated using indices such as the average system interruption period index (SAIDI) and the average system interruption frequency index (SAIFI)[63]. Using analytical or modeling methods, these indicators can be evaluated.

Analytical methods use mathematical models that are typically large and inefficient, but are used to analyze large-scale systems of complex schemes. Simulation methods based on the Monte Carlo method, on the other hand, take into account the actual procedure and random actions of network components. It takes into account component failure history as well as maintenance time data [44]. Embedded or non component-dependent faults, such as cold load pickup (CLPU), are not typically included in the estimates of these indices. As a consequence, these measurements can not accurately represent real device behaviour.

The Markov model [264], Reliability Block Diagram (RBD) [96, 209], fault-tree analysis [43], failure propagation studies [187], and state-mapping techniques [186] are some of the other works relevant to evaluating the direct cyber-to-power effect on system reliability. The majority of previous works necessitate a large amount of computational effort, and the computational time increases exponentially with the scale of the system under investigation.

The graph-theoretical approach to the smart grid is a solution to the above challenges. The aim of graphical approaches is to classify the nodes and edges that are most vulnerable to attacks and failures due to human error. The graphical reliability model takes into account both electrical (transmission line impedance) and reliability indices (probability of failure in network components). Reliability graphs were encoded in binary decision diagrams (BDD) to reduce the complexity of storage and computation [28]. Another valuable method for reliability analysis is Bayesian networks.

There are several other aspects and factors that affect the overall reliability of the network. Many techniques have been developed to determine the importance of a part in a network. An

analytical method based on state matrix which including different uncertainties of PHEV has been introduced in [142]. The criticality reliability importance to quantify the degree of impact of key component failures on system failure, mainly for fault diagnosis has been suggested in [236]. The redundancy value metric, which seeks to determine the incremental reliability growth of a system when an additional redundant variable is introduced. This metric is very useful for deciding the best degree of redundancy in reliability design [257]. The improvement potential (IP) to estimate the change in system efficiency when a part is perfectly improved [268]. Risk mitigation and risk achievement are the most widely used risk value indicators, which imply the contribution of a particular component to overall risk [103]. The Bayesian reliability value method was proposed to determine the weakest component that is more likely to be the cause of system failure [265].

However, since these approaches are heavily based on cause-and-effect relationships, they are unsuccessful in assessing the overall reliability of large interconnected ICT-EP systems and in examining the role of cyber infrastructure. As a consequence, a scalable but realistic tool is needed to assess the risk of interconnected system failure due to the reliability of the ICT system and to identify essential cyber components.

First, a graphical model is used to provide the structural significance of the ICT components within a Supervisory Control and Data Acquisition (SCADA) system. Second, a new metric named Network Accuracy Indicator (NAI) is developed to quantify the system's reliability. The Network Reliability Deterioration Worth (NRDW) index is used to rank the criticality of each node in the corresponding graphical model providing system reliability. Finally, simulations are performed on an IEEE 14-bus test case to prove that the proposed approach correctly tests the system's reliability parameters.

6.2 PROPOSED METHOD

6.2.1 Graphical modeling of Reliability Graph

To assess the risk of network failures, the network configuration is first plotted on a Reliability Graph, which is a pair of sets (V, E) where $V = V_1, V_2, V_3 ... V_m$ is the set of all vertices and $E = E_1, E_2, E_3 ... En$ is the set of all edges, with m and n being the number of nodes and edges, respectively. The paths in the graph can be broken out to understand the time constraints of a power system control action. The edge weight (E_w) has been assigned to each edge of the graph, and the vertex weight (V_w) has been assigned to each vertex, indicating the latency at each transmission path and component, respectively. The power system's latency threshold can be used to determine the possible transmission paths between a source and a target node.

The reliability of route from source node to target node with N number of nodes is the product of the each node's reliability along the path, where each node fails independently with failure rate f_n. The reliability of the path is given by the following equation:

$$R_{path} = \prod_{n=1}^{N} r_n = \prod_{n=1}^{n} 1 - f_n \tag{6.1}$$

where r_n and f_n determine the reliability and failure rate of node n, respectively.

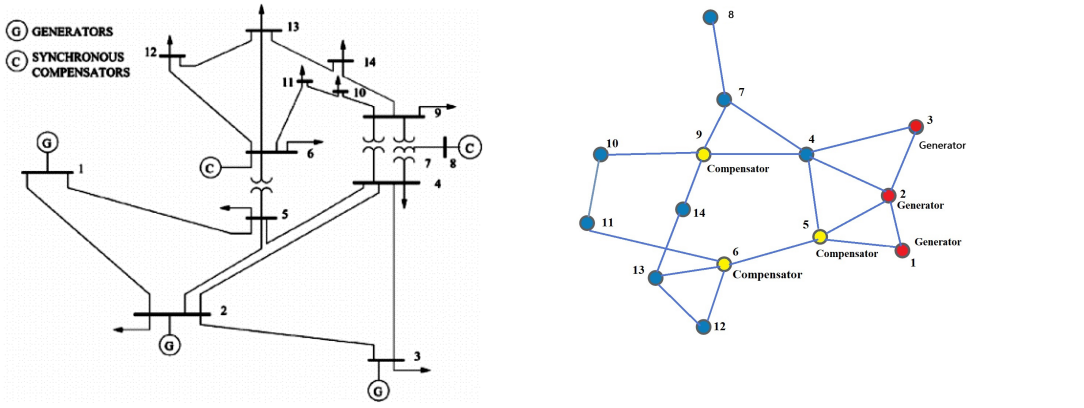

(a) IEEE-14 bus system

(b) Graphical model of IEEE-14 bus system

Figure 6.1: IEEE-14 bus system and its equivalent graph

Fig. 6.1 shows the IEEE-14 bus system and its equivalent graphical representation.

6.2.2 Reliability Analysis

Power system reliability is an important concern in the planning, construction, and operation of power distribution systems. Electric power utilities are expected to provide their customers with uninterrupted electrical service at the lowest possible cost while ensuring a reasonable level of service quality.

The value of reliability is demonstrated by the fact that it can be used to express the cost of service outages. The quality of service rendered by a distribution system can be calculated by its reliability indices, which can be enhanced by automating its feeder and related components, resulting in the desired reduction in power interruptions. Reliable power delivery networks are those that achieve a high degree of reliability.

A variety of studies have taken a systemic approach to smart grid stability, taking into account, to varying degrees, the effects of cyber network disturbances. The Dijkstra's algorithm has been used in graphical model to find reliability of each path [168]. However, 'shortest paths' may not be adequate to quantify the level of reliability of the system.

6.2.3 NETWORK ACCURACY INDICATOR (NAI)

To fix this problem, the Network Accuracy Indicator (NAI) has been introduced, which is based on complex Network Theory (CNT), and an algorithm for evaluating it is shown in Fig. 4. For a complete power system monitoring and control action, the depth-first search (DFS) has been used to explore all possible pathways between source node and target node. Then, the routes denoted by p_c that fulfil the latency requirements for a given power source has been filtered out. Subsequently, for all $p_x \in p_c$, the sum of the natural logarithm of the reliability value of each cut c_{hv} within the path p_x is determined. Finally, the NAI of the network is measured by

equation 6.2.

$$NAI = \frac{1}{N(N-1)} \prod_{x=1}^{R} \frac{1}{\prod_{h,v \in V_R} - \log c_{hv}} \tag{6.2}$$

where R is the total number of routes that meet the latency criteria and N is the total number of ICT components.

6.3 IMPORTANT MEASURES

For quantifying overall reliability of the power system, it is essential to discover metrics that quantify the relative importance of each node in the network. The two metrics, namely, Structural Importance (SI) and Total System Efficiency (TSE), have been used for this purpose. These are described in detail in following subsection.

6.3.1 STRUCTURAL IMPORTANCE

A component's structural importance (SI) is determined by the system's dependence on that component as well as the value it brings to the network's total efficiency (TSE). The structural value is calculated by the ratio of the difference between TSE(N) and TSE(N-I), which are the Total System's Efficiency with and without node I to TSE(N).

$$TSE = \frac{1}{N(N-1)} \prod_{i,j \in V_R} \frac{1}{d_{ij}} \tag{6.3}$$

$$SI = \frac{TSE(N) - TSE(N-I)}{TSE(N)} \tag{6.4}$$

where N denotes the total number of nodes in the network, and d_{ij} is the shortest path distance between node i and node j.

6.3.2 Network Reliability Deterioration Worth

Risk Achievement Worth (RAW), which calculates the refinement of a component's reliability to one to the overall device reliability, is one of the most commonly utilised punitive measure in nuclear power plant factories. Here, in power system network, it is important to deduce network reliability in terms of risk introduced by each component. Therefore, Network Reliability Deterioration Worth (NRDW) is defined by the following equation-

$$NRDW = NAI(1f)/NAI \tag{6.5}$$

where NAI stands for Network Accuracy Indicator in a normal state, and NRI(1f) stands for Network Misfiring Rate Indicator when the component's misfiring rate is one (i.e., The component is failed). The component's castigation is then measured as shown in Equation 5, where NAI(1f) is when the component's failure rate is one. When the NRDW is compared to the structural importance (SI) of a component, it can be deduced that the NRDW offers much better results than the pure structural index SI for locating the prime component in a network.

6.4 SIMULATION SETUP

Simulation is used in reliability modelling to classify nodes where the grid has the highest probability of system-level failure and to determine the system's overall criticality. The custom simulator based on PSAT [191], an open-source power system simulation environment has been utilized. The simulator sends a data file that describes the topology of the power grid and the requirements of the cyber infrastructure. The IEEE-14 bus system is used as a case study as it is a compact system with a small number of buses and transmission lines. It was important to begin with a small system in order to obtain a better understanding of the system's operation dynamics when line contingencies and distributed generation (DG) sources are implemented. The proposed method does not require a lot of computing power. The experiment we conducted can easily be applied to larger systems, such as the IEEE 57 or IEEE 118 bus systems, giving us a greater understanding of the dynamics of larger systems.

Table 6.1: All available paths from source to target.

Path No.	Path	Reliability	Latency
1	1-2	0.81	3ms
2	1-5-2	0.729	4ms
3	1-5-4-2	0.6561	5ms
4	1-5-4-3-2	0.59049	3ms
5	1-5-6-11-10-9-7-4-2	0.387420	4ms
6	1-5-6-11-10-9-7-4-3-2	0.3486784	5ms
7	1-5-6-12-13-14-9-7-4-2	0.3486784	3ms
8	1-5-6-12-13-14-9-7-4-3-2	0.3138105	4ms
9	1-5-6-13-14-9-7-4-2	0.3874204	5ms
10	1-5-6-13-14-9-7-4-3-2	0.3486784	3ms

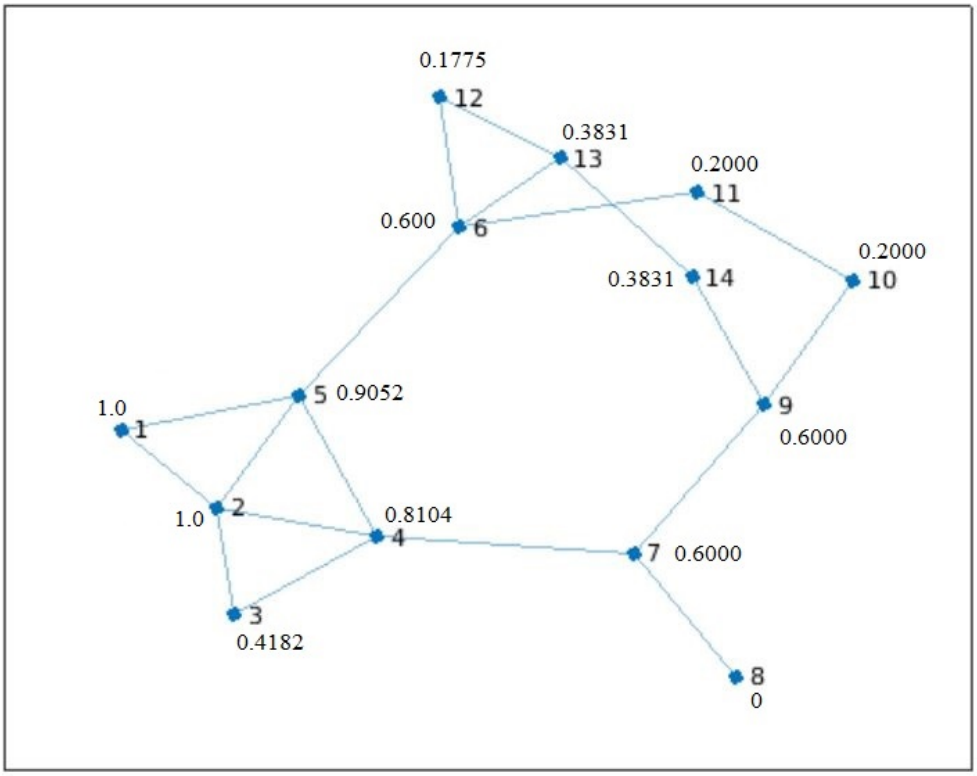

Figure 6.2: NRDW index of each node

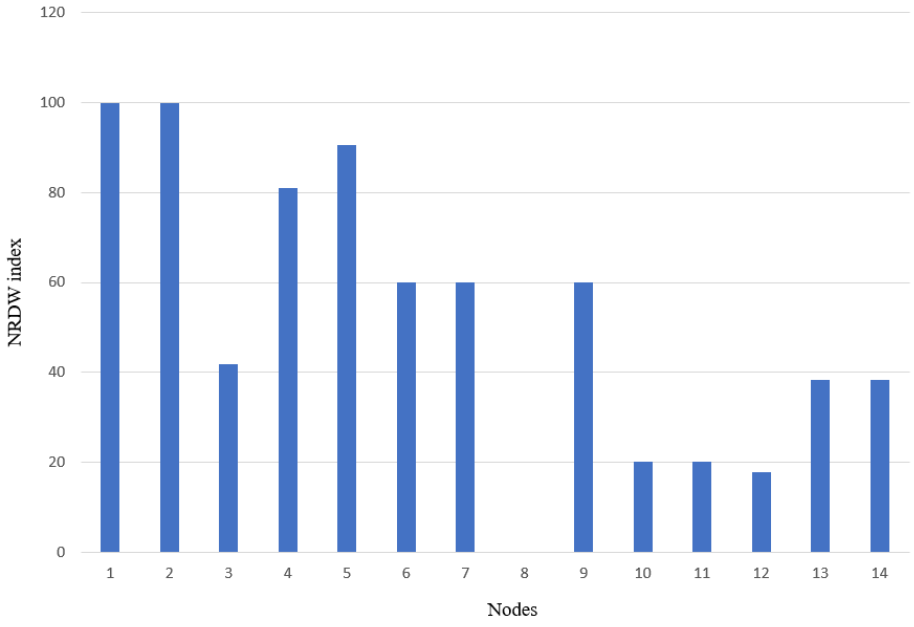

Figure 6.3: Comparing NRDW index of each node

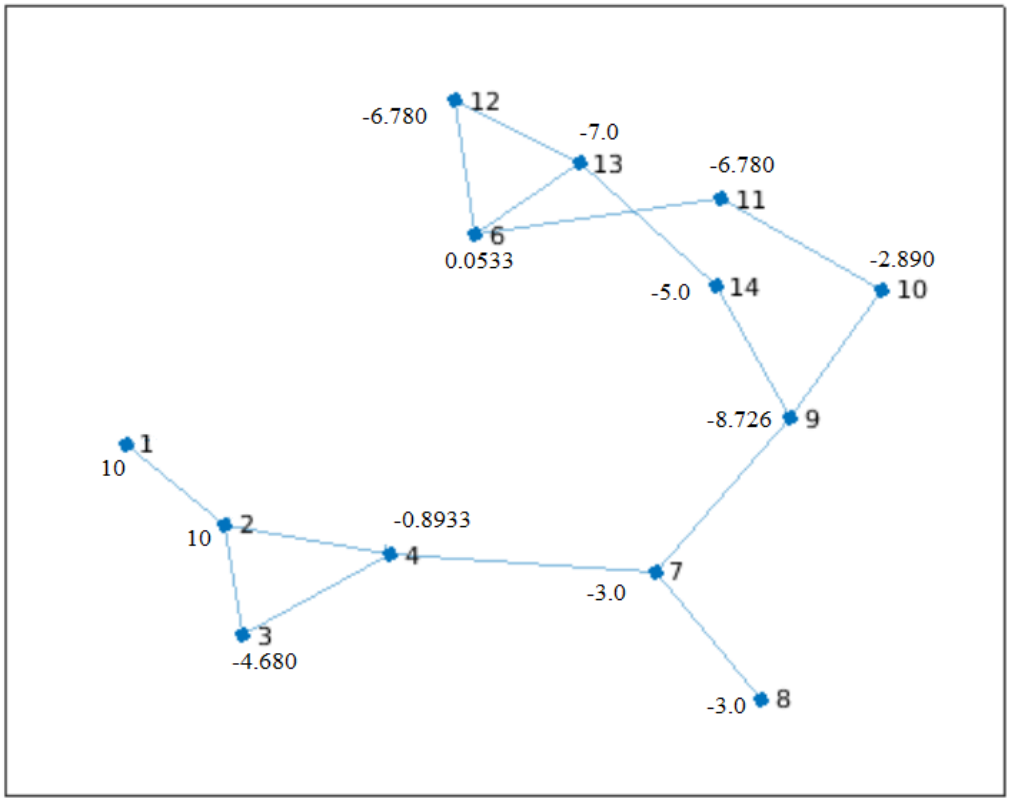

Figure 6.4: NRDW values after removal of critical node 5

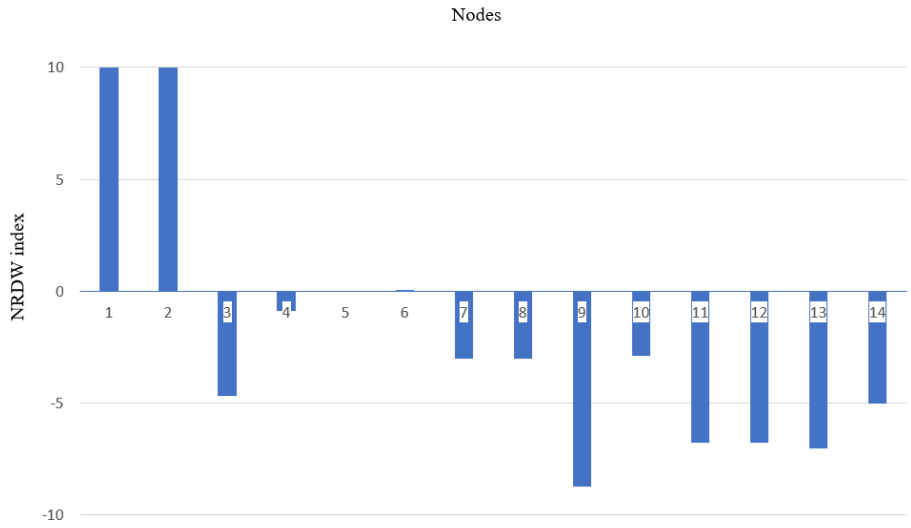

Figure 6.5: Comparing NRDW index after removal of critical Node 5

6.4.1 Case Study

The IEEE 14-bus test case is a simplified representation of the American Electric Power grid in February 1962. It has 14 buses, 5 engines, and 11 loads in total. The system's comprehensive

data can be found in [100].

6.4.2 Reliability Analysis

The failure rate of each node and the latency of each communication channel are initialized after the IEEE 14 bus system is modeled in its subsequent graph. The reliability of all N-node routes from the source to the target node is determined after this initialization. The node 1 is used as the source and node 2 as the target node in the case study.

The routing strategies and their total latencies are presented in 6.1, taking into account that the source node has a processing time of 1 sec, the target node's data collection time and command execution time are also 1 sec, and other nodes manage signals instantly. The 6.1 signifies that there are 10 different paths available from source node 1 to destination node 2. All paths have different reliability values c_{hv}. Also, all displayed paths fulfill the latency criteria, as its value has been provided with corresponding paths.

The NAI of the IEEE 14 bus system is determined using equation 6.2, it comes out to be 0.11.

6.4.3 NRDW analysis

After that, each component's NRDW index is determined using equation 5. The NRDW index of each node in the system graph is shown in Fig.6.2.

When the findings in Fig.6.3 are contrasted, the structural significance of node 5 and its effect on the system becomes apparent. Node 8 on the other hand, is not included in any of the routes and thus has no effect on the system's reliability.

Fig. 6.4 depicts the network effect of eliminating the most important node 5. The system's reliability index NAI decreases to 0.0102 from 0.1000 after node 5 is withdrawn, suggesting a 90% reduction in reliability. As a consequence, the criticality of node 5 can be deduced from the preceding observations. Node 9 is now the system's most important node, as seen from Fig. 6.5. After removal of critical node 5 we can see that there is only a single path from source i.e.

node 1 to the target node 2, so all nodes will have a negligible impact on the criticality of the system. This can be observed through the below graph. And since the critical node is also the node after removal of which, the system becomes the most fragmented, we observe that node 9 is the new critical node of the system.

6.5 Conclusion

The graphical computational model has been developed to signify the structural importance of the ICT components. The model is computationally inexpensive and easy to deploy and efficient in visualizing the contribution of each node in network reliability. The contributions are twofold: First, the overall network reliability has been calculated using network accuracy indicator (NAI) metric. Second, relative importance of each node in the network has been analyzed using structural importance (SI) and network reliability deterioration worth (NRDW). Simulations on standard IEEE-14 bus system demonstrate the most and least important node in contribution to the network reliability according to the NAI calculations. Then, the results of the network overall reliability after removal of the most important node have been discussed. It has been shown that removing the node with maximum NRDW can greatly affect the overall reliability of the network. The graphical model and the metrics introduced in the manuscript greatly help in assessing the reliability of the power network.

Chapter 7

Summary and Conclusions

Smart grid is a concept of integrating intelligent electronic devices with the existing power system network to make it more efficient and smarter, with built-in self-healing capabilities. It integrates new-age technologies at generation, transmission, and distribution levels of Power grid, thereby enhancing energy efficiency. Demand-side management plays significant role in smart grid functionality which helps the consumers to bring down the electricity cost by reducing the peak load demand through judicial use of electricity using DSM tools.

This work focuses on solving optimization problem of scheduling smart home appliances using load shifting. Firstly, the challenges related to DSM has been discussed in detail. The main challenges includes load profile of appliances, RES integration, load categorization, constraints, dynamic pricing, consumer categorization, and optimization techniques. HEMS comprising smart appliances and PV panel with greater control on electricity consumption is the integral part of the proposed optimization solution. Smart home consumers can monitor and control the energy consumption and production of energy, thereby manually controlling the energy usage within household.

The automated optimization algorithm has been proposed that minimizes electricity cost, maximizes comfort, and reduces PAR with consideration of consumer privacy. The proposed

algorithm solves the problem using different types of pricing scheme, accurate forecasting of appliances' power, and solar irradiance using deep learning techniques. The highly complex stochastic problem involving uncertainties of consumer behavior, different types of appliances, power requirement patterns, and PV power has been solved in different pricing scenarios. The least slack time based algorithm has been used which output 24 hour schedule of the smart home appliances using PV power stored in battery at peak time period.

For optimization algorithm to work accurately, there are some pre-requisites. First, solar irradiance is forecasted based on weather parameters so that the PV power produced by the PV panel can be determined in advance. This PV power is stored in the battery and is used to run appliances when the price of electricity is high. This helps the scheduling algorithm to take correct decisions to run home appliances. Secondly, Consumer behavior learning is the vital part for making scheduling decisions. Different smart home consumers have varied kind of appliances and habits. To take scheduling decisions, the power requirement and association between appliances need to be determined. This greatly helps to maintain the comfort of the consumer by running appliances according to the time preferred by the consumer.

In this thesis, different algorithms have been devised to solve the DSM multiobjective optimization problem using load shifting.Three major algorithms have been presented to solve various problems namely, solar irradiance forecasting, appliances' power forecasting, and scheduling optimization algorithm, respectively. The algorithms have been proposed and validated using publicly available data sets and compared with other state-of-art algorithms. The results obtained from these approaches have been meticulously presented with the detailed discussions in their respective sections.

- A robust multi-step solar irradiance forecasting using Transformer deep learning model. To make the model robust, interval prediction is performed using quantile regression. Annually as well as season-wise performance of the RSAM model is superior as compared to other RNN-based models.

- An Ensemble deep learning algorithm has been proposed to estimate the appliance power requirement of the smart home consumer. Furthermore, the appliance-appliance association has been determined using the Dynamic Item Set counting algorithm. In this way, it provides a complete solution to consumer behavior patterns.

- An optimization algorithm using least slack time based algorithm has been proposed to solve multi-objective optimization problem of minimizing electricity cost without affecting the comfort of consumer. The performance of the proposed algorithm has been demonstrated under different request patterns, PV generation, and pricing scenarios.
- At final, graphical computation model has been developed and different metrics are devised to quantify system's reliability assessment in ICT networks.
- An extensive survey of different optimization techniques has been carried out to solve the problem of multi-objective energy management. All different types of practical challenges imposed while implementing DSM using load shifting for IoT enabled home energy management systems (HEMS) have been discussed in detail. It helps the researchers' community utilize, explore, and contribute to the further development of advanced and realistic optimization algorithms for DSM implementation.

7.1 Scope for future research

- The more flexible optimization algorithm development incorporating EVs, more appliances, and selling extra power back to grid.
- More generalized algorithm can be developed for consumer behavior learning which can manage consumer behavior by learning more parameters.
- DSM implementation should also take care of challenges related with the distribution network. The frequency and voltage stability issues, incentive management, and government policy requirements should be taken into consideration.

Appendix

Table A1: Accuracy Metrics

Name	Acronym & Formulae
Forecast error (e_i)	$e_i = GHI_{forecast,i} - GHI_{actual,i}$
RMSE	$\sqrt{\frac{1}{N}\sum_{i=1}^{N} e_i^2}$
MAE	$\frac{1}{N}\sum_{i=1}^{N} \lvert e_i \rvert$
MBE	$\frac{1}{N}\sum_{i=1}^{N} e_i$

Table A2: Data-set Information

Parameters	Dataset-1	Dataset-2
Location	Arizona	India
Latitude	36.33	28.35
Longitude	-110.74	76.55
Weather Parameters	Dew point , cloud type, wind speed and direction , relative humidity , precipitable water, temperature, pressure, solar zenith angle	DNI, dew point, temperature, pressure, wind direction, wind speed
Climate Type	Semi-Arid	Subtropical
Size	20 years	14 years
Training Set	1-1-1998 to 31-12-2017	1-1-2000 to 31-12-2013
Testing Set	1-1-2018 to 31-12-2018	1-1-2014 to 31-12-2014
Data Resolution	Half-Hourly	Hourly

Table A3: Optimal Hyper-parameters of RSAM model

Parameters	Values	Search Range
Training Steps	50	{40, 50, 100}
Dropout rate	0.1	{0.1, 0.2, 0.3}
Mini Batch Size	256	{64, 128, 256}
Sequence Length	256	{64, 128, 256}
Learning Rate	0.001	{0.0001, 0.001, 0.01 }
FFN Size	2048	{512, 1024, 2048 }
Number of Heads	4	{1, 4, 6}

Table A4: Network Configuration of RSAM model (India)

	Layers	Input Vector	Output Vector
Pre-Net	Input Embedding	[1, 256, 15]	[1, 256, 32]
	Positional Encoding	[1, 256, 32]	[1, 256, 32]
	ReLU	[1, 256, 32]	[1, 256, 32]
	Linear	[1, 256, 32]	[1, 256, 20]
	Batch Normalization	[1, 256, 20]	[1, 20, 256]
Attention	Transformer Encoders (4)	[256, 1, 20]	[256, 1, 20]
	Flatten	[256, 1, 20]	[1, 5120]
Post-Net	Linear	[1, 5120]	[1, 512]
	ReLU	[1, 512]	[1, 512]
	Linear	[1, 512]	[1, 1]

Table A5: Optimal Hyper parameters of Ensemble model

Parameters	Values	Search Range
Training Steps	50	{40, 50, 100}
Kernel size	3	{2, 3, 4}
Pool Size	2	{2, 3, 4}
LSTM layer size	100	{50, 100, 120}
Learning Rate	0.01	{0.0001, 0.001, 0.01 }
Estimators Size	45	{30, 45, 55 }
Tree depth	5	{3, 5, 6}

Table A6:

Dishwasher Operating Cycles Specifications

Energy Phase	**Min. Power (W)**	**Max. Power (W)**	**op. time (min)**
pre-wash	16.0	140	14.9
wash	751.2	2117.8	32.1
1^{st} rinse	17.3	132.4	10.1
drain	1.6	136.2	4.3
2^{nd} rinse	572.3	2143	18.3
drain & dry	1.7	2.3	52.4

Table A7:

Washing Machine Operating Cycle Specifications

Energy Phase	**Min. Power (W)**	**Max. Power (W)**	**op. time (min)**
movement	27.2	2100	26
pre-heating	5	300	6.6
heating	206.5	2200	59.7
maintenance	11.0	200	19.9
cooling	10.8	500	10
1^{st} rinse	10.3	700	10.4
2^{nd} rinse	9.9	700	10.3
3^{rd} rinse	23.6	1170	19.8

Table A8:

Dryer Technical Specifications

Energy Phase	**Min. Power (W)**	**Max. Power (W)**	**op. time (min)**
drying	120.5	1454	120.8

References

[1] Nrel location viewer. Last Accessed: 2 Nov, 2019.

[2] Solar energy research data. Last Accessed: 21 Jan, 2020.

[3] Binary particle swarm optimisation with quadratic transfer function: A new binary optimisation algorithm for optimal scheduling of appliances in smart homes. *Applied Soft Computing*, 78:465 – 480, 2019.

[4] Irena future of solar pv 2019, November 2019. last accessed: 28 Feb, 2020.

[5] Solar energy in india, May 2019. Last Accessed: 2 Feb, 2020.

[6] Mohamed Abdel-Nasser and Karar Mahmoud. Accurate photovoltaic power forecasting models using deep lstm-rnn. *Neural Computing and Applications*, 31(7):2727–2740, Jul 2019.

[7] A. Adepetu, E. Rezaei, D. Lizotte, and S. Keshav. Critiquing time-of-use pricing in ontario. In *2013 IEEE International Conference on Smart Grid Communications (SmartGridComm)*, pages 223–228, Oct 2013.

[8] X. G. Agoua, R. Girard, and G. Kariniotakis. Probabilistic models for spatio-temporal photovoltaic power forecasting. *IEEE Transactions on Sustainable Energy*, 10(2):780–789, April 2019.

[9] Majid Ahmadi, Jay M. Rosenberger, Wei Jen Lee, and Asama Kulvanitchaiyanunt. Optimizing Load Control in a Collaborative Residential Microgrid Environment. *IEEE Transactions on Smart Grid*, 6(3):1196–1207, 2015.

[10] Hamed Ahmadi-Nezamabad, Mohammad Zand, Araz Alizadeh, Mahdi Vosoogh, and Sayyad Nojavan. Multi-objective optimization based robust scheduling of electric vehicles aggregator. *Sustainable Cities and Society*, 47:101494, 2019.

[11] Nahar Alshammari and Johnson Asumadu. Optimum unit sizing of hybrid renewable energy system utilizing harmony search, jaya and particle swarm optimization algorithms. *Sustainable Cities and Society*, 60:102255, 2020.

[12] Emanuel Federico Alsina, Marco Bortolini, Mauro Gamberi, and Alberto Regattieri. Artificial neural network optimisation for monthly average daily global solar radiation prediction. *Energy Conversion and Management*, 120:320 – 329, 2016.

[13] Benyamin Amirhosseini and S.M. Hassan Hosseini. Scheduling charging of hybrid-electric vehicles according to supply and demand based on particle swarm optimization, imperialist competitive and teaching-learning algorithms. *Sustainable Cities and Society*, 43:339 – 349, 2018.

[14] Aggeliki Androutsopoulou, Nikos Karacapilidis, Euripidis Loukis, and Yannis Charalabidis. Transforming the communication between citizens and government through ai-guided chatbots. *Government Information Quarterly*, 36(2):358 – 367, 2019.

[15] Amjad Anvari-Moghaddam, Hassan Monsef, and Ashkan Rahimi-Kian. Optimal smart home energy management considering energy saving and a comfortable lifestyle. *IEEE Transactions on Smart Grid*, 6(1):324–332, 2015.

[16] Apple. idevices smart switch, 2020. Accessed: 2020-01-30.

[17] Raji Atia and Noboru Yamada. Sizing and Analysis of Renewable Energy and Battery Systems in Residential Microgrids. *IEEE Transactions on Smart Grid*, 7(3):1204–1213, 2016.

[18] Donald Azuatalam, Wee-Lih Lee, Frits de Nijs, and Ariel Liebman. Reinforcement learning for whole-building hvac control and demand response. *Energy and AI*, 2:100020, 2020.

[19] K. Y. Bae, H. S. Jang, and D. K. Sung. Hourly solar irradiance prediction based on support vector machine and its error analysis. *IEEE Transactions on Power Systems*, 32(2):935–945, March 2017.

[20] Zahra Baharlouei and Massoud Hashemi. Efficiency-fairness trade-off in privacy-preserving autonomous demand side management. *IEEE Transactions on Smart Grid*, 5(2):799–808, 2014.

[21] Abdul Basit, Guftaar Ahmad Sardar Sidhu, Anzar Mahmood, and Feifei Gao. Efficient and Autonomous Energy Management Techniques for the Future Smart Homes. *IEEE Transactions on Smart Grid*, 8(2):917–926, 2017.

[22] Hasnae Bilil, Ghassane Aniba, and Hamid Gharavi. Dynamic Appliances Scheduling in Collaborative MicroGrids System. *IEEE Transactions on Power Systems*, 32(3):2276–2287, 2017.

[23] Robert Brown, Navid Ghavami, Hafeez-Ur-Rehman Siddiqui, Mounir Adjrad, Mohammad Ghavami, and Sandra Dudley. Occupancy based household energy disaggregation using ultra wideband radar and electrical signature profiles. *Energy and Buildings*, 141:134 – 141, 2017.

[24] Anthony Canino, Yu David Liu, and Hidehiko Masuhara. Stochastic energy optimization for mobile gps applications. In *Proceedings of the 2018 26th ACM Joint Meeting on European Software Engineering Conference and Symposium on the Foundations of Software Engineering*, ESEC/FSE 2018, page 703–713, New York, NY, USA, 2018. Association for Computing Machinery.

[25] Z. Cao, C. Wan, Z. Zhang, F. Li, and Y. Song. Hybrid ensemble deep learning for deterministic and probabilistic low-voltage load forecasting. *IEEE Transactions on Power Systems*, 35(3):1881–1897, May 2020.

[26] Bo Chai, Jiming Chen, Zaiyue Yang, and Yan Zhang. Demand response management with multiple utility companies: A two-level game approach. *IEEE Transactions on Smart Grid*, 5(2):722–731, 2014.

[27] A. K. Chakraborty and N. Sharma. Advanced metering infrastructure: Technology and challenges. In *2016 IEEE/PES Transmission and Distribution Conference and Exposition (T D)*, pages 1–5, May 2016.

[28] Sreemoyee Chatterjee and Suprovab Mandal. A novel comparison of gauss-seidel and newton- raphson methods for load flow analysis. In *2017 International Conference on Power and Embedded Drive Control (ICPEDC)*, pages 1–7, 2017.

[29] Phani Chavali, Peng Yang, and Arye Nehorai. A distributed algorithm of appliance

scheduling for home energy management system. *IEEE Transactions on Smart Grid*, 5(1):282–290, 2014.

[30] B. Chen and J. Li. Combined probabilistic forecasting method for photovoltaic power using an improved markov chain. *IET Generation, Transmission Distribution*, 13(19):4364–4373, 2019.

[31] Tianqi Chen and Carlos Guestrin. Xgboost. *Proceedings of the 22nd ACM SIGKDD International Conference on Knowledge Discovery and Data Mining - KDD '16*, 2016.

[32] Z. Chen, L. Wu, and Y. Fu. Real-time price-based demand response management for residential appliances via stochastic optimization and robust optimization. *IEEE Transactions on Smart Grid*, 3(4):1822–1831, Dec 2012.

[33] K. Chiteka and C.C. Enweremadu. Prediction of global horizontal solar irradiance in zimbabwe using artificial neural networks. *Journal of Cleaner Production*, 135:701 – 711, 2016.

[34] Tsan-Ming Choi, Ata Allah Taleizadeh, and Xiaohang Yue. Game theory applications in production research in the sharing and circular economy era. *International Journal of Production Research*, 58(1):118–127, 2020.

[35] L. Ciabattoni, G. Comodi, F. Ferracuti, and G. Foresi. Ai-powered home electrical appliances as enabler of demand-side flexibility. *IEEE Consumer Electronics Magazine*, 9(3):72–78, May 2020.

[36] Clark W. Gellings. The Concept of Demand-Side Management for Electric Utilities. *Proceedings of the IEEE*, (10):1468–1470, 1985.

[37] Carlos F.M. Coimbra, Jan Kleissl, and Ricardo Marquez. Chapter 8 - overview of solar-forecasting methods and a metric for accuracy evaluation. In Jan Kleissl, editor, *Solar Energy Forecasting and Resource Assessment*, pages 171 – 194. Academic Press, Boston, 2013.

[38] A. J. Conejo, J. M. Morales, and L. Baringo. Real-time demand response model. *IEEE Transactions on Smart Grid*, 1(3):236–242, Dec 2010.

[39] Valeria Di Cosmo and Denis O'Hora. Nudging electricity consumption using tou pricing and feedback: evidence from irish households. *Journal of Economic Psychology*, 61:1 – 14, 2017.

[40] Surya [Narayan Dash], Radha [Krushna Padhi], Tapas Dora, A. Surendar, and Karen Cristan. A robust optimization method for bidding strategy by considering the compressed air energy storage. *Sustainable Cities and Society*, 48:101564, 2019.

[41] Mathieu David, Hadja Maïmouna Diagne, and Philippe Lauret. Outputs and error indicators for solar forecasting models. May 2012.

[42] Jacob Devlin, Ming-Wei Chang, Kenton Lee, and Kristina Toutanova. Bert: Pre-training of deep bidirectional transformers for language understanding. *arXiv:1810.04805*, 2018.

[43] Elisabeth Drayer, Niki Kechagia, Jan Hegemann, Martin Braun, Mathieu Gabel, and Raphael Caire. Distributed self-healing for distribution grids with evolving search space. *IEEE Transactions on Power Delivery*, PP:1–1, 10 2017.

[44] Elisabeth Drayer and Tirza Routtenberg. Detection of false data injection attacks in smart grids based on graph signal processing. *IEEE Systems Journal*, PP:1–11, 08 2019.

[45] Yuefang F. Du, Lin Jiang, Yuanzheng Li, and Qinghua Wu. A robust optimization approach for demand side scheduling considering uncertainty of manually operated appliances. *IEEE Transactions on Smart Grid*, 9(2):743–755, 2018.

[46] A. Can Duman, Hamza Salih Erden, Ömer Gönül, and Önder Güler. A home energy management system with an integrated smart thermostat for demand response in smart grids. *Sustainable Cities and Society*, 65:102639, 2021.

[47] Ecobee. Smart thermostats, 2019. Accessed: 2019-11-20.

[48] C. Eksin, H. Deliç, and A. Ribeiro. Demand response with communicating rational consumers. *IEEE Transactions on Smart Grid*, 9(1):469–482, Jan 2018.

[49] C. Eksin, H. Deliç, and A. Ribeiro. Demand response with communicating rational consumers. *IEEE Transactions on Smart Grid*, 9(1):469–482, Jan 2018.

[50] Elattar, E.E., Sabiha, N.A., and M Alsharef. Short term electric load forecasting using hybrid algorithm for smart cities. *Appl Intell*, 50:3379–3399, 2020.

[51] Fadi Elghitani and Weihua Zhuang. Aggregating a Large Number of Residential Appliances for Demand Response Applications. *IEEE Transactions on Smart Grid*, 9(5):5092–5100, 2018.

[52] Onur Elma, Akın Taşcıkaraoğlu, A. Tahir İnce, and Uğur S. Selamoğulları. Implementation of a dynamic energy management system using real time pricing and local renewable energy generation forecasts. *Energy*, 134:206 – 220, 2017.

[53] Majid Emami Javanmard, S.F. Ghaderi, and Mohamad Sadegh Sangari. Integrating energy and water optimization in buildings using multi-objective mixed-integer linear programming. *Sustainable Cities and Society*, 62:102409, 2020.

[54] O. Erdinc, N. G. Paterakis, T. D. P. Mendes, A. G. Bakirtzis, and J. P. S. Catalão. Smart household operation considering bi-directional ev and ess utilization by real-time pricing-based dr. *IEEE Transactions on Smart Grid*, 6(3):1281–1291, May 2015.

[55] Ozan Erdinc, Nikolaos G Paterakis, Tiago D P Mendes, Anastasios G Bakirtzis, and João P S Catalão. Smart Household Operation Considering Bi-Directional EV and ESS Utilization. *IEEE Transactions on Smart Grid*, 6(3):1281–1291, 2015.

[56] S. M. Errapotu, J. Wang, Y. Gong, J. Cho, M. Pan, and Z. Han. Safe: Secure appliance scheduling for flexible and efficient energy consumption for smart home iot. *IEEE Internet of Things Journal*, 5(6):4380–4391, Dec 2018.

[57] Sai Mounika Errapotu, J. Wang, Yanmin Gong, Jin-Hee Cho, M. Pan, and Z. Han. Safe: Secure appliance scheduling for flexible and efficient energy consumption for smart home iot. *IEEE Internet of Things Journal*, 5:4380–4391, 2018.

[58] Sai Mounika Errapotu, Jingyi Wang, Yanmin Gong, Jin Hee Cho, Miao Pan, and Zhu Han. SAFE: Secure Appliance Scheduling for Flexible and Efficient Energy Consumption for Smart Home IoT. *IEEE Internet of Things Journal*, 5(6):4380–4391, 2018.

[59] Ima O. Essiet, Yanxia Sun, and Zenghui Wang. Optimized energy consumption model for smart home using improved differential evolution algorithm. *Energy*, 172:354 – 365, 2019.

[60] Ayman Faza and Amjed Al-Mousa. Pso-based optimization toward intelligent dynamic pricing schemes parameterization. *Sustainable Cities and Society*, 51:101776, 2019.

[61] C. Feng, M. Cui, B. Hodge, S. Lu, H. F. Hamann, and J. Zhang. Unsupervised clustering-based short-term solar forecasting. *IEEE Transactions on Sustainable Energy*, 10(4):2174–2185, Oct 2019.

[62] Wei Feng, Yi Zhang, Gang Rong, and Yiping Feng. Finite adaptability in data-driven robust optimization for production scheduling: A case study of the ethylene plant. *Industrial & Engineering Chemistry Research*, 58(16):6505–6518, 2019.

[63] Mohamed Amine Ferrag, Messaoud Babaghayou, and Mehmet Akif Yazici. Cyber security for fog-based smart grid scada systems: Solutions and challenges. *Journal of Information Security and Applications*, 52:102500, 2020.

[64] Nicolas Gast, Dan Cristian Tomozei, and Jean Yves Le Boudec. Optimal generation and storage scheduling in the presence of renewable forecast uncertainties. *IEEE Transactions on Smart Grid*, 5(3):1328–1339, 2014.

[65] Clark W. GELLINGS. Evolving practice of demand-side management. *Journal of Modern Power Systems and Clean Energy*, 5(1):1–9, Jan 2017.

[66] Nazeeh Ghatasheh, Hossam Faris, Ibrahim Aljarah, and Rizik M. H. Al-Sayyed. Optimizing software effort estimation models using firefly algorithm. *Journal of Software Engineering and Applications*, 08(03):133–142, 2015.

[67] Mohammad Ghiasi, Moslem Dehghani, Taher Niknam, and Abdollah Kavousi-Fard. Investigating overall structure of cyber-attacks on smart-grid control systems to improve cyber resilience in power system. 03 2020.

[68] Hessam Golmohamadi, Kim Guldstrand Larsen, Peter Gjøl Jensen, and Imran Riaz Hasrat. Optimization of power-to-heat flexibility for residential buildings in response to day-ahead electricity price. *Energy and Buildings*, 232:110665, 2021.

[69] Hessam Golmohamadi, Reza Keypour, Birgitte Bak-Jensen, and Jayakrishnan Radhakrishna Pillai. Optimization of household energy consumption towards day-ahead retail electricity price in home energy management systems. *Sustainable Cities and Society*, 47:101468, 2019.

[70] Sajjad Golshannavaz. Cooperation of electric vehicle and energy storage in reactive power compensation: An optimal home energy management system considering pv presence. *Sustainable Cities and Society*, 39, 02 2018.

[71] Nicholas Good, Keith A. Ellis, and Pierluigi Mancarella. Review and classification of barriers and enablers of demand response in the smart grid. *Renewable and Sustainable Energy Reviews*, 72:57–72, 2017.

[72] Ian Goodfellow, Yoshua Bengio, and Aaron Courville. *Deep Learning*. MIT Press, 2016. `http://www.deeplearningbook.org`.

[73] Bram L. Gorissen, Ihsan Yanikoğlu, and Dick den Hertog. A practical guide to robust optimization. *Omega (United Kingdom)*, 53:124–137, 2015.

[74] K. Greff, R. K. Srivastava, J. Koutník, B. R. Steunebrink, and J. Schmidhuber. Lstm: A search space odyssey. *IEEE Transactions on Neural Networks and Learning Systems*, 28(10):2222–2232, 2017.

[75] Katia Gregio, Di Santo, Silvio Giuseppe, Di Santo, Renato Machado Monaro, and Marco Antonio Saidel. Active demand side management for households in smart grids using optimization and arti fi cial intelligence. *Measurement*, 115(April 2017):152–161, 2018.

[76] A. Grogan. Smart appliances. *Engineering Technology*, 7(6):44–45, July 2012.

[77] Zhifeng Guo, Kaile Zhou, Xiaoling Zhang, and Shanlin Yang. A deep learning model for short-term power load and probability density forecasting. *Energy*, 160:1186 – 1200, 2018.

[78] Muhammet Gündüz and Resul Das. Cyber-security on smart grid: Threats and potential solutions. *Computer Networks*, 169:107094, 03 2020.

[79] G. Hafeez, K. S. Alimgeer, Z. Wadud, I. Khan, M. Usman, A. B. Qazi, and F. A. Khan. An innovative optimization strategy for efficient energy management with day-ahead demand response signal and energy consumption forecasting in smart grid using artificial neural network. *IEEE Access*, 8:84415–84433, 2020.

[80] Mengjie Han, Ross May, Xingxing Zhang, Xinru Wang, Song Pan, Da Yan, Yuan Jin, and Liguo Xu. A review of reinforcement learning methodologies for controlling occupant comfort in buildings. *Sustainable Cities and Society*, 51:101748, 2019.

[81] Rania Hassan, Babak Cohanim, and Olivier de Weck. A comparison of particle swarm optimization and the genetic algorithm. volume 2, 04 2005.

[82] Sepp Hochreiter and Jürgen Schmidhuber. Long short-term memory. *Neural computation*, 9:1735–80, 12 1997.

[83] Sepp Hochreiter and Jürgen Schmidhuber. Long short-term memory. *Neural Computation*, 9(8):1735–1780, 1997.

[84] Thomas E. Hoff, Richard Perez, Jan Kleissl, David Renne, and Joshua Stein. Reporting of irradiance modeling relative prediction errors. *Progress in Photovoltaics: Research and Applications*, 21(7):1514–1519, 2013.

[85] William Hoiles and Vikram Krishnamurthy. Nonparametric demand forecasting and detection of energy aware consumers. *IEEE Transactions on Smart Grid*, 6(2):695–704, 2015.

[86] Md Alamgir Hossain, Ripon K. Chakrabortty, Michael J. Ryan, and Hemanshu Roy Pota. Energy management of community energy storage in grid-connected microgrid under uncertain real-time prices. *Sustainable Cities and Society*, 66:102658, 2021.

[87] X. Hou, J. Wang, T. Huang, T. Wang, and P. Wang. Smart home energy management optimization method considering energy storage and electric vehicle. *IEEE Access*, 7:144010–144020, October 2019.

[88] X. Hu and J. Nutaro. A priority-based control strategy and performance bound for aggregated hvac-based load shaping. *IEEE Transactions on Smart Grid*, 11(5):4133–4143, 2020.

[89] Cheng-Zhi Anna Huang, Ashish Vaswani, Jakob Uszkoreit, Noam Shazeer, Ian Simon, Curtis Hawthorne, Andrew M. Dai, Matthew D. Hoffman, Monica Dinculescu, and Douglas Eck. Music transformer. *arXiv:1809.04281*, 2018.

[90] Qi Huang, Hanze Zhang, Jiaqing Chen, and Mengying He. Quantile regression models and their applications: A review. *Journal of Biometrics & Biostatistics*, 08, 01 2017.

[91] Yantai Huang, Lei Wang, Weian Guo, Qi Kang, and Qidi Wu. Chance constrained optimization in a home energy management system. *IEEE Transactions on Smart Grid*, 9(1):252–260, 2018.

[92] Tanguy Hubert and Santiago Grijalva. Modeling for residential electricity optimization in dynamic pricing environments. *IEEE Transactions on Smart Grid*, 3(4):2224–2231, 2012.

[93] Ronald Huisman, Christian Huurman, and Ronald Mahieu. Hourly electricity prices in day-ahead markets. *Energy Economics*, 29(2):240 – 248, 2007.

[94] N. S. Hussin, M. P. Abdullah, A. I.M. Ali, M. Y. Hassan, and F. Hussin. Residential electricity time of use (ToU) pricing for Malaysia. In *2014 IEEE Conference on Energy Conversion, CENCON 2014*, 2014.

[95] iDevices Thermostats. Smart thermostats, 2019. Accessed: 2019-12-10.

[96] Balaraju Jakkula, Govinda Raj Mandela, and Murthy Ch SN. Reliability block diagram (rbd) and fault tree analysis (fta) approaches for estimation of system reliability and availability–a case study. *International Journal of Quality & Reliability Management*, 2020.

[97] Nadeem Javaid, Mudassar Naseem, Muhammad Babar Rasheed, Danish Mahmood, Shahid Ahmed Khan, Nabil Alrajeh, and Zafar Iqbal. A new heuristically optimized home energy management controller for smart grid. *Sustainable Cities and Society*, 34:211 – 227, 2017.

[98] Wu Ji and Keong Chan Chee. Prediction of hourly solar radiation using a novel hybrid model of arma and tdnn. *Solar Energy*, 85(5):808 – 817, 2011.

[99] Y. Ji, E. Buechler, and R. Rajagopal. Data-driven load modeling and forecasting of residential appliances. *IEEE Transactions on Smart Grid*, pages 1–1, 2019.

[100] Jing Jiang and Yi Qian. Defense mechanisms against data injection attacks in smart grid networks. *IEEE Communications Magazine*, 55:76–82, 10 2017.

[101] Y. Jiang, H. Long, Z. Zhang, and Z. Song. Day-ahead prediction of bihourly solar radiance with a markov switch approach. *IEEE Transactions on Sustainable Energy*, 8(4):1536–1547, Oct 2017.

[102] Junchen Jin, Xiaoliang Ma, and Iisakki Kosonen. A stochastic optimization framework for road traffic controls based on evolutionary algorithms and traffic simulation. *Advances in Engineering Software*, 114:348 – 360, 2017.

[103] Zhuojun Jin, Peng Yu, Shao Yong Guo, Lei Feng, Fanqin Zhou, Minxing Tao, Wenjing Li, Xue-Song Qiu, and Lei Shi. Cyber-physical risk driven routing planning with deep reinforcement-learning in smart grid communication networks. In *2020 International Wireless Communications and Mobile Computing (IWCMC)*, pages 1278–1283, 2020.

[104] M. Kakimoto, Y. Endoh, H. Shin, R. Ikeda, and H. Kusaka. Probabilistic solar irradiance forecasting by conditioning joint probability method and its application to electric power trading. *IEEE Transactions on Sustainable Energy*, 10(2):983–993, April 2019.

[105] Vishruti Kakkad, Hitarth Shah, Reema Patel, and Nishant Doshi. A comparative study of applications of game theory in cyber security and cloud computing. *Procedia Computer Science*, 155:680 – 685, 2019. The 16th International Conference on Mobile Systems and Pervasive Computing (MobiSPC 2019),The 14th International Conference on Future Networks and Communications (FNC-2019),The 9th International Conference on Sustainable Energy Information Technology.

[106] Amanpreet Kaur, Lukas Nonnenmacher, Hugo T.C. Pedro, and Carlos F.M. Coimbra. Benefits of solar forecasting for energy imbalance markets. *Renewable Energy*, 86:819 – 830, 2016.

[107] Nikhil Kaza. Urban form and transportation energy consumption. *Energy Policy*, 136:111049, 2020.

[108] Jack Kelly and William Knottenbelt. The UK-DALE dataset, domestic appliance-level electricity demand and whole-house demand from five UK homes. *Scientific Data*, 2(150007), 2015.

[109] Ahsan Raza Khan, Anzar Mahmood, Awais Safdar, Zafar A. Khan, and Naveed Ahmed

Khan. Load forecasting, dynamic pricing and dsm in smart grid: A review. *Renewable and Sustainable Energy Reviews*, 54:1311 – 1322, 2016.

[110] Meysam Khojasteh. A robust energy procurement strategy for micro-grid operator with hydrogen-based energy resources using game theory. *Sustainable Cities and Society*, 60:102260, 2020.

[111] B. Kim, Y. Zhang, M. van der Schaar, and J. Lee. Dynamic pricing and energy consumption scheduling with reinforcement learning. *IEEE Transactions on Smart Grid*, 7(5):2187–2198, Sep. 2016.

[112] H. J. Kim, R. Sioshansi, and A. J. Conejo. Benefits of stochastic optimization for scheduling energy storage in wholesale electricity markets. *Journal of Modern Power Systems and Clean Energy*, pages 1–9, 2020.

[113] Yoon Kim. Convolutional neural networks for sentence classification. In *Proceedings of the 2014 Conference on Empirical Methods in Natural Language Processing (EMNLP)*, pages 1746–1751, Doha, Qatar, October 2014. Association for Computational Linguistics.

[114] W. Kong, Z. Y. Dong, Y. Jia, D. J. Hill, Y. Xu, and Y. Zhang. Short-term residential load forecasting based on lstm recurrent neural network. *IEEE Transactions on Smart Grid*, 10(1):841–851, 2019.

[115] Vladimir V. Kostylev and Anya Pavlovski. Solar power forecasting performance – towards industry standards. In *Proc. 1st Int. Workshop on Integration of Solar Power into Power Systems*, Aarhus, Denmark, 2011.

[116] Oleksii Kuchaiev, Jason Li, Huyen Nguyen, Oleksii Hrinchuk, Ryan Leary, Boris Ginsburg, Samuel Kriman, Stanislav Beliaev, Vitaly Lavrukhin, Jack Cook, Patrice Castonguay, Mariya Popova, Jocelyn Huang, and Jonathan M. Cohen. Nemo: a toolkit for building ai applications using neural modules, 2019.

[117] S. Kumar, L. Hussain, S. Banarjee, and M. Reza. Energy load forecasting using deep learning approach-lstm and gru in spark cluster. In *2018 Fifth International Conference on Emerging Applications of Information Technology (EAIT)*, pages 1–4, 2018.

[118] Sachin Kumar, Saibal K Pal, and Rampal Singh. A novel hybrid model based on particle swarm optimisation and extreme learning machine for short-term temperature prediction using ambient sensors. *Sustainable Cities and Society*, 49:101601, 2019.

[119] Gideon A.H. Laugs, René M.J. Benders, and Henri C. Moll. Balancing responsibilities: Effects of growth of variable renewable energy, storage, and undue grid interaction. *Energy Policy*, 139:111203, 2020.

[120] Philippe Lauret, Cyril Voyant, Ted Soubdhan, Mathieu David, and Philippe Poggi. A benchmarking of machine learning techniques for solar radiation forecasting in an insular context. *Solar Energy*, 112:446 – 457, 2015.

[121] Y. W. Law, T. Alpcan, V. C. S. Lee, A. Lo, S. Marusic, and M. Palaniswami. Demand response architectures and load management algorithms for energy-efficient power grids: A survey. In *2012 Seventh International Conference on Knowledge, Information and Creativity Support Systems*, pages 134–141, Nov 2012.

[122] Tuong Le, Minh Thanh Vo, Tung Kieu, Eenjun Hwang, Seungmin Rho, and Sung Wook Baik. Multiple electric energy consumption forecasting using a cluster-based strategy for transfer learning in smart building. *Sensors*, 20(9), 2020.

[123] Tuong Le, Minh Thanh Vo, Bay Vo, Eenjun Hwang, Seungmin Rho, and Sung Wook Baik. Improving electric energy consumption prediction using cnn and bi-lstm. *Applied Sciences*, 9(20), 2019.

[124] Jae Yong Lee and Seong Gon Choi. Linear Programming Based Hourly Peak Load Shaving Method at Home Area. *16th International Conference on Advanced Communication Technology*, pages 4–7, 2014.

[125] David Levine, Yong Liang, and Zuo-Jun Max) Shen. Thermostats for the smart grid: Models, benchmarks, and insights. *The Energy Journal*, 33, 03 2012.

[126] C. Li, X. Yu, W. Yu, G. Chen, and J. Wang. Efficient computation for sparse load shifting in demand side management. *IEEE Transactions on Smart Grid*, 8(1):250–261, Jan 2017.

[127] Junhui Li, Chenjun Sun, Haiming Zhou, Yang Zhao, Xichun Bao, and Qi Zhao. A Survey of Development and Application of Artificial Intelligence in Smart Grid. *IOP Conference Series: Earth and Environmental Science*, 186:012066, 2018.

[128] S. Li, D. Zhang, A. B. Roget, and Z. O'Neill. Integrating home energy simulation and dynamic electricity price for demand response study. *IEEE Transactions on Smart Grid*, 5(2):779–788, March 2014.

[129] Shiyang Li, Xiaoyong Jin, Yao Xuan, Xiyou Zhou, Wenhu Chen, Yu-Xiang Wang, and Xifeng Yan. Enhancing the locality and breaking the memory bottleneck of transformer on time series forecasting. *arXiv:1907.00235*, 2019.

[130] Tianyi Li and Min Dong. Real-time residential-side joint energy storage management and load scheduling with renewable integration. *IEEE Transactions on Smart Grid*, 9(1):283–298, 2018.

[131] H. Liao and J. V. Milanović. Flexibility exchange strategy to facilitate congestion and voltage profile management in power networks. *IEEE Transactions on Smart Grid*, 10(5):4786–4794, 2019.

[132] Z. Ling, J. Luo, Y. Xu, C. Gao, K. Wu, and X. Fu. Security vulnerabilities of internet of things: A case study of the smart plug system. *IEEE Internet of Things Journal*, 4(6):1899–1909, Dec 2017.

[133] Liyuan Liu, Haoming Jiang, Pengcheng He, Weizhu Chen, Xiaodong Liu, Jianfeng Gao, and Jiawei Han. On the variance of the adaptive learning rate and beyond. *arXiv:1908.03265*, 2019.

[134] N. Liu, J. Chen, L. Zhu, J. Zhang, and Y. He. A key management scheme for secure communications of advanced metering infrastructure in smart grid. *IEEE Transactions on Industrial Electronics*, 60(10):4746–4756, Oct 2013.

[135] Ren Shiou Liu and Yu Feng Hsu. A scalable and robust approach to demand side management for smart grids with uncertain renewable power generation and bi-directional energy trading. *International Journal of Electrical Power and Energy Systems*, 97(November 2017):396–407, 2018.

[136] Yi Liu, Chau Yuen, Rong Yu, Yan Zhang, and Shengli Xie. Queuing-Based Energy Consumption Management for Heterogeneous Residential Demands in Smart Grid. *IEEE Transactions on Smart Grid*, 7(3):1650–1659, 2016.

[137] Ziyao Liu, Nguyen Cong Luong, Wenbo Wang, Dusit Niyato, Ping Wang, Ying-Chang Liang, and Dong In Kim. A survey on applications of game theory in blockchain, 2019.

[138] V. B. Lobo, J. Analin, R. M. Laban, and S. S. More. Convergence of blockchain and artificial intelligence to decentralize healthcare systems. In *2020 Fourth International Conference on Computing Methodologies and Communication (ICCMC)*, pages 925–931, March 2020.

[139] T. Logenthiran, D. Srinivasan, and T. Z. Shun. Demand side management in smart grid using heuristic optimization. *IEEE Transactions on Smart Grid*, 3(3):1244–1252, Sep. 2012.

[140] Thillainathan Logenthiran, D. Srinivasan, and K. Vanessa. Demand side management of smart grid: Load shifting and incentives. *Journal of Renewable and Sustainable Energy*, 6, 05 2014.

[141] B. Lokeshgupta and S. Sivasubramani. Multi-objective home energy management with battery energy storage systems. *Sustainable Cities and Society*, 47:101458, 2019.

[142] An-Yang Lu and Guang-Hong Yang. False data injection attacks against state estimation in the presence of sensor failures. *Information Sciences*, 508:92–104, 2020.

[143] Hui Lu, Mengmeng Zhang, Zongming Fei, and Kefei Mao. Multi-Objective Energy Consumption Scheduling in Smart Grid Based on Tchebycheff Decomposition. *IEEE Transactions on Smart Grid*, 6(6):2869–2883, 2015.

[144] Xinhui Lu, Kaile Zhou, Felix T S Chan, and Shanlin Yang. Optimal scheduling of household appliances for smart home energy management considering demand response. *Natural Hazards*, 88(3):1639–1653, 2017.

[145] Juan M. Lujano-Rojas, Rodolfo Dufo-López, José L. Bernal-Agustín, and João P.S. Catalão. Optimizing Daily Operation of Battery Energy Storage Systems Under Real-Time Pricing Schemes. *IEEE Transactions on Smart Grid*, 8(1):316–330, 2017.

[146] Fengji Luo, Zhao Yang Dong, Zhao Xu, Weicong Kong, and Fan Wang. Distributed residential energy resource scheduling with renewable uncertainties. *IET Generation, Transmission & Distribution*, 12(11):2770–2777, 2018.

[147] Jianing (Tom) Luo, Mahmood Mastani Joybari, Karthik Panchabikesan, Ying Sun, Fariborz Haghighat, Alain Moreau, and Miguel Robichaud. Performance of a self-learning predictive controller for peak shifting in a building integrated with energy storage. *Sustainable Cities and Society*, 60:102285, 2020.

[148] Per Lynggaard and Knud Skouby. Deploying 5g-technologies in smart city and smart home wireless sensor networks with interferences. *Wireless Personal Communications*, 81:1399–1413, 04 2015.

[149] J. Ma, H. H. Chen, L. Song, and Y. Li. Residential load scheduling in smart grid: A cost efficiency perspective. *IEEE Transactions on Smart Grid*, 7(2):771–784, March 2016.

[150] Jiawei Ma, Zheng Shou, Alireza Zareian, Hassan Mansour, Anthony Vetro, and Shih-Fu Chang. Cdsa: Cross-dimensional self-attention for multivariate, geo-tagged time series imputation. *arXiv:1905.09904*, 2019.

[151] K Maddulety, Suneel Sharma, K Prasanna Venkatesh, and A Seetharaman. Factors Influencing Purchase of Smart Appliances in Smart Homes. Technical report, 2017.

[152] Mohamed Massaoudi, Shady S. Refaat, Ines Chihi, Mohamed Trabelsi, Fakhreddine S. Oueslati, and Haitham Abu-Rub. A novel stacked generalization ensemble-based hybrid lgbm-xgb-mlp model for short-term load forecasting. *Energy*, 214:118874, 2021.

[153] Mark P. McHenry. Technical and governance considerations for advanced metering infrastructure/smart meters: Technology, security, uncertainty, costs, benefits, and risks. *Energy Policy*, 59:834–842, 2013.

[154] Killian McKenna and Andrew Keane. Residential Load Modeling of Price-Based Demand Response for Network Impact Studies. *IEEE Transactions on Smart Grid*, 7(5):2285–2294, 2016.

[155] F. Y. Melhem, O. Grunder, Z. Hammoudan, and N. Moubayed. Energy management in electrical smart grid environment using robust optimization algorithm. *IEEE Transactions on Industry Applications*, 54(3):2714–2726, May 2018.

[156] Fan-lin Meng, Student Member, and Xiao-jun Zeng. A Profit Maximization Approach to Demand Response Management with Customers Behavior Learning in Smart Grid. *IEEE Transactions on Smart Grid*, 7(3):1516–1529, May 2016.

[157] A. Mohammadali, M. Sayad Haghighi, M. H. Tadayon, and A. Mohammadi-Nodooshan. A novel identity-based key establishment method for advanced metering infrastructure in smart grid. *IEEE Transactions on Smart Grid*, 9(4):2834–2842, July 2018.

[158] Ramyar Rashed Mohassel, Alan Fung, Farah Mohammadi, and Kaamran Raahemifar. A survey on advanced metering infrastructure. *International Journal of Electrical Power & Energy Systems*, 63:473 – 484, 2014.

[159] T. Molla, B. Khan, B. Moges, H. H. Alhelou, R. Zamani, and P. Siano. Integrated optimization of smart home appliances with cost-effective energy management system. *CSEE Journal of Power and Energy Systems*, 5(2):249–258, June 2019.

[160] A. Monacchi, D. Egarter, W. Elmenreich, S. D'Alessandro, and A. M. Tonello. Greend: An energy consumption dataset of households in italy and austria. In *2014 IEEE International Conference on Smart Grid Communications (SmartGridComm)*, pages 511–516, Nov 2014.

[161] H Morsali, S.M. Shekarabi, K Ardekani, Hossein Khayami, Alireza Fereidunian, Mona Ghassemian, and H Lesani. Smart plugs for building energy management systems. pages 1–5, 01 2012.

[162] HE Murdock. Renewables 2019 global status report, 2019.

[163] Sergio Nesmachnow. An overview of metaheuristics: accurate and efficient methods for optimisation. *International Journal of Metaheuristics*, 3(4):320, 2015.

[164] H. T. Nguyen, D. T. Nguyen, and L. B. Le. Energy management for households with solar assisted thermal load considering renewable energy and price uncertainty. *IEEE Transactions on Smart Grid*, 6(1):301–314, Jan 2015.

[165] Amir Niromandfam, Ahmad Sadeghi Yazdankhah, and Rasool Kazemzadeh. Modeling demand response based on utility function considering wind profit maximization in the day-ahead market. *Journal of Cleaner Production*, 251:119317, 2020.

[166] Martin J Osborne. *A course in Game Theory*. The MIT Press, 1994.

[167] Smart Outlet. Centralite smart outlet, 2019. Accessed: 2019-09-30.

[168] Biljana Panic, Natasa Kontrec, Mirko Vujosevic, and Stefan Panic. A novel approach for determination of reliability of covering a node from k nodes. *Symmetry*, 12:1461, 09 2020.

[169] Niki Parmar, Ashish Vaswani, Jakob Uszkoreit, Łukasz Kaiser, Noam Shazeer, Alexander Ku, and Dustin Tran. Image transformer. *arXiv:1802.05751*, 2018.

[170] N. G. Paterakis, O. Erdinç, A. G. Bakirtzis, and J. P. S. Catalão. Optimal household appliances scheduling under day-ahead pricing and load-shaping demand response strategies. *IEEE Transactions on Industrial Informatics*, 11(6):1509–1519, Dec 2015.

[171] Priti Paudyal and Zhen Ni. Smart home energy optimization with incentives compensation from inconvenience for shifting electric appliances. *International Journal of Electrical Power & Energy Systems*, 109:652 – 660, 2019.

[172] Hugo T.C. Pedro and Carlos F.M. Coimbra. Assessment of forecasting techniques for solar power production with no exogenous inputs. *Solar Energy*, 86(7):2017 – 2028, 2012.

[173] Mario Petrollese and Daniele Cocco. Robust optimization for the preliminary design of solar organic rankine cycle (orc) systems. *Energy Conversion and Management*, 184:338 – 349, 2019.

[174] Virginia Pilloni, Alessandro Floris, Alessio Meloni, and Luigi Atzori. Smart Home Energy Management Including Renewable Sources: A QoE-Driven Approach. *IEEE Transactions on Smart Grid*, 9(3):2006–2018, 2018.

[175] Matthias Pilz and Luluwah Al-Fagih. Recent advances in local energy trading in the smart grid based on game-theoretic approaches. *IEEE Transactions on Smart Grid*, 10(2):1363–1371, 2019.

[176] T. Pinto, H. Morais, T. M. Sousa, T. Sousa, Z. Vale, I. Praça, R. Faia, and E. J. S. Pires. Adaptive portfolio optimization for multiple electricity markets participation. *IEEE Transactions on Neural Networks and Learning Systems*, 27(8):1720–1733, Aug 2016.

[177] Jelena Ponocko and Jovica Milanovic. Forecasting demand flexibility of aggregated residential load using smart meter data. *IEEE Transactions on Power Systems*, PP:1–1, 01 2018.

[178] B. Qela and H. T. Mouftah. Observe, learn, and adapt (ola)—an algorithm for energy management in smart homes using wireless sensors and artificial intelligence. *IEEE Transactions on Smart Grid*, 3(4):2262–2272, Dec 2012.

[179] B. Qela and H. T. Mouftah. Peak load curtailment in a smart grid via fuzzy system approach. *IEEE Transactions on Smart Grid*, 5(2):761–768, 2014.

[180] Xiangyun Qing and Yugang Niu. Hourly day-ahead solar irradiance prediction using weather forecasts by lstm. *Energy*, 148:461 – 468, 2018.

[181] Md Moktadir Rahman, Sujeewa Hettiwatte, GM Shafiullah, and Ali Arefi. An analysis of the time of use electricity price in the residential sector of bangladesh. *Energy Strategy Reviews*, 18:183 – 198, 2017.

[182] A. Riahi Sfar, Y. Challal, P. Moyal, and E. Natalizio. A game theoretic approach for privacy preserving model in iot-based transportation. *IEEE Transactions on Intelligent Transportation Systems*, 20(12):4405–4414, 2019.

[183] Hee Tae Roh and Jang Won Lee. Residential demand response scheduling with multiclass appliances in the smart grid. *IEEE Transactions on Smart Grid*, 7(1):94–104, 2016.

[184] M. Roozbehani, M. A. Dahleh, and S. K. Mitter. Volatility of power grids under real-time pricing. *IEEE Transactions on Power Systems*, 27(4):1926–1940, Nov 2012.

[185] Cristina Rottondi, Antimo Barbato, Lin Chen, and Giacomo Verticale. Enabling privacy in a distributed game-theoretical scheduling system for domestic appliances. *IEEE Transactions on Smart Grid*, 8(3):1220–1230, 2017.

[186] Tirza Routtenberg and Yonina C. Eldar. Centralized identification of imbalances in power networks with synchrophasor data. *IEEE Transactions on Power Systems*, 33(2):1981–1992, 2018.

[187] Tirza Routtenberg and Yao Xie. Pmu-based online change-point detection of imbalance in three-phase power systems. In *2017 IEEE Power Energy Society Innovative Smart Grid Technologies Conference (ISGT)*, pages 1–5, 2017.

[188] Sarah Royston, Jan Selby, and Elizabeth Shove. Invisible energy policies: A new agenda for energy demand reduction. *Energy Policy*, 123:127 – 135, 2018.

[189] Frederik Ruelens, Bert J. Claessens, Stijn Vandael, Bart De Schutter, Robert Babuska, and Ronnie Belmans. Residential Demand Response of Thermostatically Controlled Loads Using Batch Reinforcement Learning. *IEEE Transactions on Smart Grid*, 8(5):2149–2159, 2017.

[190] M. Sajjad, Z. A. Khan, A. Ullah, T. Hussain, W. Ullah, M. Y. Lee, and S. W. Baik. A novel cnn-gru-based hybrid approach for short-term residential load forecasting. *IEEE Access*, 8:143759–143768, 2020.

[191] Jacob Sakhnini, Hadis Karimipour, and Ali Dehghantanha. Smart grid cyber attacks detection using supervised learning and heuristic feature selection. In *2019 IEEE 7th International Conference on Smart Energy Grid Engineering (SEGE)*, pages 108–112, 2019.

[192] P. Samadi, H. Mohsenian-Rad, V. W. S. Wong, and R. Schober. Tackling the load uncertainty challenges for energy consumption scheduling in smart grid. *IEEE Transactions on Smart Grid*, 4(2):1007–1016, June 2013.

[193] Pedram Samadi, Hamed Mohsenian-Rad, Vincent W.S. Wong, and Robert Schober. Real-time pricing for demand response based on stochastic approximation. *IEEE Transactions on Smart Grid*, 5(2):789–798, 2014.

[194] Pedram Samadi, Vincent W.S. Wong, and Robert Schober. Load Scheduling and Power Trading in Systems with High Penetration of Renewable Energy Resources. *IEEE Transactions on Smart Grid*, 7(4):1802–1812, 2016.

[195] M. Shafie-Khah and P. Siano. A stochastic home energy management system considering satisfaction cost and response fatigue. *IEEE Transactions on Industrial Informatics*, 14(2):629–638, 2018.

[196] Miadreza Shafie-Khah and Pierluigi Siano. A stochastic home energy management system considering satisfaction cost and response fatigue. *IEEE Transactions on Industrial Informatics*, 14(2):629–638, 2018.

[197] A. Shakya, S. Michael, C. Saunders, D. Armstrong, P. Pandey, S. Chalise, and R. Tonkoski. Solar irradiance forecasting in remote microgrids using markov switching model. *IEEE Transactions on Sustainable Energy*, 8(3):895–905, July 2017.

[198] Shengnan Shao, Manisa Pipattanasomporn, and Saifur Rahman. Grid integration of electric vehicles and demand response with customer choice. *IEEE Transactions on Smart Grid*, 3:543–550, 2012.

[199] Shaolun Zeng, J. Li, and Yulong Ren. Research of time-of-use electricity pricing models in china: A survey. In *2008 IEEE International Conference on Industrial Engineering and Engineering Management*, pages 2191–2195, Dec 2008.

[200] S. Sharda, M. Singh, and K. Sharma. Rsam: Robust self-attention based multi-horizon model for solar irradiance forecasting. *IEEE Transactions on Sustainable Energy*, pages 1–1, 2020.

[201] Swati Sharda. link.

[202] Swati Sharda, Mukhtiar Singh, and Kapil Sharma. Demand side management through load shifting in iot based hems: Overview, challenges and opportunities. *Sustainable Cities and Society*, page 102517, 2020.

[203] H. Shareef, M. S. Ahmed, A. Mohamed, and E. Al Hassan. Review on home energy management system considering demand responses, smart technologies, and intelligent controllers. *IEEE Access*, 6:24498–24509, 2018.

[204] J. . Sheen, C. . Chen, and J. . Yang. Time-of-use pricing for load management programs in taiwan power company. *IEEE Transactions on Power Systems*, 9(1):388–396, Feb 1994.

[205] Z. Sheng, H. Wang, and G. Chen. Convolutional residual network to short-term load forecasting. *Appl Intell*, 6(2):911–918, November 2020.

[206] H. Shi, M. Xu, and R. Li. Deep learning for household load forecasting—a novel pooling deep rnn. *IEEE Transactions on Smart Grid*, 9(5):5271–5280, 2018.

[207] George Sideratos, Andreas Ikonomopoulos, and Nikos D. Hatziargyriou. A novel fuzzy-based ensemble model for load forecasting using hybrid deep neural networks. *Electric Power Systems Research*, 178:106025, 2020.

[208] Hazem M. Soliman and Alberto Leon-Garcia. Game-theoretic demand-side management with storage devices for the future smart grid. *IEEE Transactions on Smart Grid*, 5(3):1475–1485, 2014.

[209] Saleh Soltan, Mihalis Yannakakis, and Gil Zussman. Power grid state estimation following a joint cyber and physical attack. *IEEE Transactions on Control of Network Systems*, 5(1):499–512, 2018.

[210] K. C. Sou, J. Weimer, H. Sandberg, and K. H. Johansson. Scheduling smart home appliances using mixed integer linear programming. In *2011 50th IEEE Conference on Decision and Control and European Control Conference*, pages 5144–5149, 2011.

[211] Kin Cheong Sou, James Weimer, Henrik Sandberg, and Karl Henrik Johansson. Scheduling smart home appliances using mixed integer linear programming. *Proceedings of the IEEE Conference on Decision and Control*, pages 5144–5149, 2011.

[212] Shikhar Srivastava and Stefan Lessmann. A comparative study of lstm neural networks in forecasting day-ahead global horizontal irradiance with satellite data. *Solar Energy*, 162:232 – 247, 2018.

[213] S.S.Rao. *Engineering optimization: theory and practice*. John Wiley & Sons, 2009.

[214] E. R. Stephens, D. B. Smith, and A. Mahanti. Game theoretic model predictive control for distributed energy demand-side management. *IEEE Transactions on Smart Grid*, 6(3):1394–1402, May 2015.

[215] Goran Strbac. Demand side management: Benefits and challenges. *Energy Policy*, 36(12):4419–4426, 2008.

[216] R. Tapakis, S. Michaelides, and A.G. Charalambides. Computations of diffuse fraction of global irradiance: Part 2 – neural networks. *Solar Energy*, 139:723 – 732, 2016.

[217] Mohammad Tasdighi, Hassan Ghasemi, and Ashkan Rahimi-Kian. Residential microgrid scheduling based on smart meters data and temperature dependent thermal load modeling. *IEEE Transactions on Smart Grid*, 5(1):349–357, 2014.

[218] Thomas Theodoridis, Vassilios Solachidis, Kosmas Dimitropoulos, Lazaros Gymnopoulos, and Petros Daras. A survey on ai nutrition recommender systems. In *Proceedings of*

the 12th ACM International Conference on PErvasive Technologies Related to Assistive Environments, PETRA '19, page 540–546, New York, NY, USA, 2019. Association for Computing Machinery.

[219] Google Nest Thermostats. Smart thermostats, 2019. Accessed: 2019-12-10.

[220] Tp-link. Tp-link smart plugs, 2019. Accessed: 2019-10-10.

[221] K. M. Tsui and S. C. Chan. Demand response optimization for smart home scheduling under real-time pricing. *IEEE Transactions on Smart Grid*, 3(4):1812–1821, Dec 2012.

[222] Mosaddek Hossain Kamal Tushar, Chadi Assi, Martin Maier, and Mohammad Faisal Uddin. Smart microgrids: Optimal joint scheduling for electric vehicles and home appliances. *IEEE Transactions on Smart Grid*, 5(1):239–250, 2014.

[223] Mosaddek Hossain Kamal Tushar, Adel W. Zeineddine, and Chadi Assi. Demand-Side Management by Regulating Charging and Discharging of the EV, ESS, and Utilizing Renewable Energy. *IEEE Transactions on Industrial Informatics*, 14(1):117–126, 2018.

[224] Wayes Tushar, Jian A. Zhang, David B. Smith, H. Vincent Poor, and Sylvie Thiébaux. Prioritizing consumers in smart grid: A game theoretic approach. *IEEE Transactions on Smart Grid*, 5(3):1429–1438, 2014.

[225] Amin Ullah, Kilichbek Haydarov, Ijaz Ul Haq, Khan Muhammad, Seungmin Rho, Miyoung Lee, and Sung Wook Baik. Deep learning assisted buildings energy consumption profiling using smart meter data. *Sensors*, 20(3), 2020.

[226] F. U. M. Ullah, A. Ullah, I. U. Haq, S. Rho, and S. W. Baik. Short-term prediction of residential power energy consumption via cnn and multi-layer bi-directional lstm networks. *IEEE Access*, 8:123369–123380, 2020.

[227] Ahmad Usman and Sajjad Haider Shami. Evolution of communication technologies for smart grid applications. *Renewable and Sustainable Energy Reviews*, 19:191 – 199, 2013.

[228] Ashish Vaswani, Noam Shazeer, Niki Parmar, Jakob Uszkoreit, Llion Jones, Aidan N. Gomez, Lukasz Kaiser, and Illia Polosukhin. Attention is all you need. *arXiv:1706.03762*, 2017.

[229] Cynthujah Vivekananthan, Yateendra Mishra, and Fangxing Li. Real-Time Price Based Home Energy Management Scheduler. *IEEE Transactions on Power Systems*, 30(4):2149–2159, 2015.

[230] Cyril Voyant, Gilles Notton, Soteris Kalogirou, Marie-Laure Nivet, Christophe Paoli, Fabrice Motte, and Alexis Fouilloy. Machine learning methods for solar radiation forecasting: A review. *Renewable Energy*, 105:569 – 582, 2017.

[231] Z. Wan, G. Wang, Y. Yang, and S. Shi. Skm: Scalable key management for advanced metering infrastructure in smart grids. *IEEE Transactions on Industrial Electronics*, 61(12):7055–7066, Dec 2014.

[232] Chengshan Wang, Yue Zhou, Jianzhong Wu, Jidong Wang, Yiqiang Zhang, and Dan Wang. Robust-Index Method for Household Load Scheduling Considering Uncertainties of Customer Behavior. *IEEE Transactions on Smart Grid*, 6(4):1806–1818, 2015.

[233] D. Wang, D. Lo, J. Bhimani, and K. Sugiura. Anycontrol – iot based home appliances monitoring and controlling. In *2015 IEEE 39th Annual Computer Software and Applications Conference*, volume 3, pages 487–492, July 2015.

[234] Kejun Wang, Xiaoxia Qi, and Hongda Liu. Photovoltaic power forecasting based lstm-convolutional network. *Energy*, 189:116225, 2019.

[235] L. Wang, Z. Wang, and R. Yang. Intelligent multiagent control system for energy and comfort management in smart and sustainable buildings. *IEEE Transactions on Smart Grid*, 3(2):605–617, June 2012.

[236] Pengyuan Wang and Manimaran Govindarasu. Multi-agent based attack-resilient system integrity protection for smart grid. *IEEE Transactions on Smart Grid*, 11(4):3447–3456, 2020.

[237] Yi Wang, Dahua Gan, Mingyang Sun, Ning Zhang, Zongxiang Lu, and Chongqing Kang. Probabilistic individual load forecasting using pinball loss guided lstm. *Applied Energy*, 235:10 – 20, 2019.

[238] Z. Wen, D. O'Neill, and H. Maei. Optimal demand response using device-based reinforcement learning. *IEEE Transactions on Smart Grid*, 6(5):2312–2324, Sep. 2015.

[239] J. Wiehagen and D. Harrell. Review of residential electrical energy use data, nahb res. center inc., upper marlboro, July 2001.

[240] Chorng-Huey Wong. Market-Based Systems of Monetary Control in Developing Countries: Operating Procedures and Related Issues. *IMF Working Papers*, 91(40):1–30, 2014.

[241] Zhi Wu, Suyang Zhou, Jianing Li, and Xiao Ping Zhang. Real-time scheduling of residential appliances via conditional risk-at-value. *IEEE Transactions on Smart Grid*, 5(3):1282–1291, 2014.

[242] Xu, W., H. Peng, and Zeng X. A hybrid modelling method for time series forecasting based on a linear regression model and deep learning. *Appl Intell*, 49:3002–3015, 2019.

[243] X. Xu, Y. Jia, Y. Xu, Z. Xu, S. Chai, and C. S. Lai. A multi-agent reinforcement learning-based data-driven method for home energy management. *IEEE Transactions on Smart Grid*, 11(4):3201–3211, 2020.

[244] Zhongwen Xu, Liming Yao, and Xudong Chen. A robust optimization for agricultural crops area planning and industrial production level in the presence of effluent trading. *Journal of Cleaner Production*, 254:119987, 2020.

[245] Naouar Yaagoubi and Hussein T. Mouftah. User-aware game theoretic approach for demand management. *IEEE Transactions on Smart Grid*, 6(2):716–725, 2015.

[246] Y. Yan, Y. Qian, H. Sharif, and D. Tipper. A survey on smart grid communication infrastructures: Motivations, requirements and challenges. *IEEE Communications Surveys Tutorials*, 15(1):5–20, First 2013.

[247] Bo Yang, Jingbo Wang, Xiaoshun Zhang, Tao Yu, Wei Yao, Hongchun Shu, Fang Zeng, and Liming Sun. Comprehensive overview of meta-heuristic algorithm applications on pv cell parameter identification. *Energy Conversion and Management*, 208:112595, 2020.

[248] Dazhi Yang, Zhen Ye, Li Hong Idris Lim, and Zibo Dong. Very short term irradiance forecasting using the lasso. *Solar Energy*, 114:314 – 326, 2015.

[249] Lei Yang, Xu Chen, Junshan Zhang, and H. Vincent Poor. Cost-effective and privacy-preserving energy management for smart meters. *IEEE Transactions on Smart Grid*, 6(1):486–495, 2015.

[250] Enxin Yao, Pedram Samadi, Vincent W.S. Wong, and Robert Schober. Residential Demand Side Management Under High Penetration of Rooftop Photovoltaic Units. *IEEE Transactions on Smart Grid*, 7(3):1597–1608, 2016.

[251] P. Yi, X. Dong, A. Iwayemi, C. Zhou, and S. Li. Real-time opportunistic scheduling for residential demand response. *IEEE Transactions on Smart Grid*, 4(1):227–234, March 2013.

[252] P. Yi, A. Iwayemi, and C. Zhou. Developing zigbee deployment guideline under wifi interference for smart grid applications. *IEEE Transactions on Smart Grid*, 2(1):110–120, March 2011.

[253] Yeliz Yoldaş, Ahmet Önen, S. M. Muyeen, Athanasios V. Vasilakos, and İrfan Alan. Enhancing smart grid with microgrids: Challenges and opportunities. *Renewable and Sustainable Energy Reviews*, 72(January):205–214, 2017.

[254] K. Yu, M. Arifuzzaman, Z. Wen, D. Zhang, and T. Sato. A key management scheme for secure communications of information centric advanced metering infrastructure in smart grid. *IEEE Transactions on Instrumentation and Measurement*, 64(8):2072–2085, Aug 2015.

[255] L. Yu, T. Jiang, and Y. Zou. Online energy management for a sustainable smart home with an hvac load and random occupancy. *IEEE Transactions on Smart Grid*, 10(2):1646–1659, March 2019.

[256] Mengmeng Yu and Seung Ho Hong. A Real-Time Demand-Response Algorithm for Smart Grids: A Stackelberg Game Approach. *IEEE Transactions on Smart Grid*, 7(2):879–888, 2016.

[257] Zong-Han Yu and Wen-Long Chin. Blind false data injection attack using pca approximation method in smart grid. *IEEE Transactions on Smart Grid*, 6(3):1219–1226, 2015.

[258] Yudong Tang, Hongkun Song, Funian Hu, and Yun Zou. Investigation on tou pricing principles. In *2005 IEEE/PES Transmission Distribution Conference Exposition: Asia and Pacific*, pages 1–9, Aug 2005.

[259] Rehman Zafar, Anzar Mahmood, Sohail Razzaq, Wamiq Ali, Usman Naeem, and Khurram Shehzad. Prosumer based energy management and sharing in smart grid. *Renewable and Sustainable Energy Reviews*, 82:1675 – 1684, 2018.

[260] A. Zakaria, Firas B. Ismail, M.S. Hossain Lipu, and M.A. Hannan. Uncertainty models for stochastic optimization in renewable energy applications. *Renewable Energy*, 145:1543 – 1571, 2020.

[261] Javier Zazo, Santiago Zazo, and Sergio Valcarcel Macua. Robust Worst-Case Analysis of Demand-Side Management in Smart Grids. *IEEE Transactions on Smart Grid*, 8(2):662–673, 2017.

[262] Jianwu Zeng and Wei Qiao. Short-term solar power prediction using a support vector machine. *Renewable Energy*, 52:118 – 127, 2013.

[263] Dong Zhang, Shuhui Li, Min Sun, and Zheng O'Neill. An Optimal and Learning-Based Demand Response and Home Energy Management System. *IEEE Transactions on Smart Grid*, 7(4):1790–1801, 2016.

[264] Hang Zhang, Bo Liu, and Hongyu Wu. Smart grid cyber-physical attack and defense: A review. *IEEE Access*, 9:29641–29659, 2021.

[265] Tian-Yu Zhang and Dan Ye. False data injection attacks with complete stealthiness in cyber–physical systems: A self-generated approach. *Automatica*, 120:109117, 2020.

[266] B. Zhao, S. Xiao, H. Lu, and J. Liu. Waveforms classification based on convolutional neural networks. In *2017 IEEE 2nd Advanced Information Technology, Electronic and Automation Control Conference (IAEAC)*, pages 162–165, 2017.

[267] L. Zhao, Z. Yang, and W. Lee. The impact of time-of-use (tou) rate structure on consumption patterns of the residential customers. *IEEE Transactions on Industry Applications*, 53(6):5130–5138, Nov 2017.

[268] Peng Zhuang, Ruilong Deng, and Hao Liang. False data injection attacks against state estimation in multiphase and unbalanced smart distribution systems. *IEEE Transactions on Smart Grid*, 10(6):6000–6013, 2019.

List of Publications

International Journals

1. **Swati Sharda**, Mukhtiar Singh, Kapil Sharma 2021,"RSAM: Robust Self-Attention Based Multi-Horizon Model for Solar Irradiance Forecasting ", *IEEE TRANSACTIONS ON SUSTAINABLE ENERGY (IF-7.9), IEEE (SCIE).*

2. **Swati Sharda**, Mukhtiar Singh, Kapil Sharma, 2021,"A complete consumer behaviour learning model for real-time demand response implementation in smart grid ", *APPLIED INTELLIGENCE (IF-5.0), Springer (SCIE).*

3. **Swati Sharda**, Mukhtiar Singh, Kapil Sharma, 2021,"Demand side management through load shifting in IoT based HEMS: Overview, challenges and opportunities ", *SUSTAINABLE CITIES and SOCIETY (IF-7.5), Elsevier (SCIE).*

4. **Swati Sharda**, Kapil Sharma, Mukhtiar Singh 2021,"A real-time automated scheduling algorithm with PV integration for smart home prosumers ", *JOURNAL of BUILDING ENGINEERING (IF-5.3), Elsevier (SCIE).*

International Conferences

1. **Swati Sharda**, Kapil Sharma, Mukhtiar Singh 2021, "Smart Grid Communication Network Reliability Assessment using Graphical Computational Model ", *3rd International Conference on Sustainable and Innovative Solutions for Current Challenges in Engineering Technology (ICSISCET) , Springer Book Series*.

2. **Swati Sharda**, Kapil Sharma, Mukhtiar Singh 2021, "False Data Injection and Detection in Smart Grid Cyber-Physical Systems by Iterative Load Flow Analysis", *3rd Interna-*

tional Conference on Advances in Information Communication Technology Computing (AICTC).